

# CHALMERS



## Dual Clutch Transmission for Plug-in hybrid electric vehicle

Comparative analysis with Toyota hybrid system

*Master's thesis in Automotive engineering*

KARTHIK UPENDRA

Department of Signal and systems  
CHALMERS UNIVERSITY OF TECHNOLOGY  
Göteborg, Sweden 2014  
Master's thesis EX061/2014

[\*https://autolibrary.ir\*](https://autolibrary.ir)

[\*https://autolibrary.ir\*](https://autolibrary.ir)

MASTER'S THESIS IN AUTOMOTIVE ENGINEERING

# Dual Clutch Transmission for Plug-in hybrid electric vehicle

Comparative analysis with Toyota hybrid system

KARTHIK UPENDRA

Department of Signal and systems  
CHALMERS UNIVERSITY OF TECHNOLOGY

Göteborg, Sweden 2014

Dual Clutch Transmission for Plug-in hybrid electric vehicle  
Comparative analysis with Toyota hybrid system  
KARTHIK UPENDRA

© KARTHIK UPENDRA, 2014

Master's thesis EX061/2014  
ISSN 1652-8557  
Department of Signal and systems  
Chalmers University of Technology  
SE-412 96 Göteborg  
Sweden  
Telephone: +46 (0)31-772 1000

Chalmers Reproservice  
Göteborg, Sweden 2014

Dual Clutch Transmission for Plug-in hybrid electric vehicle  
Comparative analysis with Toyota hybrid system  
Master's thesis in Automotive engineering  
KARTHIK UPENDRA  
Department of Signal and systems  
Chalmers University of Technology

## ABSTRACT

Depleting oil resources and global warming has lead to a continual search in the automotive sector to find a cost effective solution to develop more and more fuel efficient vehicles. As a result of this, a new concept called the hybrid dual clutch transmission (HDCT) has recently been developed. This thesis aims to compare the new concept (HDCT) to the state of art electric continuously variable transmission (ECVT) used for example by Toyota.

The investigated power train in this thesis is the HDCT with six speed built by a German company called Getrag. In order to evaluate the HDCT concept, three hybrid power train design are compared for their working principle, functionality and cost with that of the HDCT design. The three power trains used for comparison are 'voltec 4ET50', used in Chevrolet volt, 'GM 2MT70', not in production for cars but is used in bus, and 'THS-III generation', used in Toyota Prius. Later, for simulation using Matlab and Simulink, THS-III generation design is used as a benchmark for the HDCT design to compare the fuel and electric efficiency and performance.

The Simulation results shows that the HDCT design is better than the ECVT design in terms of fuel efficiency on all three driving cycle (NEDC, UDDS and HWFET). A functionality comparison shows that HDCT design can offer all the functionalities that ECVT design offers. In addition to this, a rough cost estimate shows that HDCT design is probably cheaper than ECVT design. The performance comparison indicates that HDCT design is clearly better than ECVT design. In addition to this, HDCT design can be made modular, that is, with little modifications it can be combined easily with heavy vehicles, light vehicles, conventional vehicles or hybrid vehicles.

The HDCT in general is found better regarding all the above compared properties. The differences may depend on some assumptions. However, for many vehicles the HDCTs are expected to be a better solution than the ECVT.

Keywords: plug-in hybrid vehicle, PHEV, Hybrid electric vehicle, HEV, Dual clutch transmission, DCT, HDCT equivalent consumption minimisation strategy, ECMS, cost, performance, efficiency, comparison, THS-III, GM 2MT70, Voltec 4ET50, state of art, charge sustaining and charge depletion, CDCS.

## ACKNOWLEDGEMENTS

First and foremost, I would like to thank my supervisor professor Anders Grauers for having faith in me and considering me for this thesis work. It wouldn't have been possible for me to have completed this thesis work without the motivating discussion and valuable guidance.

I would also like to thank my advisor Victor Judez for all the suggestions and discussions. You helped me take the first step in the correct path and direction. It wouldn't have been possible for me to have developed controls without your guidance and support.

This master thesis analyses a new promising powertrain concept developed in the EU project Optimore. The financial support and the support of data are gratefully acknowledged.

My sincere thanks to Aziz Mohammed from Volvo cars for providing me with the data necessary for simulation.

My sincere thanks also go to Nikolce Murgovcki for valuable discussion regarding dynamic programming and matlab script for object files for simulation. I would also like to thank my friend Pavan Balram for helping me with the Latex format and files. Last but not the least, I would like to thank my family for supporting me.

## CONTENTS

<b>Abstract</b>	<b>i</b>
<b>Acknowledgements</b>	<b>ii</b>
<b>Contents</b>	<b>iii</b>
<b>1 Introduction</b>	<b>5</b>
1.1 Background . . . . .	5
1.2 The Optimore project . . . . .	6
1.3 Aim of this project . . . . .	6
1.4 Assumptions . . . . .	6
1.5 Thesis Outline . . . . .	7
<b>2 Hybrid Power-train Architectures</b>	<b>8</b>
2.1 Series hybrid power-train architecture . . . . .	8
2.2 Parallel hybrid power-train architecture . . . . .	8
2.3 Series-Parallel hybrid power-train architecture . . . . .	9
2.4 Plug-in Hybrid Electric vehicle (PHEV) . . . . .	9
<b>3 Current state of art in Hybrid power-trains</b>	<b>10</b>
3.1 Toyota hybrid system (THS) . . . . .	10
3.1.1 THS-II Architecture and working principle . . . . .	10
3.1.2 THS-III Architecture and working principle . . . . .	12
3.1.3 Constraints on Engine and MG1 (generator) speed for THS-III . . . . .	13
3.2 General Motors two mode hybrid system . . . . .	15
3.2.1 General Motors '2MT70', Architecture and working principle . . . . .	15
3.2.2 Constraints on engine speed and motor-generator units speed . . . . .	18
3.3 GMs 'Voltec-4ET50' . . . . .	20
3.3.1 'Voltec-4ET50' Architecture and working principle . . . . .	20
3.3.2 Constrains on motor-generator speeds and engine speed for Voltec-4ET50 in ER mode only . . . . .	23
3.4 Hybrid dual clutch transmission . . . . .	23
3.4.1 Dual clutch transmission . . . . .	23
3.4.2 Hybrid Dual clutch transmission for PHEV . . . . .	24
<b>4 Hybrid power-train control</b>	<b>28</b>
4.1 Charge Depletion and Charge Sustaining (CDCS) . . . . .	28
4.2 Equivalent Consumption minimization strategy (ECMS) . . . . .	28
<b>5 Comparisons of different power-train</b>	<b>30</b>
5.1 Cost comparison . . . . .	30
5.2 Functionality comparison . . . . .	32
5.3 Comparison on different configurations possible for HDCT design . . . . .	32
5.4 Sizing of Motor generator unit and Battery . . . . .	35
5.5 Conclusion of different comparison . . . . .	36
<b>6 Simulation model of power-trains</b>	<b>37</b>
6.1 Object file . . . . .	37
6.2 Driving cycle model . . . . .	37
6.3 Chassis model . . . . .	38
6.4 Hybrid dual clutch transmission model . . . . .	39
6.5 ECVT model (similar to THS-III generation design) . . . . .	40
6.6 Hybrid Power-train control model . . . . .	42
6.6.1 Power-train control flow chart . . . . .	43
6.6.2 Input/Output signals of hybrid power-train control . . . . .	44

6.7	Internal combustion engine model . . . . .	48
6.8	Motor-generator model . . . . .	48
6.9	Battery . . . . .	49
<b>7</b>	<b>Simulation Result and discussion</b>	<b>51</b>
7.1	Efficiency results and discussion . . . . .	51
7.1.1	Efficiency of both architectures during CD mode (electric mode) . . . . .	51
7.1.2	Efficiency of both architectures during CS mode (ECMS mode) . . . . .	55
7.1.3	Summary of additional losses in ECVT design . . . . .	61
7.1.4	Summary of additional losses in HDCT design . . . . .	64
7.1.5	Comparison of additional losses within both the architectures . . . . .	66
7.2	Performance capability of both architectures . . . . .	66
7.2.1	Performance capability of both architectures in pure electric mode . . . . .	66
7.2.2	Performance capability of both architectures in ICE mode when battery power is zero . . . . .	66
7.2.3	Performance capability of both architectures in Boost mode when battery power is positive . . . . .	67
7.2.4	Performance capability of ECVT architecture in ICE mode when battery power is zero (reference figure 7.27) . . . . .	68
<b>8</b>	<b>Conclusion and future work</b>	<b>72</b>
8.1	Conclusion . . . . .	72
8.2	Future work . . . . .	72
	<b>References</b>	<b>73</b>
	<b>Appendices</b>	<b>74</b>
A	THS-III generatoin power-train parameters used for drawing graph shown in figure 3.5 and 3.6	75
B	GM 2MT70 power-train parameters used for drawing graph shown in figure 3.10 and 3.11	75
C	Voltec 4ET50 power-train parameters used for drawing graph shown in figure 3.14 and 3.15	75
D	Graphs relating to NEDC driving cycle	76
E	Efficiency simulation results for both architectures in UDDS driving cycle	77
E.1	Efficiency of both architectures during CD mode (electric mode) in UDDS . . . . .	77
E.2	Efficiency of both architectures during CS mode (ECMS mode) in UDDS . . . . .	81
F	Efficiency simulation results for both architectures in HWFET driving cycle	82
F.1	Efficiency of both architectures during CD mode (electric mode) in HWFET . . . . .	89
F.2	Efficiency of both architectures during CS mode (electric mode) in HWFET . . . . .	92

## List of Figures

2.1	Series hybrid power-train architecture . . . . .	8
2.2	Parallel hybrid power-train architecture . . . . .	9
3.1	A power flow view of THS-II generation power-train architecture. C= carrier gear shaft, S = sun gear shaft, R= ring gear shaft. . . . .	10
3.2	Mechanical view of THS-II generation power-train architecture. Note, battery, power electronics and electrical connection between the motor-generator units are not shown for clarity. C= carrier gear shaft, S = sun gear shaft, R= ring gear shaft. . . . .	11
3.3	Power flow view of THS-III hybrid power-train architecture. C= carrier gear shaft, S = sun gear shaft, R= ring gear shaft. . . . .	12
3.4	Mechanical view of THS-III generation power-train architecture. Note differential, battery, power electronics and electrical connection between the MGs are not shown for clarity. C= carrier gear shaft, S = sun gear shaft, R= ring gear shaft. . . . .	13
3.5	Allowed operating region for THS-III with separation factor . . . . .	13
3.6	Allowed operating region for THS-III with generator speed (RPM) . . . . .	14
3.7	Power flow view of the GMs '2MT70' power-train architecture. Modified and redrawn from [13]. C= carrier gear shaft, S = sun gear shaft, R= ring gear shaft. . . . .	15
3.8	Mechanical view of the GMs '2MT70' power-train architecture. Note differential, battery, power electronics and electrical connections between the motor-generator unit are not shown for clarity. Modified and redrawn from [7]. C= carrier gear shaft, S = sun gear shaft, R= ring gear shaft. . . . .	16
3.9	Mechanical view of different modes in GMs '2MT70' power-train architecture. Note: Battery, power electronics and connection between motor-generator units are not shown for clarity. C= carrier gear shaft, S = sun gear shaft, R= ring gear shaft. . . . .	17
3.10	Allowed operating region for GMs '2MT70' power-train architecture. Redrawn from [15] . . . . .	18
3.11	Allowed operating region for GMs '2MT70' power-train architecture as a function of separation factor and generator speed. Redrawn from [15] . . . . .	20
3.12	Power flow view of 'Voltec-4ET50' power-train architecture. C= carrier gear shaft, S = sun gear shaft, R= ring gear shaft. . . . .	21
3.13	Mechanical view of 'Voltec-4ET50' power-train architecture. Note: Battery, power electronics and the connections between the motor-generator units are not shown for clarity. C= carrier gear shaft, S = sun gear shaft, R= ring gear shaft. . . . .	22
3.14	Motor-generator speed vs Vehicle velocity for Voltec-4ET50 . . . . .	22
3.15	Allowed operating region for Voltec 4ET50 in ER mode . . . . .	23
3.16	Schematic of Dual clutch transmission . . . . .	24
3.17	Schematic of Hybrid Dual clutch transmission. Complete arrangement of gears and synchronizers not shown for confidentiality reasons . . . . .	25
3.18	HDCT transmission plot; Possible combinations of engine, motor and vehicle speed . . . . .	26
3.19	HDCT transmission plot; Bottom view . . . . .	26
3.20	HDCT transmission plot; Side view . . . . .	26
4.1	Hybrid energy management control . . . . .	28
5.1	Rough Cost comparison of Voltec 4ET50, THS-III generation, GM 2MT70, and HDCT . . . . .	32
5.2	Different parallel hybrid architecture configuration based on the position of the motor-generator . . . . .	33
6.1	Urban dynamo meter driving cycle . . . . .	37
6.2	Highway fuel economy test cycle . . . . .	38
6.3	New European driving cycle . . . . .	38
6.4	Stick model of HDCT design . . . . .	40
6.5	Stick model of Ecvt THS-III type design . . . . .	41
6.6	Hybrid power-train control topology . . . . .	42
6.7	First level of supervisory control run at each time step . . . . .	43
6.8	CD mode supervisory control run at each time step . . . . .	44
6.9	CS mode supervisory control run at each time step . . . . .	45
6.10	ICE map with efficiency line. Efficiency values not shown due to confidentiality reasons . . . . .	48
6.11	Motor-generator 2 map with efficiency line . . . . .	49

6.12	Motor-generator 1 map with efficiency line. Note, the distorted efficiency line along the edges of the torque at high speed is a numerical error caused by manual sizing of the MG2 map. However these region in the map is not used in any of the driving cycle and simulation results are not affected. . . . .	49
6.13	Battery model . . . . .	50
6.14	$V_{OC}$ as a function of SOC . . . . .	50
7.1	Energy loss accrued in each component in NEDC cycle for both architectures in CD/electric mode	52
7.2	'No-load' losses in MG1 in ECVT design in CD mode in NEDC cycle . . . . .	52
7.3	ECVT design, MG2 map and operating points in CD mode in NEDC . . . . .	53
7.4	HDCT design, MG map and operating points in CD mode in NEDC . . . . .	53
7.5	ECVT design, MG1 map and operating points in CD mode in NEDC . . . . .	54
7.6	SOC variations for both architectures in CD mode in NEDC . . . . .	54
7.7	Energy loss accrued in each component in NEDC cycle for both architectures in CS/ECMS mode	56
7.8	No-load and No-spin losses in ECVT design in MG1 in CS mode in NEDC . . . . .	56
7.9	ICE power output for both architectures in CS mode in NEDC . . . . .	57
7.10	ECVT design, MG2 map and operating points in CS mode in NEDC . . . . .	57
7.11	HDCT design, MG map and operating points in CS mode in NEDC . . . . .	58
7.12	ECVT design, MG1 map and operating points in CS mode in NEDC . . . . .	58
7.13	SOC variation in both architectures in CS mode in NEDC . . . . .	59
7.14	ECVT design, ICE map and operating points in CS mode in NEDC . . . . .	59
7.15	HDCT design, ICE map and operating points in CS mode in NEDC . . . . .	60
7.16	Power map for both architecture with operating points and road load . . . . .	60
7.17	No-load loss in MG1 in ECVT deign when the vehicle is in pure electric mode . . . . .	62
7.18	Double energy conversion loss in ECVT design when the separation factor is greater than zero but lesser than one. Note, in this figure the losses are assumed to be supplied by the battery . . . . .	62
7.19	No-load and No-spin loss in MG2 and MG1 respectively in ECVT design when the power request at the wheels is met by ICE only via mechanical path. Note, in this figure the losses are assumed to be supplied by the battery . . . . .	62
7.20	Double energy conversion loss and loss due to circulation of energy when separation factor is greater than one. Note, in this figure the losses are assumed to be supplied by the battery . . . . .	63
7.21	Separation factor chosen by power-train control in CS mode in NEDC in ECVT design . . . . .	63
7.22	No-load losses in HDCT design when the power request at the wheels is supplied by ICE alone via the even gears . . . . .	64
7.23	Energy loss during charging via the odd gear in HDCT design . . . . .	64
7.24	Engine speed vs vehicle velocity and operating points in CS mode in NEDC in HDCT design . . . . .	65
7.25	MG speed vs vehicle velocity and operating points in CS mode in NEDC in HDCT design . . . . .	65
7.26	Acceleration capability of both architectures in pure electric mode . . . . .	67
7.27	Acceleration capability of both architectures in ICE mode when power from the battery is zero . . . . .	67
7.28	Acceleration capability of both architectures in Boost mode when power from the battery is positive . . . . .	68
7.29	Transmission gear combinations possible in HDCT design . . . . .	68
7.30	Separation factor chosen by power-train control for maximum acceleration in pure ICE mode in ECVT design . . . . .	69
7.31	MG1 speed for maximum acceleration in ICE mode in ECVT design . . . . .	69
7.32	Operating points on ICE map for maximum acceleration in ICE mode for ECVT design . . . . .	70
7.33	Operating points on MG2 map for maximum acceleration in ICE mode for ECVT design . . . . .	71
7.34	Operating points on MG1 map for maximum acceleration in ICE mode for ECVT design. Note, the MG1 (generator map) used here is different than what is used in chapter 6 in figure 6.12 . . . . .	71
D.1	HDCT architecture, power-train control signals in NEDC in CS mode . . . . .	76
D.2	ECVT architecture, power-train control signals in NEDC in CS mode . . . . .	77
E.1	Energy loss accrued in each component in UDDS cycle for both architectures in CD/electric mode	78
E.2	'No-load' losses in MG1 in ECVT design in CD mode in UDDS cycle . . . . .	78
E.3	ECVT design, MG2 map and operating points in CD mode in UDDS . . . . .	79
E.4	HDCT design, MG map and operating points in CD mode in UDDS . . . . .	79
E.5	ECVT design, MG1 map and operating points in CD mode in UDDS . . . . .	80
E.6	SOC variations for both architectures in CD mode in UDDS . . . . .	80

E.7	Energy loss accrued in each component in UDDS cycle for both architectures in CS/ECMS mode	81
E.8	No-load and No-spin losses in ECVT design in MG1 in CS mode in UDDS	81
E.9	ICE power output for both architectures in CS mode in UDDS	82
E.10	ECVT design, MG2 map and operating points in CS mode UDDS	82
E.11	HDCT design, MG map and operating points in CS mode in UDDS	83
E.12	ECVT design, MG1 map and operating points in CS mode in UDDS	83
E.13	SOC variation in both architectures in CS mode in UDDS	84
E.14	ECVT design, ICE map and operating points in CS mode in UDDS	84
E.15	HDCT design, ICE map and operating points in CS mode in UDDS	85
E.16	Power map for both architecture with operating points and road load in UDDS	85
E.17	Separation factor chosen by power-train control in CS mode in UDDS in ECVT design	86
E.18	Engine speed vs vehicle velocity and operating points in CS mode in UDDS in HDCT design	86
E.19	MG speed vs vehicle velocity and operating points in CS mode in UDDS in HDCT design	87
E.20	HDCT architecture, power-train control signals in UDDS in CS mode	87
E.21	ECVT architecture, power-train control signals in UDDS in CS mode	88
F.1	Energy loss accrued in each component in HWFET cycle for both architectures in CD/electric mode	89
F.2	'No-load' losses in MG1 in ECVT design in CD mode in HWFET cycle	89
F.3	ECVT design, MG2 map and operating points in CD mode in HWFET	90
F.4	HDCT design, MG map and operating points in CD mode in HWFET	90
F.5	ECVT design, MG1 map and operating points in CD mode in HWFET	91
F.6	SOC variations for both architectures in CD mode in HWFET	91
F.7	Energy loss accrued in each component in HWFET cycle for both architectures in CS/ECMS mode	92
F.8	No-load and No-spin losses in ECVT design in MG1 in CS mode in HWFET	92
F.9	ICE power output for both architectures in CS mode in HWFET	93
F.10	ECVT design, MG2 map and operating points in CS mode HWFET	93
F.11	HDCT design, MG map and operating points in CS mode in HWFET	94
F.12	ECVT design, MG1 map and operating points in CS mode in HWFET	94
F.13	SOC variation in both architectures in CS mode in HWFET	95
F.14	ECVT design, ICE map and operating points in CS mode in HWFET	95
F.15	HDCT design, ICE map and operating points in CS mode in HWFET	96
F.16	Power map for both architecture with operating points and road load in HWFET	96
F.17	Separation factor chosen by power-train control in CS mode in ECVT in HWFET design	97
F.18	Engine speed vs vehicle velocity and operating points in CS mode in HDCT in HWFET design	97
F.19	MG speed vs vehicle velocity and operating points in CS mode in HWFET in HDCT design	98
F.20	HDCT architecture, power-train control signals in HWFET in CS mode	99
F.21	ECVT architecture, power-train control signals in HWFET in CS mode	100

## List of Tables

3.1	Clutch selection for different operating modes . . . . .	16
3.2	Clutch selection for different operating modes for Voltec-4ET50 . . . . .	21
5.1	Rough cost estimate of power-trains Voltec 4ET50, THS-III generation, GM 2MT70, and HDCT . . . . .	31
5.2	Individual component cost table derived from Argonne lab research data and Environmental protection agency (EPA) cost analysis . . . . .	31
5.3	Comparison on functionality of Voltec 4ET50, THS-III generation, GM 2MT70, and HDCT. Note, blue color is just for visual comparison . . . . .	32
5.4	Comparison on different parallel HDCT configuration based on the position of the motor-generator unit. Note, green color indicates that particular configuration is better when compared to the rest for that specific discussion . . . . .	34
5.5	Comparison on number of electric components and if the primemovers are assisted by gear box or not. Note, blue color is just for visual comparison . . . . .	35
5.6	Sizing of the motor-generator unit comparison table. Note, blue color is just for visual comparison . . . . .	35
5.7	Cost comparison of different power train configurations normalised to THS -III power train cost. . . . .	36
6.1	Rolling resistance coefficient as a function of vehicle velocity . . . . .	39
6.2	Vehicle parameters used for simulation. Some values not given due to confidentiality reasons . . . . .	39
6.3	Combination of control output signals possible for HDCT design . . . . .	46
6.4	Combination of output signals possible for ECVT THS-III generation type design . . . . .	47
6.5	Battery parameters . . . . .	50
7.1	Efficiency in CD mode for both architectures in NEDC, UDDS and HWFET driving cycle . . . . .	51
7.2	Efficiency in CS mode for both architectures in NEDC, UDDS and HWFET driving cycle . . . . .	55
7.3	Comparison of additional losses within both the architectures . . . . .	66
A.1	THS-III generation power-train parameters used for drawing the graph shown in figure 3.5 and 3.6 . . . . .	75
B.1	GM 2MT70 power-train parameters used for drawing graph shown in figure 3.10 and 3.11 . . . . .	75
C.1	Voltec 4ET50 power-train parameters used for drawing graph shown in figure 3.14 and 3.15 . . . . .	75

# 1 Introduction

## 1.1 Background

Rapidly depleting oil resources and global warming are some of the major issues around the globe which has led many countries to set more stringent regulations for emissions and fuel consumption. The increasing customer demand and emission regulations has kept the automotive industry on a constant run to find a cost effective technology which satisfies higher and higher demands. One of the solutions that appears inevitable in the years to come would be a more widespread 'Hybridisation'.

The key benefit of hybridisation is to lower the fuel consumption which can be achieved through :-

- Recuperating kinetic energy during deceleration.
- Turn off the engine during standstill.
- Turn off the engine while coasting.
- Utilize the on-board stored electric energy from the grid which is cheaper and has lower  $CO_2$  emission than fuel.

The other benefits of hybridisation would be improved acceleration performance and lower particulate, hydrocarbon and nitrogen oxide emission. Considering the cost and maturity of the battery technology, employing all of these characteristics and simultaneously satisfying the customer demand will result in very high cost per vehicle. Therefore, most of the vehicle manufacturers employ some of the characteristics mentioned above for example, recuperation of kinetic energy during deceleration, turn off the engine when the vehicle is at standstill and use energy from battery for initial acceleration in their vehicle, thus maintaining comparable characteristic to cost ratio to that of a conventional power train. This leads to one of the classifications, mild hybrids (also sometimes referred to as weak hybrids) and full hybrids (also sometimes referred to as strong hybrids). Hybrid vehicles employing just some of the above mentioned characteristics such as recuperation of kinetic energy and using electric energy for initial acceleration from standstill are usually referred to as mild hybrid, e.g. Saturn Vue (2007-09). Hybrid vehicles employing all of the above characteristics are usually referred to as strong hybrids, e.g. Toyota Prius.

Depending on the architecture of the power-train, hybrid vehicles can be classified into series, parallel and series-parallel hybrid architecture, each having its own advantages and disadvantage for specific classes of vehicles and specific type of driving. Hybrid vehicles employing series architecture are usually beneficial for fuel economy in urban driving cycle. Hybrid vehicles employing parallel architecture have good performance and is more fuel efficient than hybrid vehicle employing series architecture. Hybrid vehicle employing series-parallel hybrid architecture have good fuel economy but usually comes with increase in number and size of prime movers when compared to hybrid vehicle employing parallel architecture.

It is clear from the hybrid vehicles in the market, that the two major companies in the automotive sector; the General Motor(GM) and Toyota are preferring series-parallel hybrid architecture with electro-mechanical continuously variable transmission (ECVT) over the other architectures, to achieve better fuel consumption. In doing so, the number and size of the components increases which in turn increases the mass and overall complexity of the power-train, thereby increasing the overall cost of the vehicle. Some inherent and inevitable power losses in the series-parallel architecture itself decreases the fuel efficiency benefit of ECVT. On the other hand, parallel hybrid architecture has the benefit of using the already in-house conventional transmission technology having high performance capability. By smartly incorporating the electric prime mover, all of the required functionality of that of a series-parallel architecture can be accomplished with low cost per vehicle.

The recent development in battery technology and its reduced price has resulted in slow transition from Hybrid electric vehicles (HEV) to plug-in hybrid electric vehicles (PHEV). The main difference between HEV and PHEV is that, in PHEV the battery is bigger and can be charged through a charging cable which can be plugged into household outlet or industrial grid.

## 1.2 The Optimore project

Within the EU project Optimore, Volvocars and Getrag are developing a new type of powertrain for electric vehicles using a hybridized version of a dual clutch transmission to serve both as the electric powertrain and also as a range extender for long trips. Even though this may look as a mechanically very complicated range extender solution, a closer look shows that it seems to be a very attractive not only for hybrid vehicles but also as an electric vehicle with a range extender. Within the Optimore project, detailed design and analysis of this powertrain is carried out for one specific range extended electric vehicle.

Within this master thesis a general comparison is made between the hybrid dual clutch transmission and state of the art hybrid power trains, to draw general conclusions about the strengths and weaknesses of this new power train concept.

## 1.3 Aim of this project

Based on data for one of the Optimore vehicle, this report aims at determining how well the new hybrid dual clutch power train competes with some state-of-the-art hybrid power trains such as the Toyotas THS (Toyota hybrid system). To draw general conclusions about its strengths and weaknesses on a detailed level, an evaluation on various levels such as functionality, fuel economy, size of prime mover, performance and cost are essential. Therefore, a comparison between the state-of-the-art hybrid power train and new hybrid dual clutch power train with same size of electric machine, ICE and controls is required which forms the basis for this thesis work.

The aim of this thesis is to study the current state of art in the area of hybridisation and compare the fuel consumption and performance of two different type of architectures; a series-parallel hybrid architecture using a electrically controlled variable transmission (same as that in Toyota Prius) and parallel hybrid architecture using a Dual clutch transmission by simulation using Matlab and Simulink. The primary objective of this thesis is to identify the conceptual differences between the above mentioned architectures that leads to better fuel economy.

## 1.4 Assumptions

Taking all the factors into account will lead to more complex simulation model which consumes more time for execution. The main focus is on identifying the steady state losses pertaining to respective architecture while a small discussion will be provided wherever necessary in-case the dynamic losses plays an important role. Hence, certain assumptions are made which are listed below.

- The gear shift dynamics involved in the power-train are not considered in this thesis.
- The efficiency of meshing gears is assumed to be 97% and that of the differential is assumed to be 95%.
- The dynamic losses in the HDCT gear box such as clutch slipping, gear shifting are assumed to be very low and ignored here.
- Losses in hydraulics due to controlling the pre selection of the gear in HDCT design is ignored.
- The power loss resulting due to the control of the speed of the electric machines are considered to be low and ignored here.
- The cooling requirements of the power-train are not considered here.

An electric motor in general can be made to operate as a generator. Hence the term electric machine is used more often in this thesis report. However, at some places the word 'motor-generator' is also used.

Note: The words electric machine and motor-generator(MG) have been used interchangeably in this thesis report.

## 1.5 Thesis Outline

This thesis work is divided into 8 chapters. After the introduction in chapter 1, different types of hybrid power-train architecture are discussed in chapter 2, followed by current state of art in the hybrid technology in chapter 3. Then a brief discussion is made on the Hybrid power-train control used for simulation in chapter 4. In chapter 5, a brief comparison in terms of cost, functionality and size of the electric components for four selected hybrid power-train design namely, the Voltec 4ET50 (used in Chevrolet Volt), GM 2MT70, THS-III (used in Toyota Prius) and Hybrid dual clutch transmission (HDCT) is presented. Chapter 6 discusses the modelling of HDCT and ECVT THS III generation type power-train using matlab and simulink. Section 7 presents the result and discussion and chapter 8 presents the conclusion and the potential future work.

## 2 Hybrid Power-train Architectures

Depending on how the components are arranged in a power-train, the hybrid power-train can be classified into three categories namely series, parallel and series-parallel hybrid power-train architectures.

### 2.1 Series hybrid power-train architecture

In series hybrid power-train architecture, ICE is coupled to a motor-generator (MG) usually functioning as generator (MG1) which is together called the Engine generator unit (EGU). Another motor-generator unit usually functioning as motor (MG2) is coupled to the wheels which propels the vehicle. The architecture of series hybrid power-train is shown in figure 2.1.

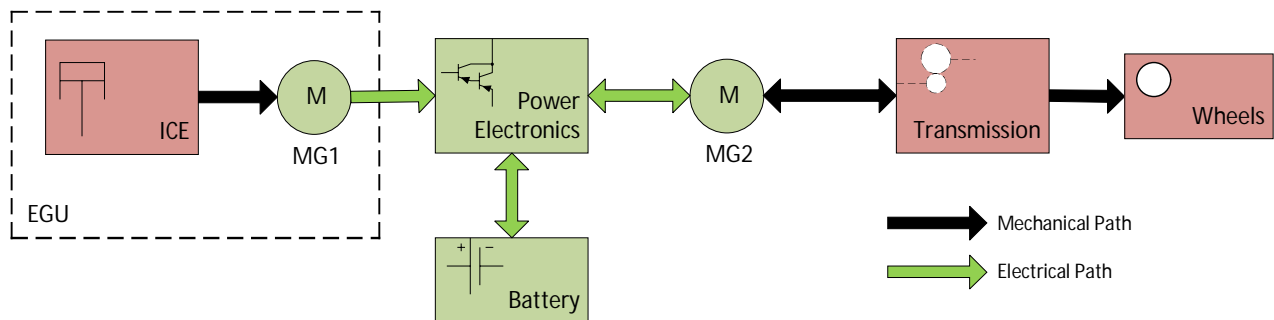


Figure 2.1: *Series hybrid power-train architecture*

The engine generator unit is used only to replenish the battery when it is depleted or sometimes directly feed the power to the MG2 connected to the wheels.

One of the advantages in series hybrid power-train architecture is that, the internal combustion engine (ICE) can be operated independent of the wheel speed and load. Hence, the engine can be tuned to operate at its most efficient point. However, this type of architecture will lead to double energy conversion losses, i.e. energy loss while converting mechanical energy from engine to electrical energy and then back to mechanical energy to the wheels.

The MG2, has to be sized based on the acceleration performance of the vehicle. In hybrid vehicles the battery is usually small and will deplete rather quickly which requires the EGU to supply the electrical power directly to MG2 connected to the wheels. Therefore, the EGU has to be sized based on start-ability, grade-ability and top speed requirement of the vehicle. Series hybrid power-train architecture is best suited for urban traffic and is typically used in some city buses.

### 2.2 Parallel hybrid power-train architecture

In parallel hybrid power-train architecture, as the name suggests, power to the wheels can be supplied in parallel through electrical and mechanical path. The number of components in parallel architecture can be fewer than that in the series hybrid power-train architecture. It usually consist of an ICE, one motor-generator, battery and power electronics. A typical architecture of parallel hybrid power-train is shown in figure 2.2.

The control for the parallel hybrid power-train architecture can be designed in such a way that the electric machine is used for initial acceleration when the power demand is low and the later power demand is met by the engine thus improving the fuel economy. This architecture has the ability to reduce the fuel consumption and also at the same time enhance the performance of the vehicle.

The power required at the wheels can be supplied by both motor-generator (MG1) and ICE independently or simultaneously. Thus, for the same performance as that of the series hybrid power-train architecture, the sum of the power of the engine and motor-generator in parallel hybrid power-train architecture can be made smaller. However, the complexity of regulating the power flow increases which will lead to more complex controls and mechanical devices.

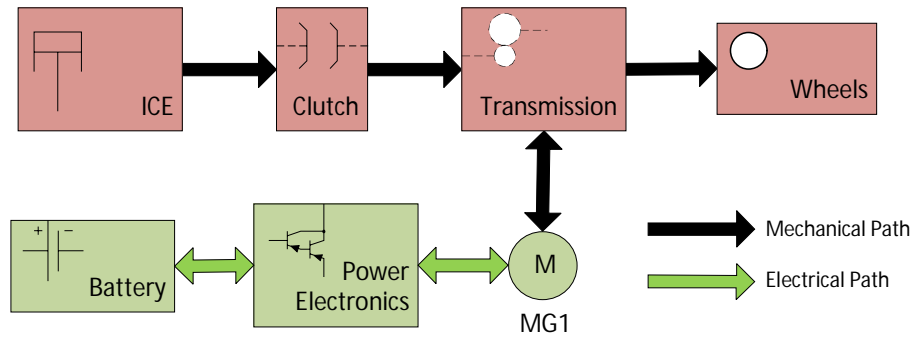


Figure 2.2: *Parallel hybrid power-train architecture*

## 2.3 Series-Parallel hybrid power-train architecture

Series-parallel hybrid power-train architecture is a blend of the advantages of series and parallel type hybrid power-train architecture. It usually consists of a mechanical or electrical power split device. Planetary gears are typically used as mechanical power split device while the power electronics itself is used as electrical power split device. An example of series-parallel hybrid power-train architecture involving planetary gear is the Toyota hybrid system (THS) generation II which is shown in figure 3.1. The working of the Toyota hybrid system will be presented in chapter 3.

As the name suggests, the series-parallel hybrid power-train architecture can be operated as either series or parallel or series-parallel type architecture. In this type of architecture, the engine speed can be made independent of the vehicle speed and at the same time provide power boost from the battery. The planetary gear set splits the power from the engine into an electrical and mechanical path. The power flow through the electrical path can be used to either charge the battery or propel the vehicle. Therefore, this type of architecture operates the engine at higher efficiency points when compared to parallel architecture. However, the efficiency of the whole power train is not necessarily high.

In this type of architecture the sizing of the prime movers directly connected to the planetary gear is interdependent. That is, for example in figure 3.1, the sizing of MG1 is dependent on the engine rated speed and torque.

## 2.4 Plug-in Hybrid Electric vehicle (PHEV)

The power train architecture of a PHEV is usually the same as that of hybrid architecture explained in section 2.1, 2.2 and 2.3, except that the energy storage capacity of the battery in a PHEV is much larger than that in a HEV. This enables the PHEV to run in pure electric mode for a certain distance, say about 20-60 km and then function as a HEV when the battery is depleted, thus maintaining the charge level in the battery at minimum level until the end of the journey. The battery in a PHEV can be charged on board using the ICE (during HEV operation) but is intended to be charged as much as possible through a charging cable which can be plugged into household outlet or industrial grid. The bigger the battery, the higher the flexibility for efficient energy control.

### 3 Current state of art in Hybrid power-trains

This section will explain the current state of art in hybrid power-trains within the strong/full hybrid power-train classification. Only the power-trains with transverse front wheel drive will be discussed in this report.

#### 3.1 Toyota hybrid system (THS)

Toyota entered the hybrid market in 1997 by the name Toyota hybrid system (THS or THS I<sup>st</sup> generation) used in the 'P111' transaxle which was installed in Toyota Prius. Later in 2003-04, they developed THS-II generation in 'P112' transaxle having the same power train architecture as that of the THS-I generation but with improvements of the individual components leading to major improvements in the performance and fuel economy [18], [17]. THS-II generation and further architectures are marketed as HSD (Hybrid synergy drive) in order for Toyota to be able to use the hybrid technology outside the Toyota brand such as Lexus, highlander etc. From 2004 onwards, various versions of HSD have evolved with improvements/modifications to the base line THS-II design to match the different classes of vehicles for example LHD (Lexus hybrid drive) in 2006 installed in Lexus LS600hL for luxury cars [9].

##### 3.1.1 THS-II Architecture and working principle

The power-train hybrid architecture used in THS-II generation is of series-parallel hybrid architecture with one simple planetary gear set, two motor-generator unit, one battery and power electronics. The system architecture of THS-II generation is shown in figure 3.1.

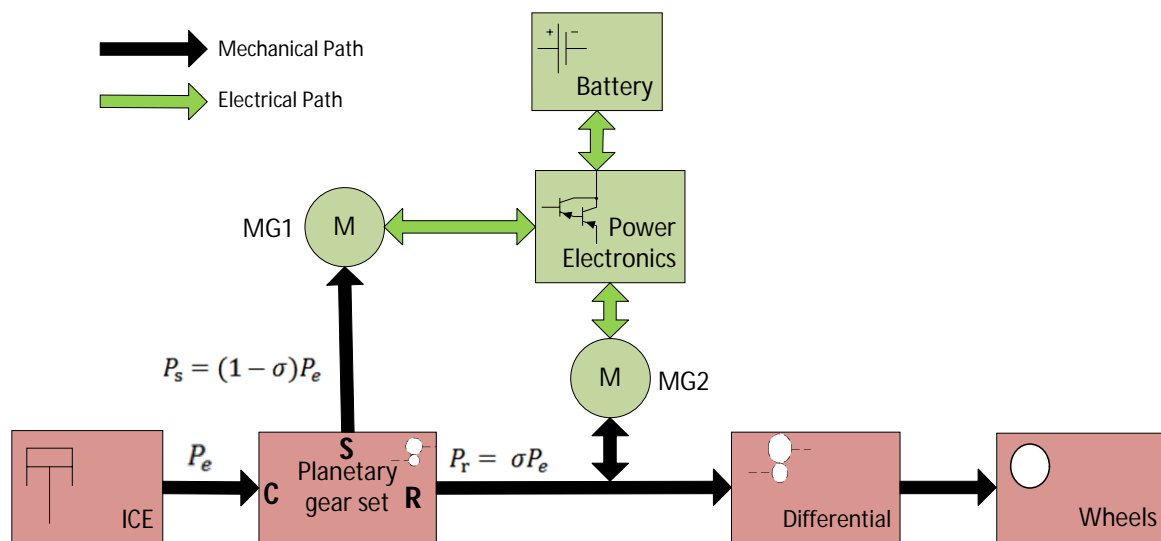


Figure 3.1: A power flow view of THS-II generation power-train architecture. C= carrier gear shaft, S = sun gear shaft, R= ring gear shaft.

The key component in THS design is the simple planetary gear which splits the engine power into mechanical and electrical path. The carrier, sun and the ring gear of the simple planetary gear set are connected to the engine, MG1 and MG2 respectively. The MG2 is mounted on a common shaft which is in turn connected to the wheels through the differential. A more exact mechanical view is shown in figure 3.2.

This type of hybrid power-train architecture enables to control the engine speed by controlling the MG1 speed. Thus the engine can be operated at its most efficient operating point irrespective of the vehicle speed. The power flow coming out of the engine is split into mechanical and electrical path via the planetary gear set (refer figure 3.1). The amount of power-split is determined by the dimensionless term called the 'Separation factor',  $\sigma$ , as introduced in [13].  $\sigma$  times the engine output ( $P_e$ ) flows mechanically through the ring gear shaft ( $P_r$ ) while  $1 - \sigma$  times the engine output flows mechanically to MG1 where it is converted to electrical energy as given by equations :-.

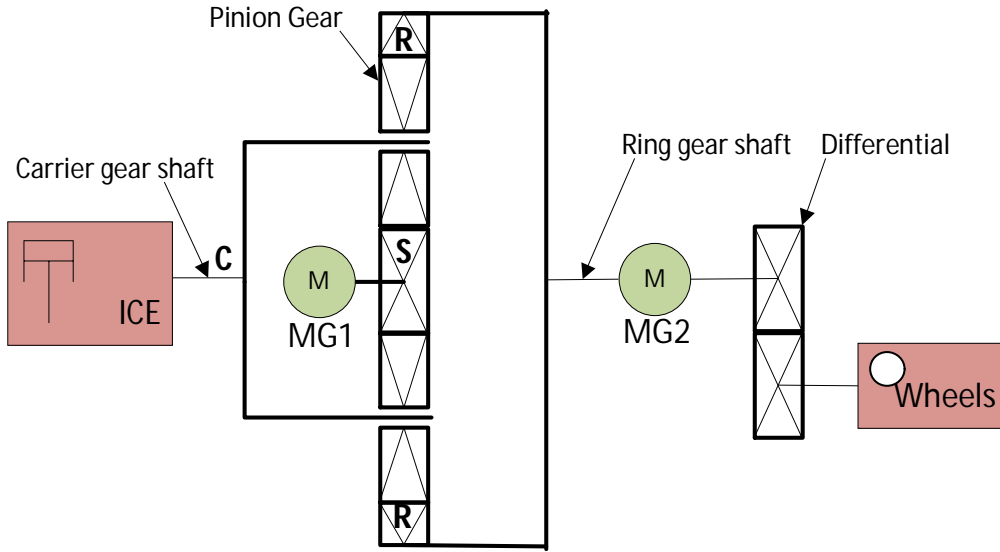


Figure 3.2: Mechanical view of THS-II generation power-train architecture. Note, battery, power electronics and electrical connection between the motor-generator units are not shown for clarity. C= carrier gear shaft, S = sun gear shaft, R= ring gear shaft.

$$P_r = \sigma P_e \quad (3.1)$$

$$P_s = (1 - \sigma)P_e \quad (3.2)$$

The separation factor determines the amount of power output of the engine flowing through electrical path and mechanical path. It depends on the vehicle velocity ( $v$ ), engine speed ( $w_e$ ), differential gear ratio ( $\gamma_{diff}$ ), radius of the wheel ( $R_w$ ) and the characteristic ratio of the simple planetary gear set ( $\rho$ ). It is defined as

$$\sigma = \frac{\gamma_{diff}}{(1 + \rho)R_w} \left( \frac{v}{w_e} \right), \quad \forall (0 \leq \sigma \leq \sigma_{max}(v)) \quad (3.3)$$

Since there are limits to the engine speed, there will be upper and lower limits for separation factor at each particular vehicle velocity. In other words, for each vehicle velocity there exists a range of separation factor whose limits are determined by the engine idling speed and maximum engine speed.

To understand the working principle, like in all analysis, let's assume there is no loss during the power transfer through the planetary gears, then, power through the sun gear shaft is the input to the generator and power through the ring gear shaft is the input to the differential. Depending on the value of the separation factor there are four possible modes of operation, they are:

1.  $\sigma = 0$ ; When the separation factor is zero, the entire power output of the engine flows mechanically to MG1 where it is converted to electrical energy and finally flows into the battery (refer figure 3.1). Here the entire system is essentially functioning as a series hybrid vehicle. Note from equation 3.3, the separation factor can be zero only when the vehicle velocity is zero. Therefore the entire system can function as a series hybrid only during stand still.
2.  $1 > \sigma > 0$ ; Here the system is functioning as a series-parallel hybrid, splitting the engine output power into electrical and mechanical path.  $\sigma$  times the engine output ( $P_e$ ) flows mechanically through the ring gear while  $1 - \sigma$  times the engine output, flows electrically through MG1 (refer figure 3.1).
3.  $\sigma = 1$ ; Here the system is functioning such that all the power output of the engine flows only through mechanical path to the wheels (refer figure 3.1). The sun gear shaft speed or the MG1 speed is zero when  $\sigma = 1$ . During this mode, the engine speed is no longer independent of the vehicle speed, that is, there is a fixed ratio between the engine speed and vehicle speed similar to a single speed gear train.
4.  $1 < \sigma \leq \sigma_{max}(v)$ ; This mode is when the separation factor is greater than one but less than the maximum separation factor possible for that particular vehicle velocity. In this mode, the functioning of the MG

units are reversed, that is, MG2 which is usually functioning as a motor, will operate as a generator and sends the energy to the MG1 (which is usually functioning as a generator) now functioning as a motor and adds the energy to the planetary gear set. This results in circulation of part of the energy through electrical path. This mode is essentially a part of the THS design, however, it leads to low efficiency of the power-train and is mostly avoided.

The ECVT action of THS-III power-train can be used only when either  $1 < \sigma \leq \sigma_{max}(v)$  or when  $1 > \sigma > 0$ . When  $1 > \sigma > 0$  part of the engine output flowing through the electrical path encounters the double energy conversion loss. When  $1 < \sigma \leq \sigma_{max}(v)$ , along with the double energy conversion loss there exist transmission losses caused by circulation of energy. Hence the fuel economy benefit of the ECVT transmission comes at the expense of double energy conversion loss and loss of energy due to circulation.

Overall, it looks like the series-parallel hybrid power-train architecture has lot of flexibility in choosing the operation mode, but the choice of operating mode that can be made considering the fuel consumption is less which is discussed in detail in section 7. For more information about the working of THS-II the reader is advised to refer to [13] and [15].

Apart from the above four modes which depends on the separation factor, it is also possible to drive the vehicle by simultaneously or separately using the stored energy from the battery which will make the vehicle essentially function as pure electric vehicle or parallel hybrid vehicle. For example, with the separation factor equal to one ( $\sigma = 1$ ) and the battery powering the motor, the system will work as parallel hybrid.

### 3.1.2 THS-III Architecture and working principle

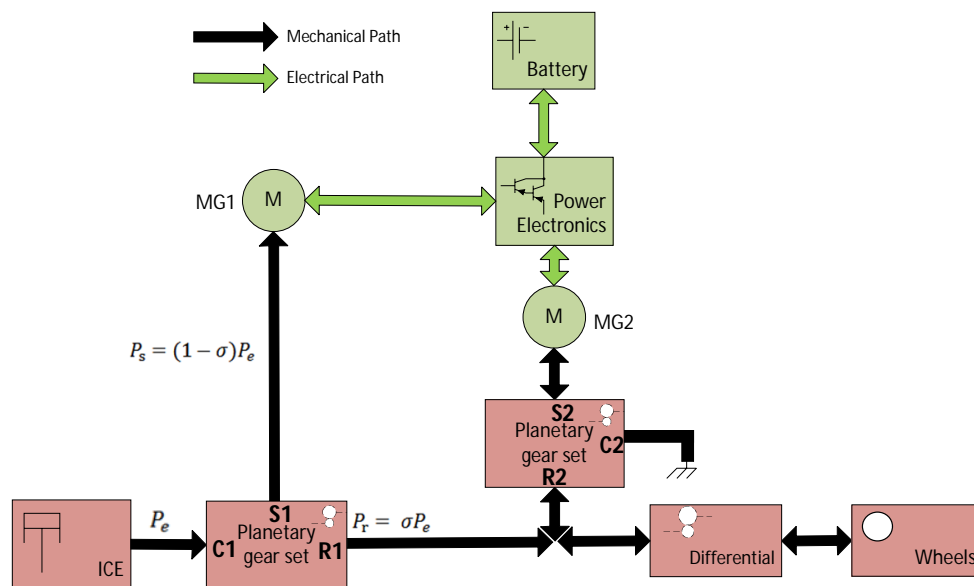


Figure 3.3: Power flow view of THS-III hybrid power-train architecture. C= carrier gear shaft, S = sun gear shaft, R= ring gear shaft.

The working principle of THS-III generation is similar to that of THS-II generation except that in THS-III generation, an additional planetary gear set is used in between the MG2 and rest of the system. The P410 transaxle uses THS-III design [17]. The system architecture of THS-III generation is shown in figure 3.3. A more exact mechanical view is shown in figure 3.4.

Besides the addition of second planetary gear set, the maximum speed rating of the MG is increased and the differential gear ratio is changed [17].

The carrier gear of the second planetary gear set is braked which gives a fixed single speed gear ratio between the sun and the ring gear of second planetary gear set. This Fixed ratio has two functions, a) It decreases the relative speed between the two motor-generator unit and b) It multiplies the torque output of the MG2 going to the wheels, hence a small and cheaper MG2 can be used.

The top speed capability in THS-III in electric mode is increased which can be attributed to the increase in speed operating range of the MG units and by the addition of second planetary gear set.

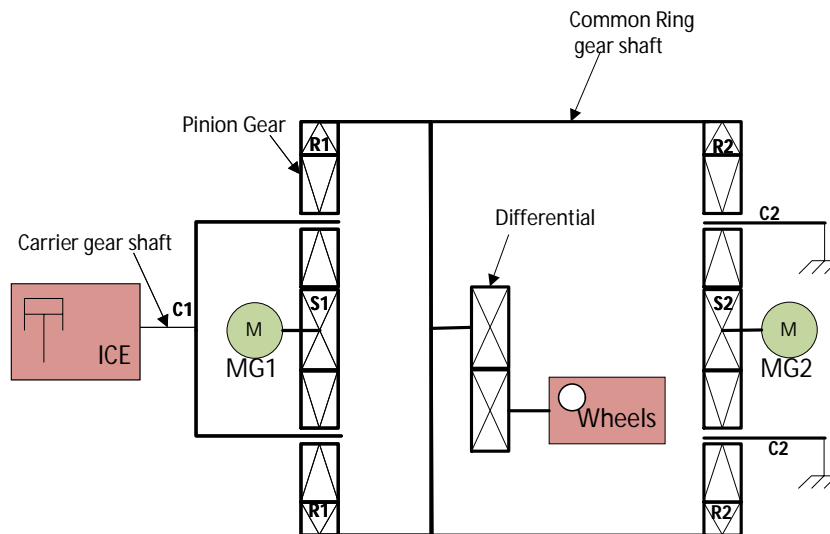


Figure 3.4: Mechanical view of THS-III generation power-train architecture. Note differential, battery, power electronics and electrical connection between the MGs are not shown for clarity. C= carrier gear shaft, S = sun gear shaft, R= ring gear shaft.

### 3.1.3 Constraints on Engine and MG1 (generator) speed for THS-III

As discussed in section 3.1.1, for each vehicle velocity there exists a range of separation factor determined by the engine speed. The limits of the separation factor for a particular vehicle speed is determined by the engine idling speed and maximum engine speed. The thick black line in figure 3.5 which is drawn using equation 3.3 indicates the separation factor limit line for range of vehicle velocities. Point 'a' (see bottom right corner of the graph) indicates the maximum speed achievable in pure electric mode. Unlike in THS-II where the top speed in electric mode is limited by the maximum speed of the MG1, in THS-III the top speed in electric mode is limited by the maximum speed of the MG2. This improvement in top speed can be attributed to the addition of second planetary gear having a single fixed gear ratio, and the increase in speed range of the MGs.

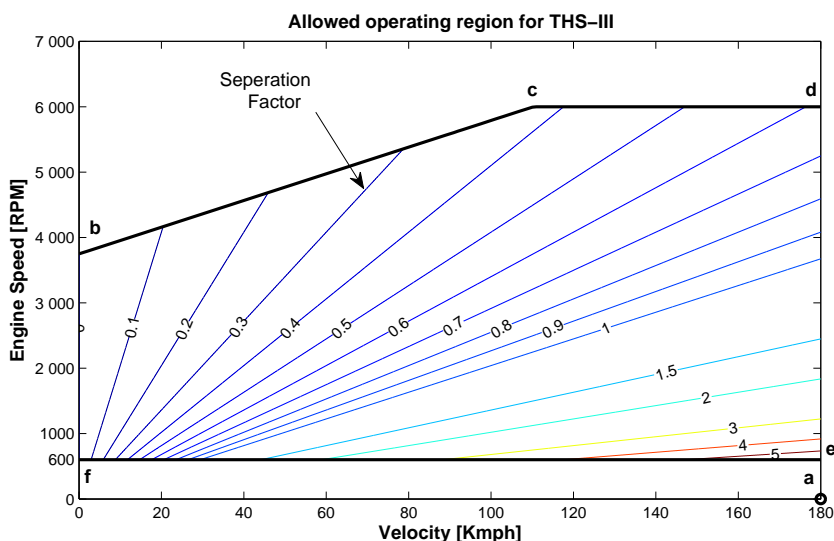


Figure 3.5: Allowed operating region for THS-III with separation factor

An alternate view of the allowed operating region of the engine as a function of MG1 speed is shown in figure 3.6, which is drawn using equation 3.4. It also indicates the engine speed that can be obtained by controlling the generator speed for various vehicle velocity. The power-train parameters used to draw the figure 3.6 and 3.5 is given in appendix A.

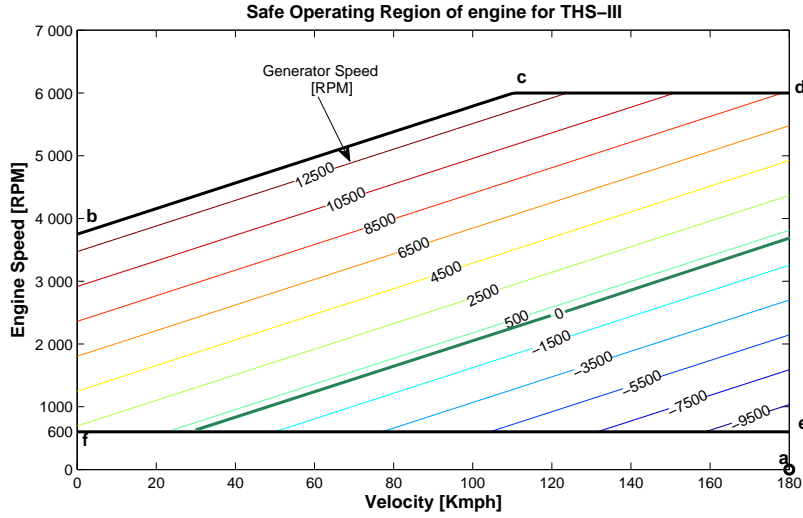


Figure 3.6: Allowed operating region for THS-III with generator speed (RPM)

$$\text{Generator speed, } w_g = \frac{v\gamma_{diff}}{\rho R_w} \left[ \frac{1}{\sigma} - 1 \right] \quad (3.4)$$

- X-axis represents pure electric vehicle operation.  $w_e = 0$
- Y-axis represents pure series hybrid vehicle which will only occur at stand still.
- Point 'a' indicates the top speed achievable in pure electric mode.
- Line 'bc' represents the upper limit on the MG1 speed.
- Line 'cd' represents the upper limit on the engine speed.
- Line 'de' represents the upper limit on the MG2 speed.
- Line 'ef' represents the lower limit on the engine speed. (engine idle speed)

The area 'bcdef' represents the series-parallel operation except at the line where generator speed is zero. Generator speed equal to zero line in figure 3.6 corresponds to separation factor equal to one line in figure 3.5. This line indicates that the entire power flow from the engine to the wheels flows through the mechanical path.

The size of the MG2 depends on the performance requirement of the vehicle. The size of the MG1 is dependent on the engine torque and speed (given by equations 3.4, 3.3 and 3.5), hence it cannot be independently sized.

$$\frac{T_e}{T_{MG1}} = \frac{1 + \rho}{\rho} \quad (3.5)$$

where,

$T_e$  = Torque of engine.

$T_{MG1}$  = Torque of MG1.

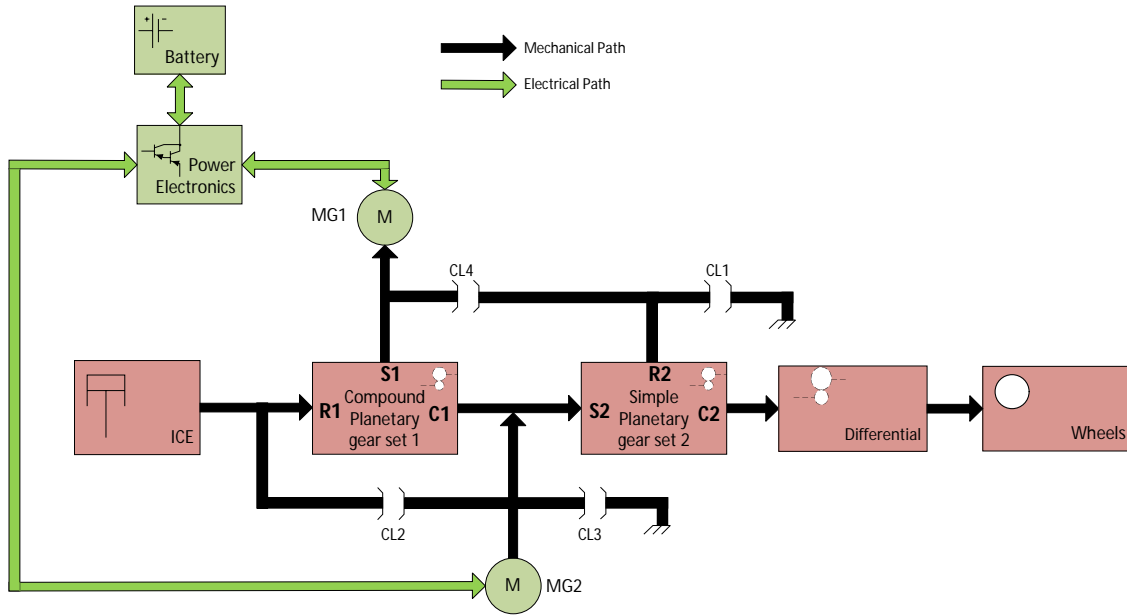


Figure 3.7: Power flow view of the GMs '2MT70' power-train architecture. Modified and redrawn from [13]. C= carrier gear shaft, S = sun gear shaft, R= ring gear shaft.

## 3.2 General Motors two mode hybrid system

General motors (GM) have developed various version of single and two mode hybrid. The first production of the two mode hybrid was for transit buses in 2003. From then on various versions of two mode hybrid are developed to suit different classes of vehicles [6]. The two mode hybrid developed by General motors for transverse front wheel drive called the '2MT70' will be briefly discussed below.

### 3.2.1 General Motors '2MT70', Architecture and working principle

The power-train architecture of the GMs '2MT70' is a more complex version of the series-parallel hybrid power-train architecture. It consists of two planetary gear set (one compound and one simple planetary gear set), two motor-generator unit, two transfer clutches, two brake clutches, power electronics and battery [7]. The system architecture of GMs '2MT70' is shown in figure 3.7. A more exact mechanical view of the connection of the parts is shown in figure 3.8 which depicts a quarter sectional view of the transmission.

The output of the ICE is connected to the ring gear (R1) of the Compound planetary gear set. The ring gear (R2) of the simple planetary gear set and the generator is connected to the sun gear (S1) of the compound planetary gear set. The sun gear (S2) of the simple planetary gear set and the motor is connected to the carrier shaft (C1) of the compound planetary gear set. The carrier shaft (C2) of the simple planetary gear set is connected to wheels through differential.

CL1 is a brake clutch which brakes the ring gear (R2) of the simple planetary gear set. CL2 is transfer clutch which locks the compound planetary gear set for rotation. CL3 is a brake clutch which brakes the sun gear (S2) of the simple planetary gear set. CL4 is a transfer clutch which locks the sun gear S1 of the compound planetary gear set and ring gear R2 of the simple planetary gear set for rotation.

The number of components in THS-II is less which makes it easy to be packaged in a transverse front wheel drive. The number of components in '2MT70' is more when compared to THS-II. The electric machines in '2MT70' have large internal diameter which enables them to be mounted over the planetary gear set thus allowing them to be packaged in transverse front wheel drive vehicles [7].

GMs '2MT70' has two ECVT modes, one for lower speed range and another for higher speed ranges for better efficiency. In addition, it has four fixed gear ratios which provides better towing capabilities than THS-III power-train. By applying either clutch CL1 or CL4 individually will provide two ECVT modes, whereas

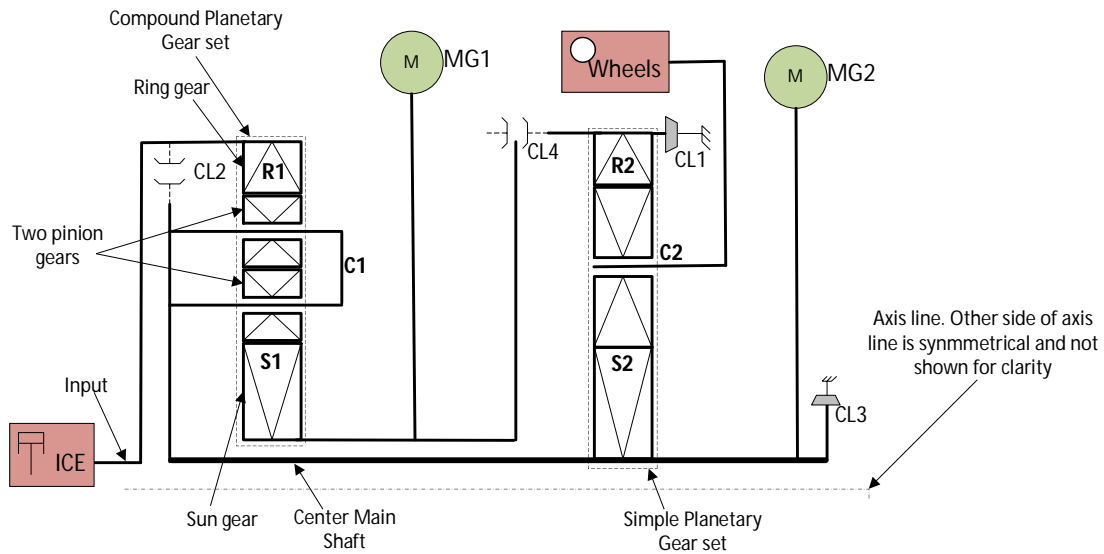


Figure 3.8: Mechanical view of the GMs '2MT70' power-train architecture. Note differential, battery, power electronics and electrical connections between the motor-generator unit are not shown for clarity. Modified and redrawn from [7]. C= carrier gear shaft, S = sun gear shaft, R= ring gear shaft.

Table 3.1: Clutch selection for different operating modes

Modes/Clutch	CL1	CL2	CL3	CL4
ECVT mode 1	on	off	off	off
1st gear	on	on	off	off
2nd gear	on	off	off	on
ECVT mode 2	off	off	off	on
3rd gear	off	on	off	on
4th gear	off	off	on	on

operating specific combination of four clutches (CL1, CL2, CL3, and CL4) will lead to four fixed gear ratio. The clutch combination which leads to different modes is shown in table 3.1.

**ECVT mode-1:** By operating the brake clutch CL1, ring gear R2 of the simple planetary gear is held stationary. The power flow from the ICE to the output is from C1 to S2 through the main centre shaft of the transmission as indicated by the cyan colour line in figure 3.9. The ECVT mode operation is possible by controlling the speed of motor-generator 1 which is connected to the sun gear S1 of the compound planetary gear, thus allowing the engine to be operated at its efficient operating point. When the engine is switched off, electric motor can be used to drive the vehicle allowing it to function as a pure electric vehicle. Also, both electric motor and ICE can be used to drive the vehicle. The ECVT Mode-1 in '2MT70' is very much similar to the single ECVT mode of THS-III.

**ECVT mode-2:** By disengaging the brake clutch CL1 and engaging the transfer clutch CL4, the sun gear S1 of the compound planetary gear is locked to ring gear R2 of the simple planetary gear and thus ECVT mode-2 is activated. The power flow is through 2 paths, one is through S1-R2 and the other is through C1-S2 as indicated by the cyan colour line in figure 3.9. It is possible to operate as pure electric vehicle and also as parallel hybrid in ECVT mode-2. By controlling the speed of either of the motor-generator unit, the engine speed can be controlled. The reader is directed to refer [14], [15] for more information.

**Fixed gear 1:** By engaging the brake clutch CL1 and transfer clutch CL2, first gear ratio is achieved. By activating Clutch CL2 the compound planetary gear is locked and rotates as a single unit. The power flow is through C1 to S2 through the main centre shaft of the transmission as indicated by the cyan colour line in figure 3.9.

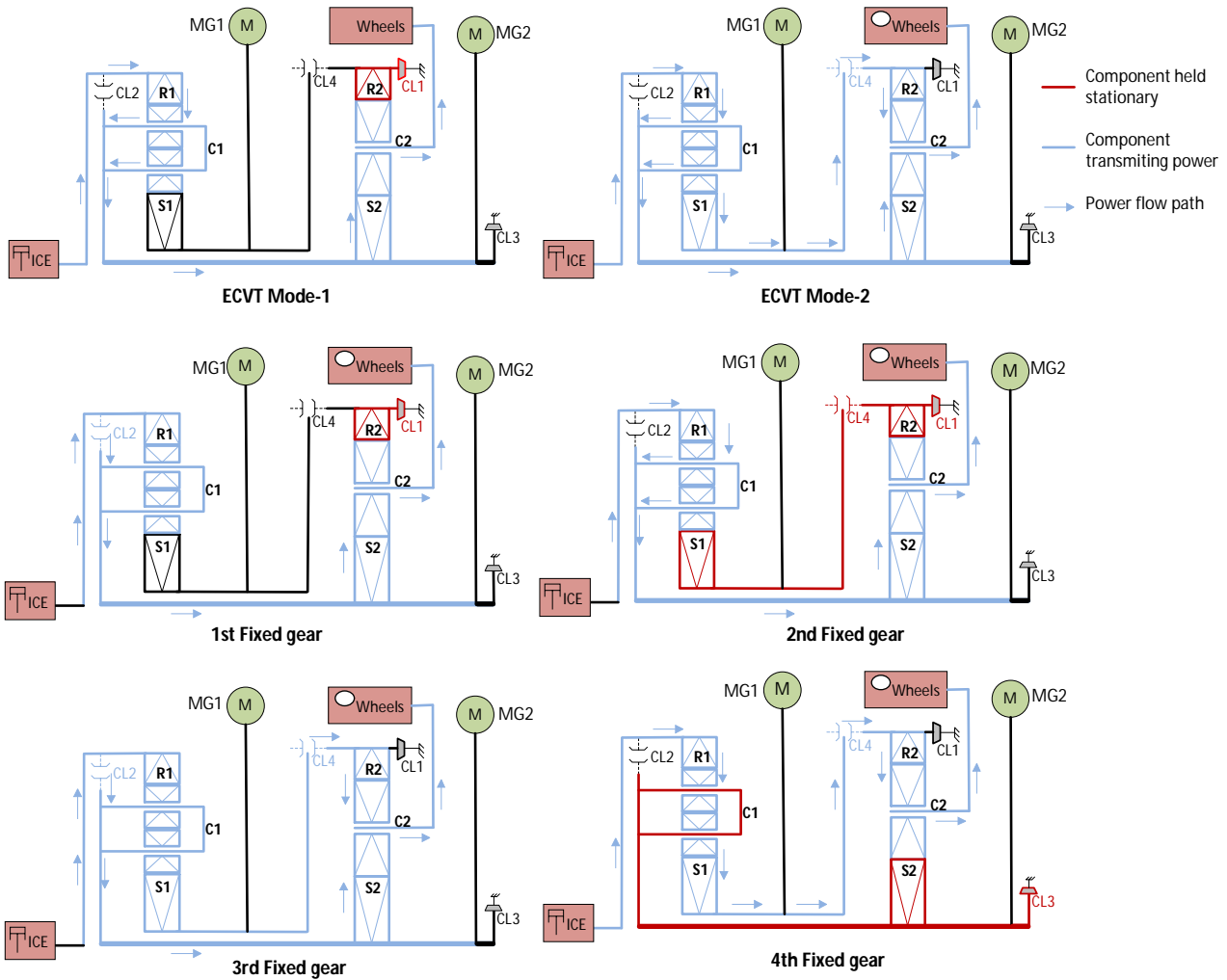


Figure 3.9: Mechanical view of different modes in GMs '2MT70' power-train architecture. Note: Battery, power electronics and connection between motor-generator units are not shown for clarity. C= carrier gear shaft, S = sun gear shaft, R= ring gear shaft.

**Fixed gear 2:** By engaging brake clutch CL1 and transfer clutch CL4, second gear ratio is achieved. Sun gear S1 of compound planetary gear is locked to ring gear R2 of the simple planetary gear through transfer clutch CL4 and then braked via brake clutch CL1. The power flow is through C1 to S2 through the main centre shaft of the transmission as indicated by the cyan colour line in figure 3.9.

**Fixed gear 3:** By engaging the transfer clutches CL2 and CL4, third gear is achieved. Clutch CL2 locks the compound planetary gear set and makes it to rotate as a single unit. Clutch CL4 locks the sun gear S1 of the compound planetary gear set and ring gear R2 of the simple planetary gear. Now since the speed of sun gear S1 is equal to the speed of the compound planetary gear set, both the planetary gear set locks and rotates as a single unit thus achieving direct drive with gear ratio 1 as indicated in figure 3.9

**Fixed gear 4:** By engaging the brake clutch CL3 and transfer clutch CL4, fourth gear is achieved. The power flow is through S1-R2 as indicated by the cyan colour line in figure 3.9.

In all the above mentioned fixed gear, the engine output flows through mechanical path and no power flows electrically through the motor-generator units. Therefore either or both the motor-generator units can be used in conjunction with the engine to power the vehicle thus obtaining parallel hybrid functionality depending on the activation/dis-activation of the brake clutches (CL1 and CL4).

### 3.2.2 Constraints on engine speed and motor-generator units speed

Similar to THS-III, there exists specific range of separation factor for particular vehicle velocity beyond which the generator will reach an over speeding condition. Reference [15] introduces the dimensionless term called the separation factor for each ECVT mode of GMs '2MT70'. These separation factor governs the power split between the mechanical and electrical paths.

By using equation 3.6 to 3.13 the allowed operating region of GMs '2MT70' is redrawn from [15] and is shown in figure 3.10.

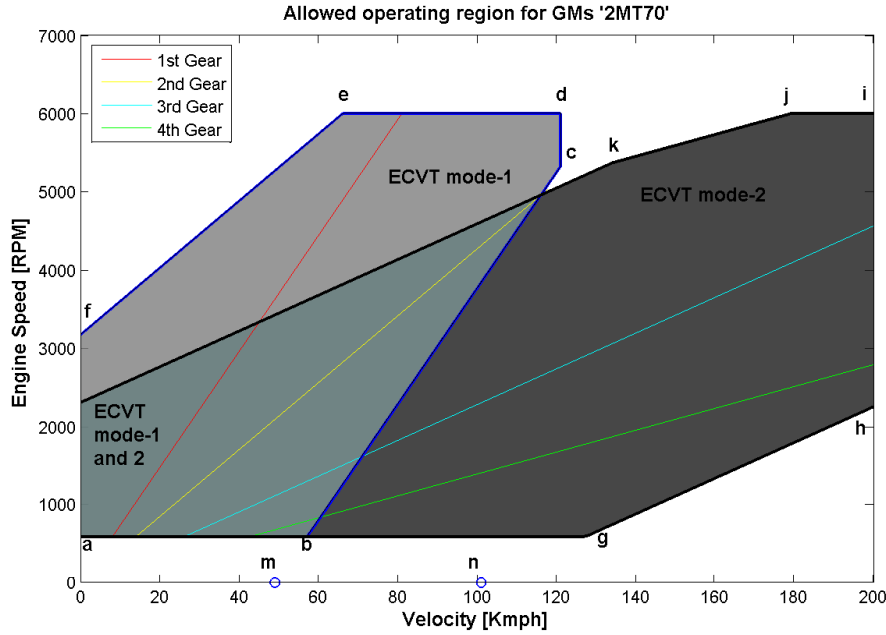


Figure 3.10: Allowed operating region for GMs '2MT70' power-train architecture. Redrawn from [15]

The separation factor for ECVT mode-1 ( $\sigma_1$ ) and ECVT mode-2 ( $\sigma_2$ ) are given by

$$\sigma_1 = \frac{(1 - \rho_1)(1 + \rho_2)\gamma_{diff}}{\rho_2 R_w} \left( \frac{v}{w_e} \right) \quad (3.6)$$

$$\sigma_2 = \frac{1 - \rho_1}{1 - \rho_1 - \rho_1 \rho_2} \left[ 1 - \frac{\rho_1(1 + \rho_2)\gamma_{diff}}{R_w} \left( \frac{v}{w_e} \right) \right] \quad (3.7)$$

The speed of motor-generator 1 in ECVT mode-1 ( $w_{g1}$ ) and mode-2 ( $w_{g2}$ ) and speed of motor generator 2 in ECVT mode-1 ( $w_{m1}$ ) and ECVT mode-2 ( $w_{m2}$ ) are given by

$$w_{g1} = \frac{w_e}{\rho_1} (1 - \sigma_1) \quad (3.8)$$

$$w_{g2} = \frac{w_e}{\rho_1} (1 - \sigma_2) \quad (3.9)$$

$$w_{m1} = \frac{\sigma_1}{(1 - \rho_1)} w_e \quad (3.10)$$

$$w_{m2} = \frac{\sigma_2}{(1 - \rho_1)} w_e \quad (3.11)$$

Speed of the pinion gear of compound planetary gear touching the sun gear in ECVT mode-1 ( $w_{pin_1}$ ) and

mode-2 ( $w_{pin_2}$ ) are given by

$$w_{pin_1} = \frac{N_{s_1}}{N_{P1S}} \frac{w_e}{\rho_1(1-\rho_1)} [1 - \rho_1 - \sigma_1] \quad (3.12)$$

$$w_{pin_2} = \frac{N_{s_1}}{N_{P1S}} w_e \left[ \frac{1}{\rho_1(1-\rho_1-\rho_1\rho_2)} - \frac{\sigma_2}{\rho_1(1-\rho_1)} - \frac{1+\rho_2}{1-\rho_1-\rho_1\rho_2} \right] \quad (3.13)$$

Where,

$\rho_1$  = Characteristic ratio of compound planetary gear.

$\rho_2$  = Characteristic ratio of simple planetary gear.

$N_{s_1}$  = Number of teeth on sun gear of compound planetary gear.

$N_{P1S}$  = Number of teeth on the pinion gear touching the sun gear in compound planetary gear.

- Area 'a-b-c-d-e-f-a' indicates ECVT mode-1 allowed operating region (Refer figure 3.10).
- Area 'a-c-g-h-i-k-a' indicates ECVT mode-2 allowed operating region.
- Line 'a-b and 'a-g' represents the lower limit on engine speed (idling speed) in ECVT mode-1 and ECVT mode-2 respectively.
- Line 'b-c' and 'g-h' represents the lower limit on the pinion gear speed of compound planetary gear which is touching the sun gear in ECVT mode-1 and ECVT mode-2 respectively. Note, lower limit of the pinion gears here means the limiting speed in the opposite direction.
- Line 'c-d' and 'j-k' represents the upper limit on the speed of the motor in ECVT mode-1 and ECVT mode-2 respectively.
- Line 'd-e' and 'i-j' represents the upper limit on engine speed in ECVT mode-1 and ECVT mode-2 respectively.
- Line 'e-f' and 'k-l' represents the upper limit on generator speed ECVT mode-1 and ECVT mode-2 respectively.
- Line 'h-i' represents the maximum vehicle speed. Here it is assumed to be 200 kmph.
- Point 'm' represents the maximum vehicle speed possible in ECVT mode-1 in pure electric mode.
- Point 'n' represents the maximum vehicle speed possible in ECVT mode-2 in pure electric mode. Beyond point 'n' the engine has to be turned on in order to avoid over speeding condition in the pinion gears.

An alternate figure showing the allowed operating region in both the ECVT modes as a function of separation factor and generator speed are shown in figure 3.11. The power-train parameters used to draw the figure 3.11 and 3.10 is given in appendix B.

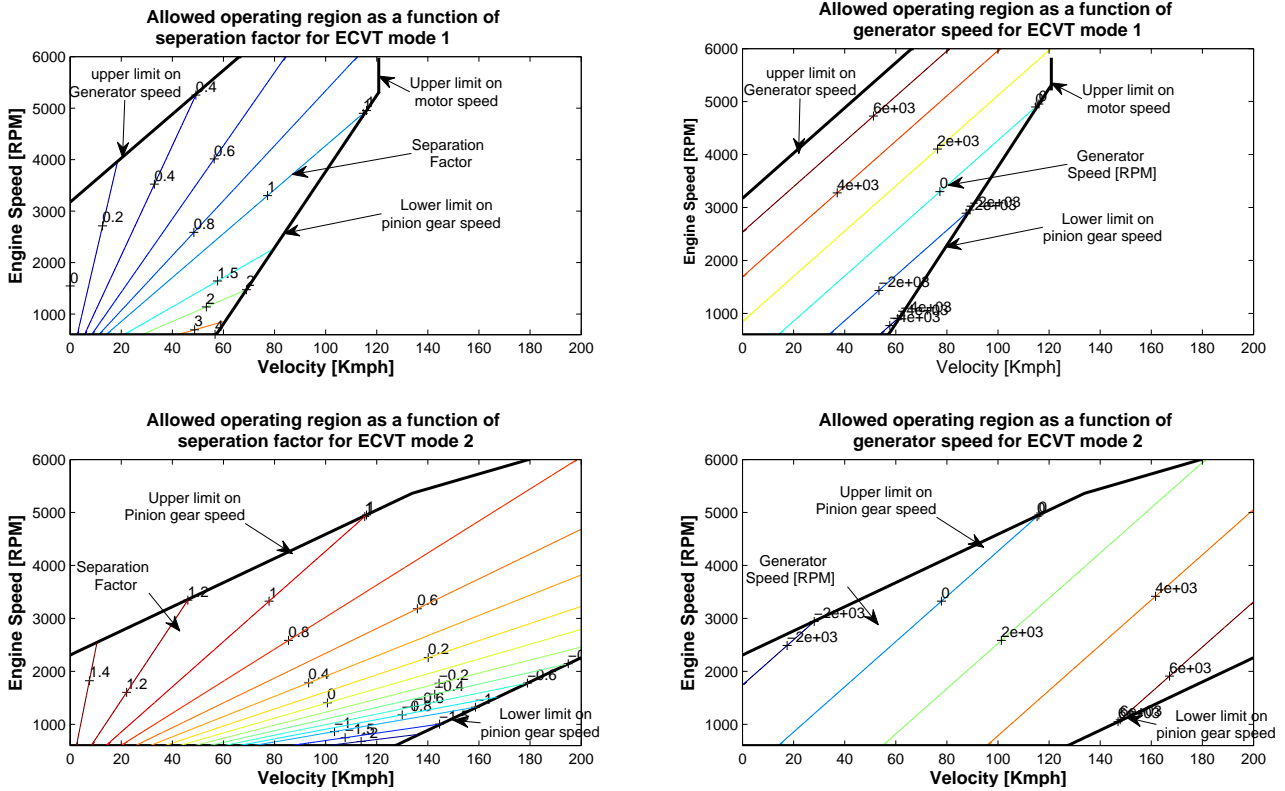


Figure 3.11: Allowed operating region for GMs '2MT70' power-train architecture as a function of separation factor and generator speed. Redrawn from [15]

### 3.3 GMs 'Voltec-4ET50'

The 'Voltec-4ET50' is the transaxle design used in the Chevrolet volt and it is a modified version of the GMs '2MT70' design. Few of the main modifications from the GM 2MT70 relevant to arrangement of system components are removing of the compound planetary gear set and one brake clutch CL3. Voltec-4ET50 offers two electric vehicle (EV) drive modes and two extended range (ER) drive modes. One of the unique feature of voltec-4ET50 design is the two motor EV drive and the combined two motor ER drive which has better efficiencies over the conventional EV drives and series operation [16].

#### 3.3.1 'Voltec-4ET50' Architecture and working principle

The system architecture of 'Voltec-4ET50' resembles the series-parallel architecture similar to THS-II but the functionality is based on the series hybrid architecture. After the battery is depleted, the power from the engine along with one of the motor-generator unit together called the EGU is used to produce electricity which drives the motor-generator (functioning as a motor) connected to the wheels or feeds the battery. Therefore the Volt is also referred to as an extended range vehicle.

The system architecture of the 'Voltec-4ET50' transaxle is shown in figure 3.12. It consists of one simple planetary gear set, two motor-generator units, three clutch set, power electronic and a battery. Note the difference in connection of the components from that of THS-II (refer figure 3.1).

As mentioned earlier Voltec-4ET50 is a modified version of GMs 2MT70 design. The compound planetary gear set of GM 2MT70 design is removed. Clutch CL1 and CL4 are retained and serves identical functionality. Clutch CL2 is also retained but the functionality here is different. It is used to couple the ICE to the transmission during extended range (ER) operation. The motor-generator unit 2 (MG2) connected to the wheels is increased in size since it has to cater to the power demands and not the engine [16]. A more exact mechanical view is shown in figure 3.13.

Voltec-4ET50 has four modes of operation depending on the combination of the clutches used as shown in table 3.2

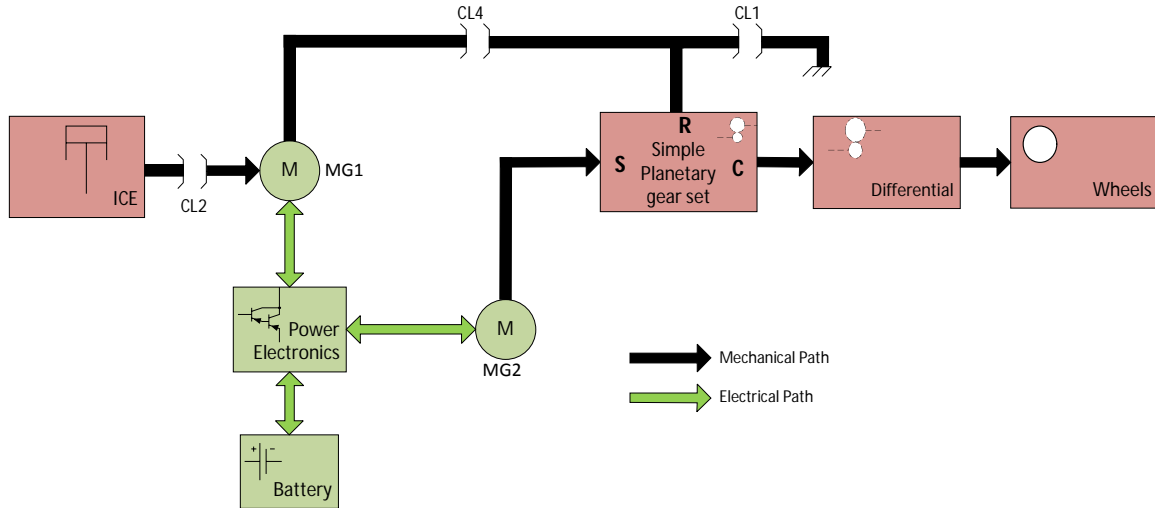


Figure 3.12: Power flow view of 'Voltec-4ET50' power-train architecture. C= carrier gear shaft, S = sun gear shaft, R= ring gear shaft.

Table 3.2: Clutch selection for different operating modes for Voltec-4ET50

Modes/Clutch	CL1	CL2	CL4
One motor EV operation	<b>On</b>	<i>off</i>	<i>off</i>
Two motor EV operation	<i>off</i>	<i>off</i>	<b>On</b>
One motor ER operation	<b>On</b>	<b>On</b>	<i>off</i>
Two motor ER operation	<i>off</i>	<b>On</b>	<b>On</b>

**One motor EV operation:** One motor EV operation mode is activated by engaging brake clutch CL1. In this mode, motor-generator 2 (MG2) alone is used to drive the vehicle. The power flows from MG2 to the wheels via the sun and the carrier gears of the simple planetary gear set. This mode is selected when the vehicle velocity is low.

**Two motor EV operation:** By disengaging brake clutch CL1 and engaging the transfer clutch CL4, Two motor EV operation is activated. In this mode both motor-generator units (MG1 and MG2) are used to drive the vehicle. The power flows from MG1 and MG2 to the wheels via the simple planetary gear set. This mode is selected when the vehicle velocity is high.

**One motor ER operation:** ER mode is used after the battery is depleted. One motor ER operation mode is activated by engaging the brake clutch CL1 and transfer clutch CL2. The engine and motor-generator 1 (MG1) together functions as EGU to produce electricity which is either stored in the battery or delivered to motor-generator 2 (MG2). This mode is selected when the vehicle velocity is low and the battery is depleted.

**Two motor ER operation:** Two motor ER operation mode is activated by engaging the transfer clutches CL2 and CL4. This mode is selected when the vehicle velocity is high and the battery is depleted.

The motor-generator units cannot be independently sized and are related by the equations 3.14 and 3.15 in the two motor EV and ER modes.

$$\frac{T_{MG2}}{T_{MG1}} = \rho \quad (3.14)$$

$$\frac{T_w}{T_{MG1}} = \gamma_{diff}(1 + \rho) \quad (3.15)$$

Where,  
 $T_{MG2}$ =Torque of MG2.

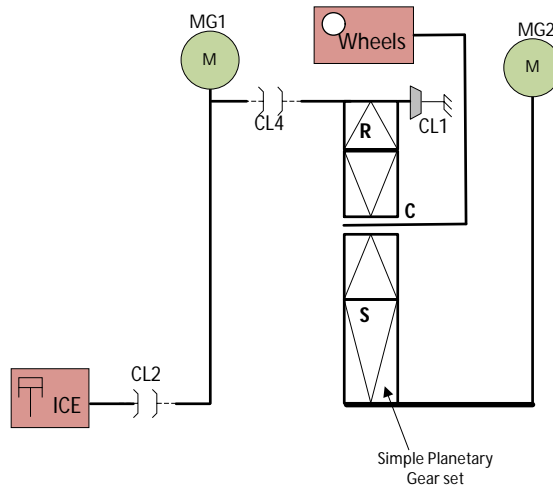


Figure 3.13: Mechanical view of 'Voltec-4ET50' power-train architecture. Note: Battery, power electronics and the connections between the motor-generator units are not shown for clarity. C= carrier gear shaft, S = sun gear shaft, R= ring gear shaft.

$T_{MG1}$ =Torque of MG1.

$T_w$ =Torque at the wheels.

$\rho$ = Characteristic ratio of simple planetary gear.

The variation of the motor-generator speed as a function of vehicle speed is shown in figure 3.14 which is based on equation 3.16.

$$\text{Vehicle velocity, } v = \frac{R_w}{\gamma_{diff}(1 + \rho)} (\rho w_{MG2} + w_{MG1}) \quad (3.16)$$

Where,

$w_{MG2}$ = Speed of MG2.

$w_{MG1}$ = Speed of MG1.

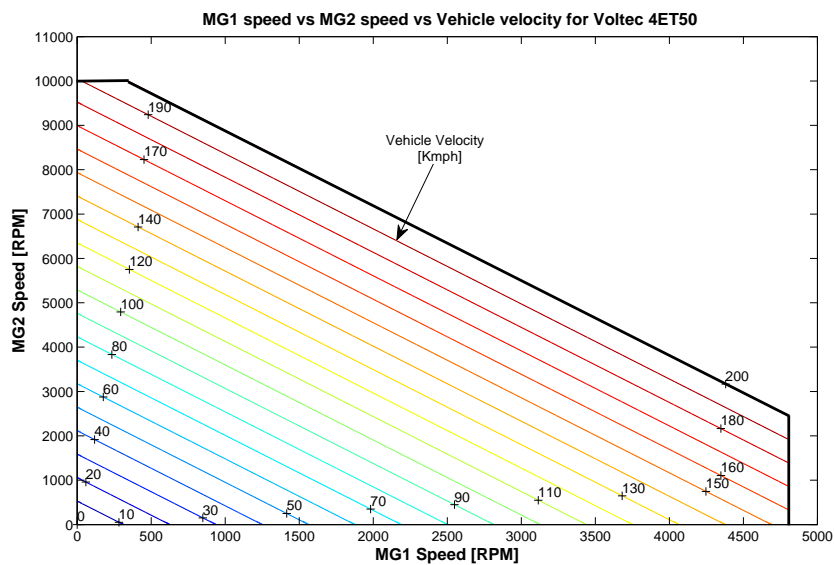


Figure 3.14: Motor-generator speed vs Vehicle velocity for Voltec-4ET50

### 3.3.2 Constrains on motor-generator speeds and engine speed for Voltec-4ET50 in ER mode only

Similar to THS-III, Voltec-4ET50 also has safe operating region in the extended range mode only which depends on the speed of the motor-generator units and engine. figure 3.15 shows the allowed operating region for ER mode drawn using equation 3.16. Note that in the EV mode the generator speed is not dependent on the engine speed since the clutch CL2 is open. The power-train parameters used to draw the figure 3.15 and 3.14 is given in appendix C

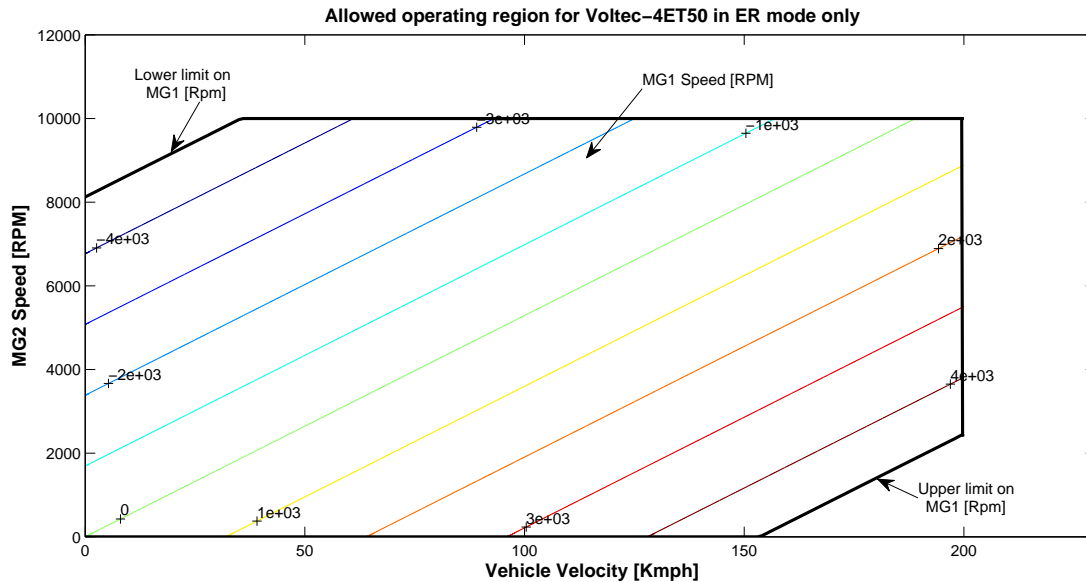


Figure 3.15: Allowed operating region for Voltec 4ET50 in ER mode

## 3.4 Hybrid dual clutch transmission

In this section a brief introduction to the conventional dual clutch transmission is presented first which is then extended to the hybrid version of dual clutch transmission.

### 3.4.1 Dual clutch transmission

Dual clutch transmission (DCT) technology was patented in 1940 and was applied in a truck that never went into production. It is later in 1980s, DCT came into limelight when Porsche demonstrated its performance in a race car. It is because of the high cost involved in its production it was not implemented in production cars. After overcoming all the hurdles, in 2003, BorgWarner and Volkswagen released it to production labelled as DSG (direct shifting gearbox).[12]

Few of the main advantage of DCT are, it has excellent response, excellent fuel efficiency, excellent shift and launch control without the requirement of a torque converter [12]. Due to the increase focus on fuel economy, there has been a growing demand for more fuel efficient replacement for the conventional automatic transmission with the torque converter. This has made DCT an attractive solution.

The Automotive sector in Japan is in favour of the ECVTs while the European automotive sector is in favour of the DCTs. Reference [12] suggests that one of the reasons the European market is sticking to DCT is because almost half of the European passenger car market is already covered with direct injection diesel engines and DCTs are flexible in that they can be easily adapted to both diesel and gasoline engines.

For simplicity, DCT can be considered as two lay shaft transmissions in one. Odd gears are connected to one shaft while the even gears are connected to the other. With the vehicle standing still the first gear is engaged. When the driver is ready to drive, clutch one is activated and the vehicle starts to move. While the vehicle still in gear 1 and moving, gear 2 is preselected. By disengaging clutch 1 and engaging clutch 2, the

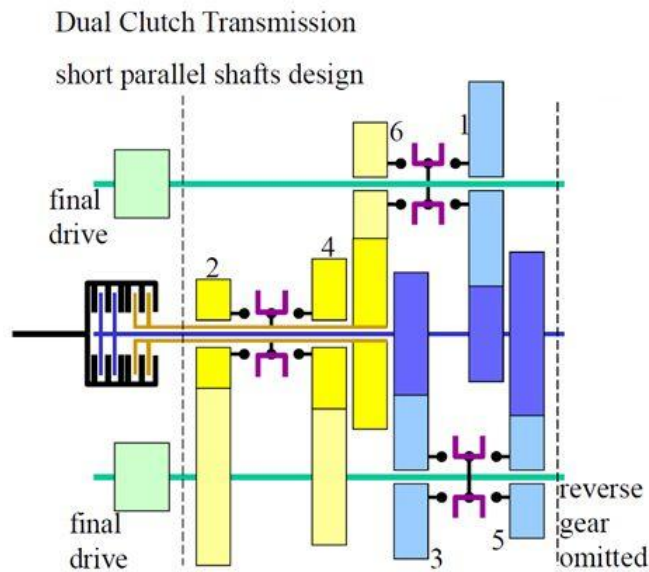


Figure 3.16: Schematic of Dual clutch transmission

vehicle is shifted to gear 2. This action provides a smooth shift with negligible power loss attributed only to slipping of clutch. Figure 3.16 shows the schematic of one of the versions of dual clutch transmission.

### 3.4.2 Hybrid Dual clutch transmission for PHEV

The DCTs have two input shafts. Therefore by connecting an electric machine on one of the shaft, a hybrid dual clutch transmission can be obtained. Getrag is one of the suppliers which produces a hybrid dual clutch transmission [5]. One motor-generator can be made to work both as a generator and motor thereby obtaining full hybrid functionality. In addition, a set of gear ratios are available in electric mode thus the size of the motor-generator unit can be made a little smaller.

#### Working principle of Hybrid dual clutch transmission

The system architecture of Hybrid dual clutch transmission (HDCT) is of a parallel hybrid type architecture. Unlike in ECVT operated hybrid vehicle, where the engine speed is independent of the vehicle speed, in HDCT the engine speed is dependent on the vehicle speed. The power-train consists of only one electric machine which can be made to operate both as generator and motor depending on the requirement. Clutch 1 is used for odd gears and clutch 2 is used for even gear. The electric machine is connected to one of the input shafts and can use 2, 4, 6 and reverse gear whereas the engine can use all the gears including the reverse gear. A schematic of the HDCT is shown in figure 3.17

For example, consider a driving scenario where the vehicle is accelerating from standing still. When the vehicle is standing still, second gear is preselected and motor is ready to drive the wheels by drawing power from the battery thus making the vehicle to operate in electric mode. While the vehicle still in second gear, any odd gear on the other shaft can be preselected. Let's assume third gear is preselected. When clutch 1 is closed both motor and engine will drive the vehicle without any power loss during shifting unlike in the conventional manual and automatic transmission.

When the vehicle is standing still, clutch 2 can be activated without selecting any gears on the output shaft thus charging the battery using the electric machine as a generator.

The engine can be used to charge the battery while the vehicle is moving via two paths. First path is when the engine is using odd gears to drive the vehicle. Some part of the engine output via the odd gears can be transmitted through the final drive to the motor-generator via one of the even gears. The second path is when the engine is using odd gears to drive the vehicle and some part of the engine output is directly transmitted

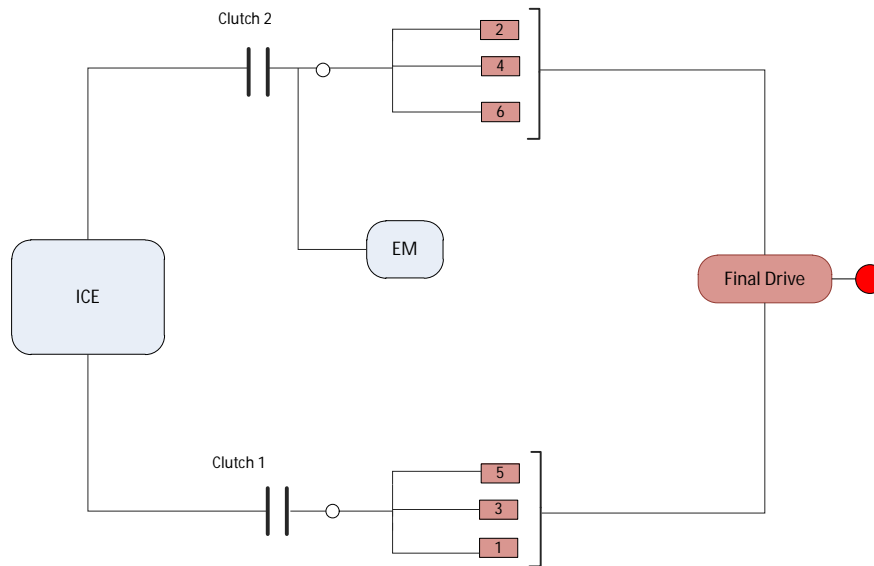


Figure 3.17: Schematic of Hybrid Dual clutch transmission. Complete arrangement of gears and synchronizers not shown for confidentiality reasons

via clutch 2 to the motor-generator. Note that non of the other even gears can be active while second path is active.

### Constraints on engine and motor-generator speed

$$w_{MG} = w_e \frac{\gamma_{MG}}{\gamma_e} \tag{3.17}$$

Where,

$\gamma_{MG}$ = Gear ratio used by MG.

$\gamma_e$ = Gear ratio used by engine.

An alternate view of figure 3.18 is shown in figure 3.19 and figure 3.20. As shown in figure 3.18 and figure 3.20 the 5-2 gear combination, that is, fifth gear used by the engine and second gear used by the motor, has a speed limit on the engine to be around 3800 rpm beyond which the motor-generator speed will exceed its maximum speed limit.

### Gear shifting in electric mode

Due to the good torque characteristic and high rated speed of the electric machine, there is essentially no requirement for a transmission during pure electric vehicle mode other than one fixed gear for appropriately sizing the electric machine[8]. Reference [19] shows that by using multi-speed gear box, the efficiency and performance can be further improved.

In HDCT design, the motor is located after the clutch and can use either 2nd, 4th or 6th gear. As mentioned earlier, a single gear can be used to avoid frequent shifting while in electric mode. However, to obtain better performance and efficiency, clutch-less gear shifting while in electric mode becomes inevitable even though less gear shifts may be sufficient. Also, unlike in the conventional dual clutch transmission, preselecting the gear is not possible during pure electric mode.

Many researches and on-road tests have been carried out to evaluate the shift quality and time for clutch-less gear shifting in different power-trains. Reference [2] describes a method used for clutch-less gear shifting in 2009 Saturn Vue hybrid power-train, where in a motor is used to synchronise the speed between the transmission

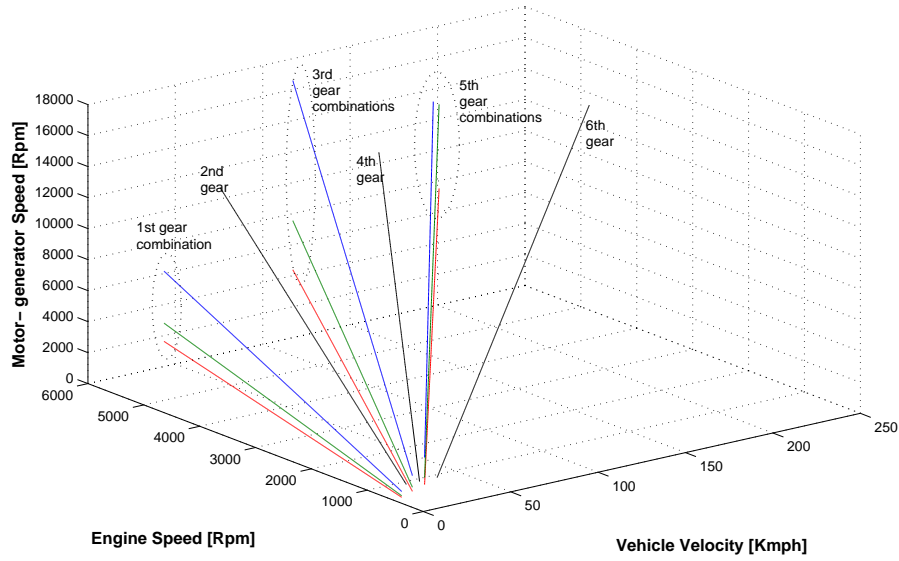


Figure 3.18: HDCT transmission plot; Possible combinations of engine, motor and vehicle speed

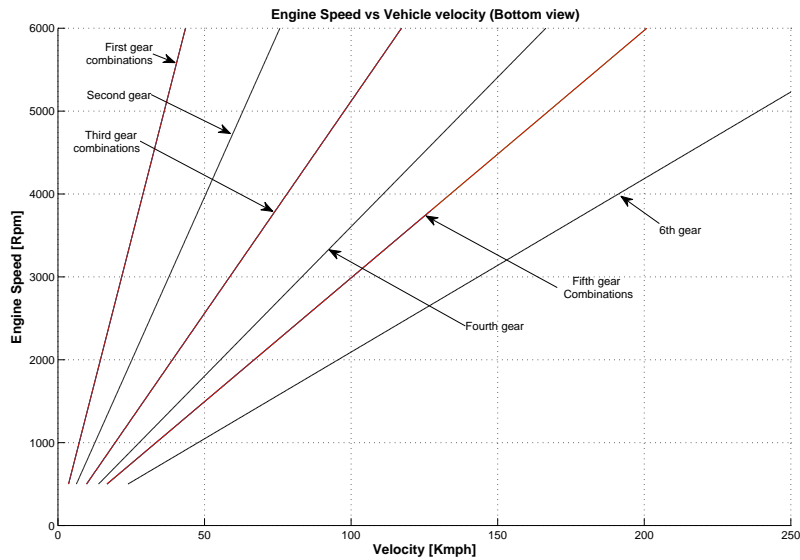


Figure 3.19: HDCT transmission plot; Bottom view

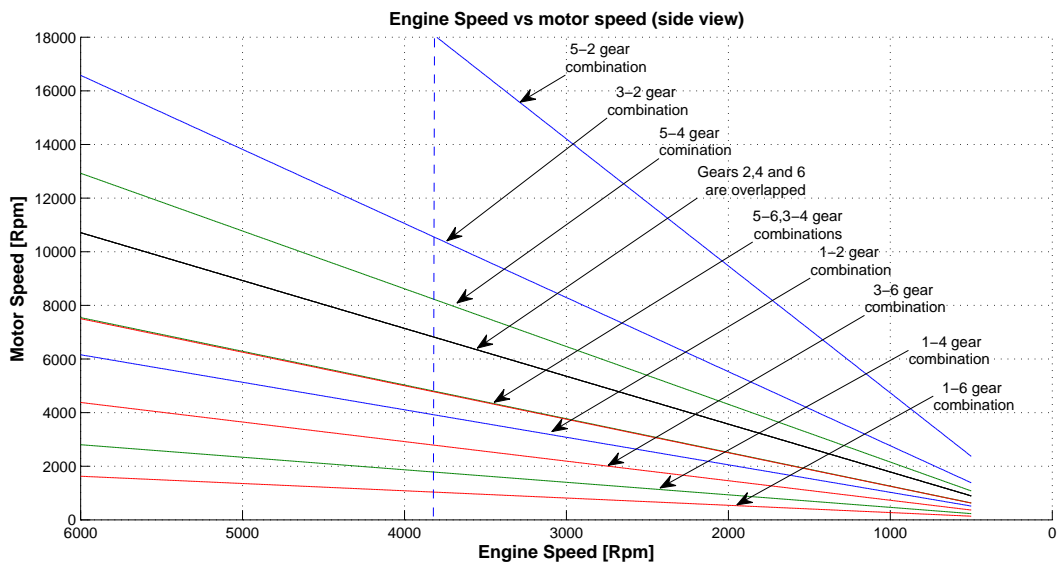


Figure 3.20: HDCT transmission plot; Side view

shaft and engine shaft. Reference [20] describes a method for clutch-less gear shifting by controlling the engine torque. He performs an on road test to compare the time for gear shifting with and without releasing the clutch and concludes that the new method produces improvements in shifting time, torque interruption and shifting comfort.

However, the clutch-less gear-shifting encountered in [2] and [20] are slightly different from that encountered in electric mode in HDCT design. In HDCT design in electric mode, speed synchronisation between motor and the transmission shaft is required. Reference [11] describes a gear shift strategy for clutch-less automated manual transmission in battery operated electric bus. On-road test conducted shows that a total time for 1st to 2nd gear up shift where the motor speed drops from 2800 rpm to 1300 rpm takes approximately 0.89 sec. He concludes that total time for clutch-less gear shifting depends on the gear step, fast mode switching capability of motor and precise control of motor speed.

Considering the fact that the gear step in electric mode (2nd gear to 4th; 4th gear to 6th) in HDCT is high, testing might be required to evaluate the shift quality, time, and power loss. Also, it must be noted that due to the torque characteristic and high rated motor-generator speed the frequency of the gear shifting in electric mode can be made less.

## 4 Hybrid power-train control

Hybrid vehicles consist of more than one power source. Regulating the energy flow from different power sources with the goal of optimizing one or more parameters such as the fuel economy or performance or efficiency is a much more complex job than for a conventional power-train. This has to be accomplished by the a energy management control.

Of the various casual and non casual energy management controllers discussed in [10], a causal controller called the 'Charge Depletion and Charge Sustaining' (CDCS) is used. In charge sustaining mode, a sub optimal control strategy called the 'Equivalent Consumption Minimization Strategy' (ECMS) is used in this thesis work as shown in figure 4.1.

For PHEV, assuming that the battery is fully charged via the electric grid, charge depletion (CD) mode is activated first, where in the power required to drive the vehicle comes from the battery alone until the state of charge (SOC) reaches the minimum limit. Once the SOC reaches the minimum limit, ECMS is activated where in the power required to drive the vehicle comes from both or either of the power source with the main objective of minimizing the cost of operation and also maintaining the SOC level in the battery close to its minimum limit for the remaining trip.

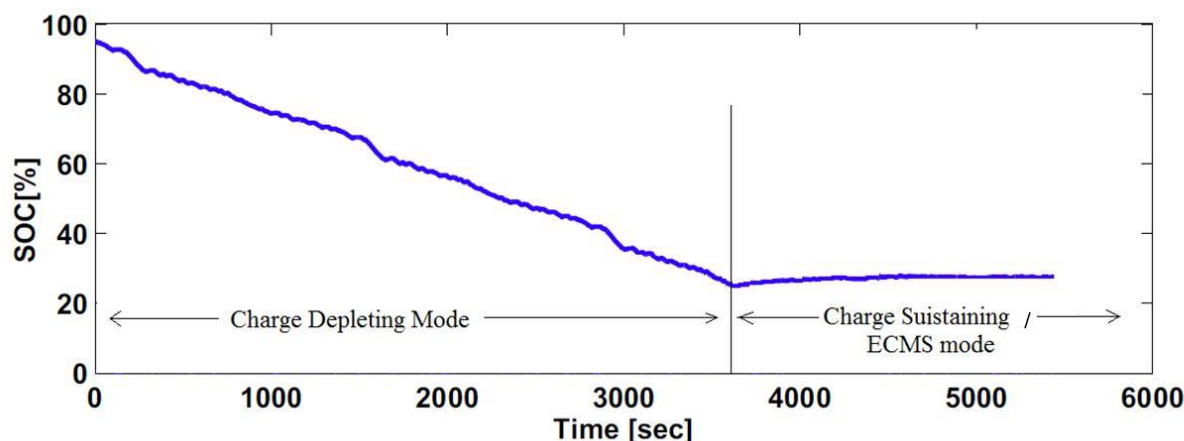


Figure 4.1: Hybrid energy management control

### 4.1 Charge Depletion and Charge Sustaining (CDCS)

Unlike in HEVs, all PHEVs has the capability of storing the electric energy from the grid in an on-board energy buffer and utilize it whenever required. Therefore, utilizing the electric grid energy which is much cheaper than the fuel energy during the initial trip is the main principle on which CDCS energy management control works. The vehicle behaves as an electric vehicle during the initial phase until the SOC reaches its minimum limit. Once the SOC reaches the minimum limit, charge sustaining mode is activated, in this case ECMS control is activated.

### 4.2 Equivalent Consumption minimization strategy (ECMS)

Once the SOC reaches its minimum limit, the power-train behaves as a hybrid vehicle maintaining the SOC close to the minimum limit. The main principle of ECMS is to minimize the overall cost of operation by optimal use of two energy sources. This means that the controller at each time instance minimises a cost function which is a weighted sum of power from the engine and power from the battery, and is mathematically given by

$$C(t) = [P_f(t)C_f] + s[P_{elc}(t)C_e] \quad (4.1)$$

Where,

$C(t)$  = Total cost of operation at time  $t$  (currency).

$P_f(t)$  = Fuel power at time  $t$  (kW).

$C_f$  = A constant equivalent to fuel cost (currency/kW).

$P_{elc}(t)$  = Electrical power at time  $t$ .(kW)

$C_e$  = A constant equivalent to grid electricity cost (currency/kW).

$s$  = Fuel equivalence factor.

ECMS is a control strategy to find the optimal control over a complete driving cycle. However, determining the fuel equivalence factor ( $s$ ), which varies from one driving condition to another is a complex task. Various authors have described various methods to determine the equivalence factor for a real time controller. However for this thesis work, an iterative method is used such that the SOC at the beginning and the end of the trip when the ECMS (Charge sustaining) mode begins, will remain the same. The power split is controlled such that total cost  $C(t)$  is minimised at every time instant. This will give us an optimal control over the entire driving cycle similar to dynamic programming (DP) strategy. A detailed flowchart of the control for HDCT is presented later in section 6.

The size of the battery has an effect on the design of controls. In hybrid vehicles, the battery size is usually small and hence the amplitude of rate of change of SOC is high which will result in smaller window for efficient control. In PHEV the battery size is usually big and has much bigger window to design an efficient control. Therefore, ECMS control strategy works well for PHEVs in charge sustaining modes.

## 5 Comparisons of different power-train

When discussing hybrid power-train, its not just sufficient to evaluate fuel efficiency. One of the crucial parameters that needs to be considered is the 'characteristic to cost ratio' of the power train itself. Characteristic to cost ratio summarises the overall value for money of the hybrid power train. Higher the value of the ratio, higher is the value for money. In recent years there has been a significant development in the battery and motor technology and their prices have reduced. This has resulted in increase in the characteristic to cost ratio of the hybrid power train. This has made the PHEV technology more attractive to vehicle manufacturers. In fact, several vehicle manufacturers have gone one step ahead to have pure electric vehicles in their fleet of vehicles.

This section will first begin with a very rough cost estimate of different power-train configurations discussed in chapter 3, followed by a comparison on functionalities. A comparison on different types of parallel hybrid configuration is then discussed followed by a brief discussion on the size of the electric components. Then a brief conclusion is drawn to give an idea of the cost to characteristic ratio of each power-train discussed in this report.

### 5.1 Cost comparison

One of the factors that is limiting the hybrid market share in the automotive sector is the cost of the power-train. Therefore, it becomes necessary to compare the cost of the power-trains. The power-train configurations discussed in chapter 3 are considered here for cost comparison. Note that, it is a very rough estimate aimed to find the relative differences and complement the comparison of performance and fuel efficiency discussed in chapter 7 and should not be used as a value for real cost of the power-train. Vehicle manufacturers treat certain specification of the power-train as confidential and therefore obtaining the exact specification is difficult. The red font in table 5.1 indicates the assumed values. Also, it is assumed that all the power-trains are designed for PHEV application having the same battery capacity for equivalent all electric range.

Table 5.1 Is derived from taking individual component costs from the Argonne lab research data and Environmental protection agency (EPA) cost analysis as shown in table 5.2 [3],[4],[1].

Note on assumed values

- Toyota prius plug-in model using P410 transaxle [17] consists of two simple planetary gear set. The size of the generator is assumed.
- Obtaining the specification for GM 2MT70 design is difficult and hence the same specifications as that of prius plug-in model 2012 are assumed where ever necessary.

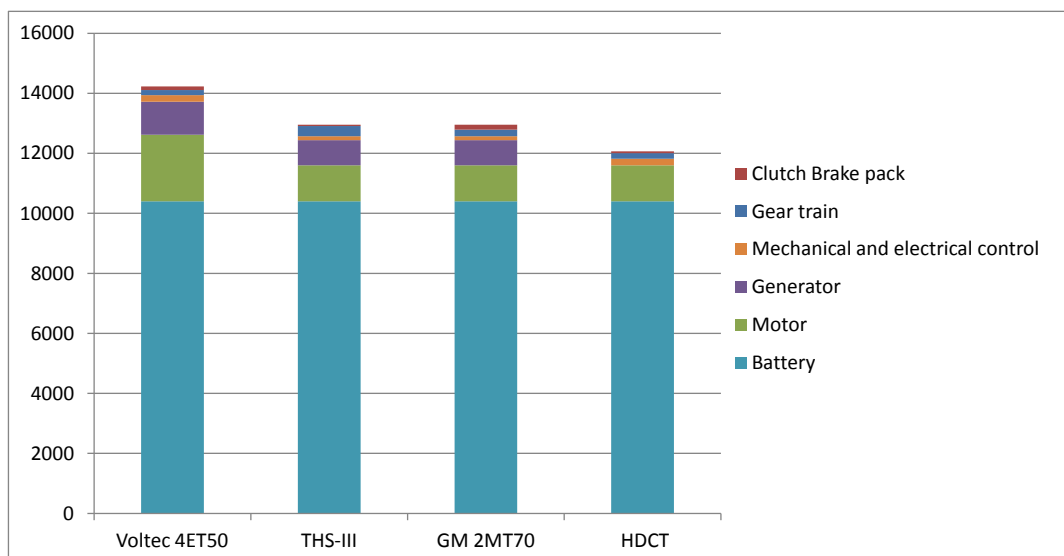


Figure 5.1: Rough Cost comparison of Voltec 4ET50, THS-III generation, GM 2MT70, and HDCT

Table 5.1: Rough cost estimate of power-trains Voltec 4ET50, THS-III generation, GM 2MT70, and HDCT

Hardware Component	Voltec 4ET50 Chevy Volt 2011		THS-III Prius 2012		GM 2MT70		HDCT	
	Size/Qty	Cost (\$)	Size/Qty	Cost (\$)	Size/Qty	Cost (\$)	Size/Qty	Cost (\$)
Gear Train (Qty)	1	170	2	340	2	220	1	185
Clutch brake pack (Qty)	3	121.2	1	40.4	4	161.6	1	64
Motor (kW)	111 kW	2220	60 kW	1200	60 kW	1200	60 kW	1200
Generator (kW)	55 kW	1100	42 kW	840	42 kW	840	0	0
Battery (kWh)	16	10400	16	10400	16	10400	16	10400
Mechanical and electrical control	1	220	0.6	132	0.6	132	1	220
Total cost (\$)		<b>14011.2</b>		<b>12820.4</b>		<b>12953.6</b>		<b>12069</b>

Table 5.2: Individual component cost table derived from Argonne lab research data and Environmental protection agency (EPA) cost analysis

Approximate cost of Li-Ion battery for energy application in 2012-13 for PHEV-40 taken from Argonne lab research data (\$/kWh) [1].	650
Approximate cost of motor with controller in 2012-13 taken from Argonne Lab research data (\$/kW) [1]	20
Cost for one simple planetary gear train. Taken from EPA cost estimate on 2010 ford fusion HEV (\$) [3]	170
Cost for ravigneaux and underdrive planetary gear set. Taken from EPA cost estimate on 2007-09 Toyota camery (\$) [4]	220
Cost for (5)Internal clutch brake pack and . Taken from EPA cost estimate on 2007-09 Toyota camery. (\$) [4]	202
Cost for mechanical and electrical controls. Taken from EPA cost estimate on 2007-09 Toyota camery. (\$) [4]	220
Cost for DCT Gear train. Taken from EPA cost estimate on 2007-09 VW jetta 6 speed DCT (\$) [4]	185
Cost for Internal clutch etc required for gearing. Taken from EPA cost estimate on 2007-09 VW jetta 6 speed DCT (\$) [4]	64

Table 5.1 represented as a column graph is shown in figure 5.1. From figure 5.1, it can be inferred that battery covers the major part of the plug-in hybrid power-train cost followed by number of electrical components and their respective size. The key difference between the systems are

- HDCT design has only one motor-generator which makes it cheaper when compared to rest of the power-train design.
- Voltec 4ET50 uses one of the motor-generator unit as a primary prime mover and has to be sized for start-ability and grade-ability which increases the overall power-train cost.
- Size of the electrical components also plays an important role in the overall cost of the power-train.

A brief comparison on size of the components required for different power-train configuration is presented in section 5.4.

## 5.2 Functionality comparison

The cost to characteristic ratio plays an important role when it comes to hybridising the vehicle. The customer, demands higher functionality for cheaper price. Therefore, it becomes necessary to compare the functionality possible for different power-trains. Table 5.3 presents the functionality comparison between Voltec 4ET50, THS-III generation, GM 2MT70, and HDCT.

Table 5.3: Comparison on functionality of Voltec 4ET50, THS-III generation, GM 2MT70, and HDCT. Note, blue color is just for visual comparison

Parameters	Voltec 4ET50	THS-III	GM 2MT70	HDCT
Electric Launch	Y	Y	Y	Y
Cranking the Engine	Y	Y	Y	Y
Charging at idle	Y	Y	Y	Y
Pure electric mode	Y	Y	Y	Y
Pure ICE mode	Y	Y	Y	Y
Partial charging partial propulsion	Y	Y	Y	Y
Boost mode	Y	Y	Y	Y
Prime movers supporting boost mode	Two motor-generator unit	ICE + motor-generator unit	ICE + motor-generator unit	ICE + motor-generator unit
Onboard energy convertor 'connected to wheels'	Two motor-generator unit	ICE + motor-generator unit	ICE + motor-generator unit	ICE + motor-generator unit

From table 5.3 it is inferred that HDCT design is capable of providing all the functionalities that THS-III generation or GM 2MT70 design can offer.

## 5.3 Comparison on different configurations possible for HDCT design

In general, for parallel hybrid power-train architecture, there are three configuration possible depending on where the motor-generator is placed. Similar configuration can be extended to HDCT design and is shown in figure 5.2. This comparison is made to understand the constraints within each configuration and to see which HDCT configuration suits best for PHEV especially when the European automotive sector is depending on dual clutch transmission and not the ECVT design.

The first configuration has motor-generator unit before the transmission. The second configuration has motor-generator connected within the transmission This configuration is the one discussed earlier referred to as HDCT design. The third configuration has motor-generator after the transmission.(Refer figure 5.2).

Table 5.4 presents the comparison on different configuration possible for HDCT design. From table 5.4 it is inferred that the second configuration, that is, connecting the MG inside of transmission has more advantages when compared to rest of the configurations. It should be noted that the acceleration performance for the

Table 5.4: Comparison on different parallel HDCT configuration based on the position of the motor-generator unit. Note, green color indicates that particular configuration is better when compared to the rest for that specific discussion

MG connected before transmission (1st configuration)	MG connected within transmission (2nd configuration)	MG connected after transmission (3rd configuration)
Since engine and motor are on same shaft, an extra clutch in addition to dual clutch is required to decouple the engine from the motor in pure electric mode. Alternative would be to deactivate the cylinder or cut off fuel which will result in small loss due to engine inertia.	The same dual clutch can be used to decouple the engine from motor and hence no additional clutch required.	The same dual clutch can be used to decouple the engine from motor and no additional clutch required.
MG and ICE should have the same maximum speed since they are mounted on the same shaft. Since the cost of MG is inversely proportional to its maximum speed, cost of the MG required here would be high.  $w_{MG} = w_e$	MG and ICE need not have same maximum speed. However the maximum speed of MG will depend on the ICE speed and gear ratio selected for MG and ICE.  $w_{MG} = \frac{w_e \gamma_{MG}}{\gamma_e}$	MG and ICE need not have same maximum speed but the Maximum speed range of MG will depend on the maximum vehicle velocity.  $w_{MG} = \frac{v \gamma_{diff}}{R}$
Gears are common for MG and ICE. Therefore for six speed gear box six different speed ratios are possible. (Note: same gear has to be used for MG and ICE)	Gears for MG and ICE can be same or different. Therefore for a six speed gear box, twelve different gear combinations are possible.	ICE can use any of the six gears of the six speed gear box but MG cannot use the gears since it is located after transmission. Therefore, for six speed gear box, six different speed ratios are possible.
Torque range of MG (size of MG) need not be high since MG can be assisted by transmission. But speed range of MG should match ICE as discussed earlier.	Torque range of MG (size of MG) need not be high since MG can be assisted by transmission.	MG is not assisted by transmission since it is located after transmission. Therefore for same acceleration performance, Size of the MG or ICE required might be high.
Acceleration performance in this configuration might be <i>slightly</i> higher in all modes (Pure ICE mode, Pure electric mode, boost mode) than the configuration with EM inside transmission for same MG and ICE specification.	Acceleration performance is high but <i>slightly</i> less than the configuration where MG is connected before the transmission	As discussed earlier for same MG and ICE size, the acceleration performance is low.
In regeneration mode, gear ratio can be selected such that MG operates at its efficient operating point possible.	In regeneration mode, gear ratios can be selected to operate the MG at its best operating point possible	In regeneration mode, MG is not assisted by transmission since it is located after transmission.
Preselecting the gear ratios will be similar to that of the conventional DCT	Pre-selecting the gear ratios will be a complex task.	Preselecting the gear ratios will be similar to that of the conventional DCT.

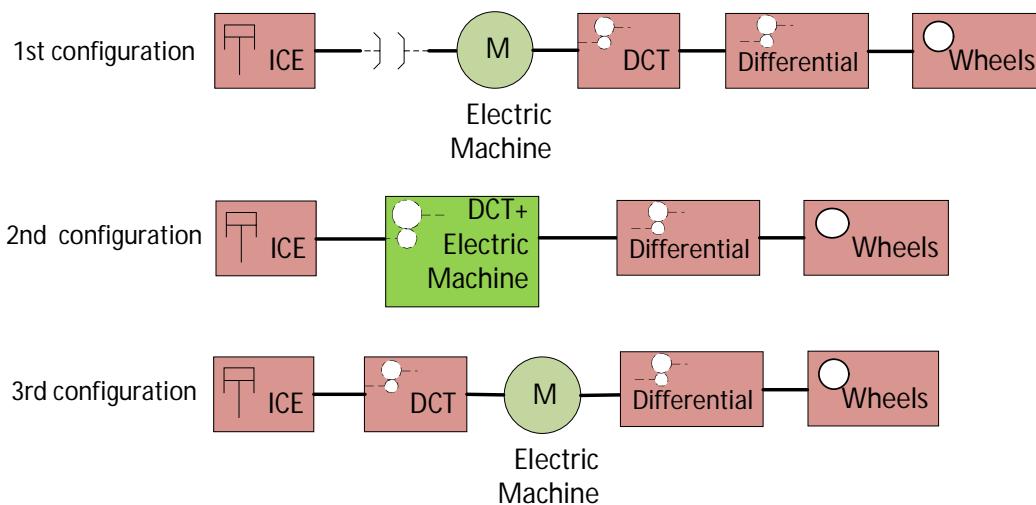


Figure 5.2: Different parallel hybrid architecture configuration based on the position of the motor-generator

second configuration is slightly less than the first configuration since the the first configuration has the ability to use the first gear ratio with both MG and ICE providing the power required for acceleration.

The first and third configuration discussed above is similar to the power-train of 'Audi A3-etron' and 'P1-Mclaren' respectively exhibited in March 2013 Geneva motor show. The second configuration is neither in production nor exhibited in any motor show. However researches are going on at Volvo.

## 5.4 Sizing of Motor generator unit and Battery

In GM 2MT70 and THS-III generation design, the battery is assisted by ICE and MG (functioning as generator) together. Therefore maximum power rating of the battery can be made smaller than the maximum power rating of the motor-generator (functioning as motor). However, this will result in decline in the performance of pure electric mode such as the all electric range and acceleration. In Voltec 4ET50 and HDCT design, the maximum power rating of the battery is mainly dependent on the maximum power rating of the MG (functioning as motor).

In THS-III design, MG is assisted by the second planetary gear set with only one fixed gear ratio but ICE is not assisted by the gears except for the differential. In Voltec 4ET50 design, both MG can be used to provide the driving torque to the wheels with assistance from the gear box. In the HDCT design, MG is assisted by the three different gear ratios but the sizing of the MG depends on the smallest gear (highest gear ratio). In GM 2MT70 design, both MG can be sometimes used to provide the driving torque to the wheels with assistance from the gears depending upon the clutch activation.

Table 5.5: Comparison on number of electric components and if the primemovers are assisted by gear box or not. Note, blue color is just for visual comparison

Parameters	Voltec 4ET50	THS-III	GM 2MT70	HDCT
MG Assisted by gearbox ?	Y	Y	Y	Y
ICE Assisted by gearbox ?	Not Required	N	Y	Y
Number of electric prime movers	2	2	2	1
Mass of the electric components (Only major electric components)	2 MG + Battery	2 MG + Battery	2 MG + Battery	1 MG + Battery

Sizing of the MG also depends on the mass of the vehicle it needs to propel. Each configuration has its own way of reducing the mass of the Vehicle. HDCT design consists of one MG less than the other configurations.

The size of the MG for GM 2MT70 and Voltec 4ET50 required can be made less. However, in general size of the battery has major effect on the total weight of the power train.

Table 5.6: Sizing of the motor-generator unit comparison table. Note, blue color is just for visual comparison

Parameters	Voltec 4ET50	THS-III	GM 2MT70	HDCT
Size of MG can be made less because it is assisted by gear?	Y	Y	Y	Y
Size of MG can be made less because Both MG can be used together ?	Y	N	Y	N

Reference [14] performs an analytical comparison on THS II generation design and GM 2MT70 design and concludes that the size of the MGs required for THS-II design is bigger than that for GM 2MT70 design. A comparison on power losses is also made and it is found that GM 2MT70 design is more efficient than THS-II design. But it must be noted that the improvement in efficiency comes at the expense of more complex architecture.

Reference [6] presents the performance of GM 2 mode hybrid in general with and without the fixed gears. This gives an idea about the advantages of using fixed gear ratio (like in conventional transmission) over the ECVT transmission. Fixed gears increases the acceleration performance and increases the towing capability of the vehicle. GM 2MT70 design has the advantage of reducing or eliminating the motor operation when its temperature is at its peak by using the fixed gear ratio where in the power flow to the wheels from the engine will be only through mechanical path.

It is evident from [6] and [14] that GM 2MT70 design is more efficient than THS-II design. However, for modelling and simulation in this thesis work, THS-III architecture is selected as bench mark over the GM-2MT70 design to compare it with HDCT design, due to its simple architecture and comparatively less complex control requirement.

## 5.5 Conclusion of different comparison

In table 5.7, the cost of different power train configurations summarised in section 5.1 is presented again, but here, the costs are normalised to THS-III power train cost. Voltec 4ET50 power train costs more, mainly because it is assumed here that the electric machine is the primary energy converter and is sized bigger (when compared to other configurations) to meet the minimum performance criteria. GM 2MT70 costs slightly more than THS-III configuration because of the additional mechanical components like clutches and brakes. HDCT configurations is cheaper than the other configurations mainly because it uses one electric machine less when compared to other configurations.

Functionality comparison in section 5.2 shows that HDCT configuration, even though cheaper, is capable of providing all the functionalities that other configurations offers to the customer.

In Section 5.3, comparison of different HDCT configurations that are possible is presented. It is found that, connecting the electric machine in the transmission allows for more flexibility for the power train designer.

Therefore, the HDCT configuration discussed in this project seems to have a good *characteristic to cost ratio*. Also, one more advantage of HDCT solution is that it can be used for different levels of hybridisation with very less change, or in other words, it is good solution for modular architecture point of view.

Different power train configuration	Cost (Normalised to THS-III cost)(%)
Voltec 4ET50	109.3
GM 2MT70	101
HDCT	94.1

Table 5.7: Cost comparison of different power train configurations normalised to THS -III power train cost.

## 6 Simulation model of power-trains

This section describes the method used for modelling of each component of the power-train. Matlab and Simulink software is used for modelling. A backward simulation approach is employed to simulate the fuel efficiency and performance of the selected two power-train architecture.

For modelling and simulation, THS-III architecture is selected over the GM-2MT70 design due to its simple architecture and comparatively less complex control requirement. A HDCT model is also built for comparative analysis.

### 6.1 Object file

Already available object oriented programming format at the university is used to create the object file for individual components. This will ensure the consistency of the type of data. The object file created is then used to load all the predetermined values of the power-train such as mass of the vehicle, drag coefficient, rolling resistance, engine dynamo meter test data etc. Separate blocks are created for each power-train component in Simulink.

### 6.2 Driving cycle model

Three driving cycle were used to compare the power-trains in different types of driving. The driving cycle used in this thesis work are Urban dynamo meter driving schedule (UDDS) for light duty vehicles, Highway fuel economy test cycle (HWFET) and New European driving schedule (NEDC). UDDS represents the urban style driving cycle , HWFET represents highway driving style and NEDC is a combination of urban and highway cycle. The acceleration and velocity profile of the driving cycle as a function of time are shown in figure 6.1, 6.2 and 6.3.

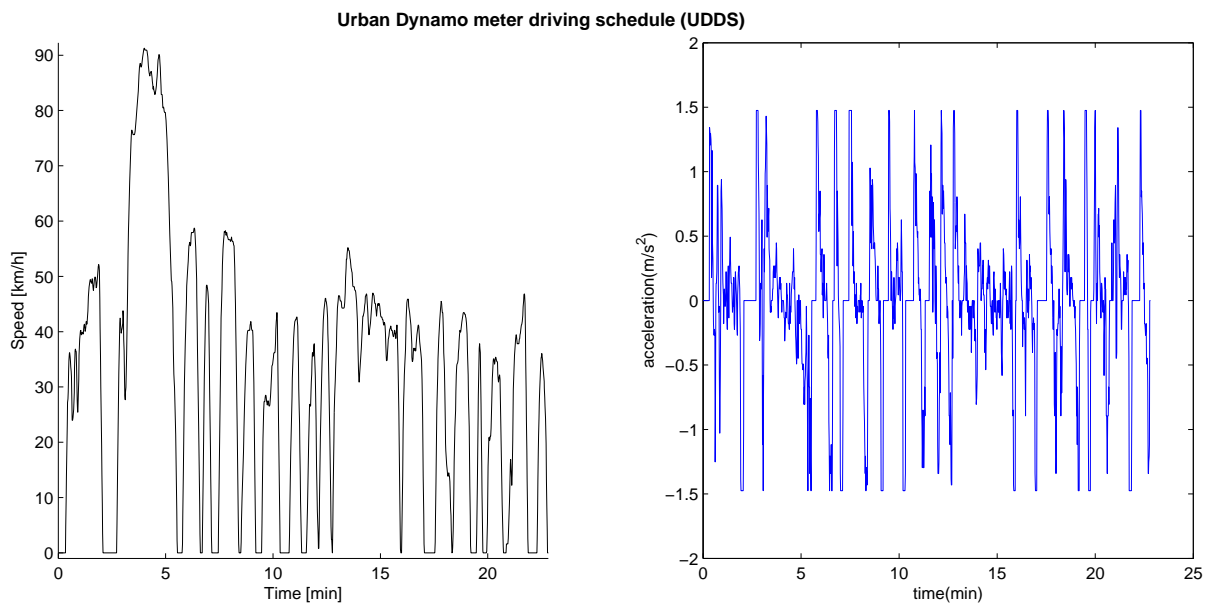


Figure 6.1: *Urban dynamo meter driving cycle*

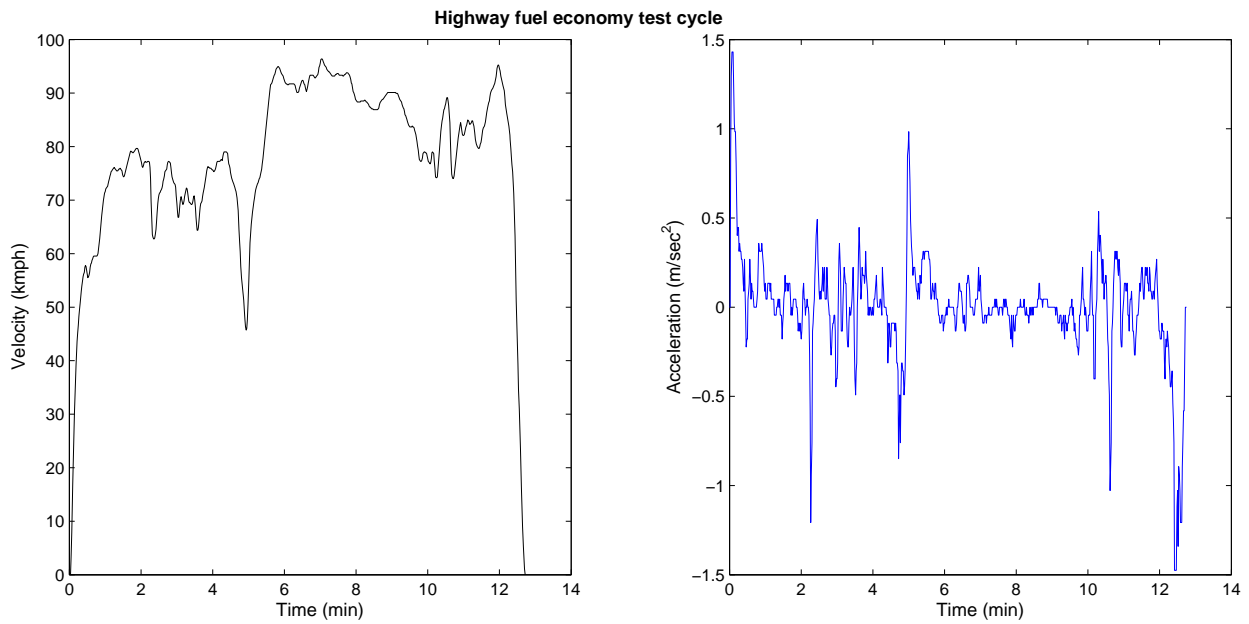


Figure 6.2: Highway fuel economy test cycle

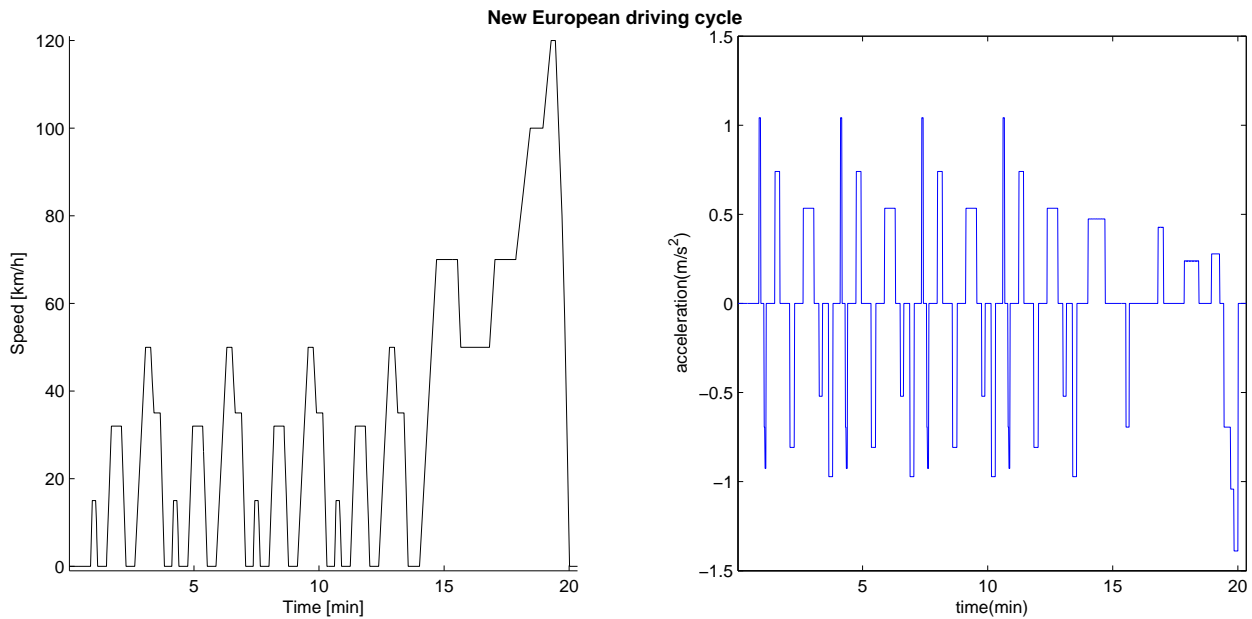


Figure 6.3: New European driving cycle

### 6.3 Chassis model

Longitudinal dynamics of the road vehicle depends on the Aerodynamic resistance ( $F_a$ ), Rolling resistance ( $F_r$ ), Grade resistance ( $F_g$ ) and inertia ( $F_i$ ). The aerodynamic resistance depends on the air density ( $\rho_a$ ), Frontal area ( $A_f$ ), drag coefficient ( $c_d$ ) and velocity of vehicle ( $v$ ). Rolling resistance and grade resistance depends on mass of the vehicle ( $m_v$ ), acceleration due to gravity ( $g$ ), coefficient of rolling resistance ( $c_r$ ), and the grade of the road ( $\alpha$ ). Inertia depends on mass of the vehicle ( $m$ ), inertia of rotating parts on the wheel side of transmission ( $j$ ), radius of wheel ( $R_w$ ) and acceleration ( $a$ ).

The traction force is given by

$$F_t = F_a + F_r + F_g + F_i \quad (6.1)$$

Table 6.1: Rolling resistance coefficient as a function of vehicle velocity

Velocity (Kmph)	Rolling resistance
0	0.0093
50	0.0093
80	0.0095
90	0.0097
120	0.01
150	0.0108
180	0.0115
210	0.0133
240	0.017

Table 6.2: Vehicle parameters used for simulation. Some values not given due to confidentiality reasons

Parameters	Values
Vehicle mass, ( $m$ )	1730 kg
Drag coefficient X frontal area, ( $c_d * A_f$ )	0.660
Rolling radius of the wheels, ( $R_w$ )	0.3067 m
Inertia of the wheels and rotating parts that are present on the wheel side of the gear box, ( $j$ )	-
Differential gear ratio for HDCT, ( $\gamma_{diff}$ )	-
Differential gear ratio for ECVT type, ( $\gamma_{diff}$ )	3.267
Efficiency of differential, ( $\eta_{diff}$ )	95%

The Aerodynamic resistance  $F_a$ , rolling resistance  $F_r$ , grade resistance  $F_g$  and inertia resistance  $F_i$  are given by

$$F_a = \frac{1}{2} \rho_a A_f c_d v^2 \quad (6.2)$$

$$F_r = m g c_r(v) \cos \alpha \quad (6.3)$$

$$F_g = m g \sin \alpha \quad (6.4)$$

$$F_i = \left( m + \frac{j}{R_w^2} \right) a \quad (6.5)$$

The torque request  $T_w$  at the wheels is given by

$$T_w = F_w R_w \quad (6.6)$$

Longitudinal and lateral vehicle dynamics are not considered in this thesis work. A look up table for Rolling resistance as function of vehicle velocity is used for simulating the fuel efficiency which is shown in table 6.1. The vehicle parameters used for simulation are shown in table 6.2.

## 6.4 Hybrid dual clutch transmission model

Hybrid dual clutch transmission is modelled as two simple manual transmissions in one, with even and odd gears on two different shafts as shown in figure 6.4. The power loss during shifting is attributed only to clutch losses during its engagement which is assumed to be very small and is not taken into consideration in this thesis work. The efficiency of each meshing gears are assumed to be 97% and the efficiency of the differential is assumed to be 95%.

The power split ratio ( $u$ ) for HDCT design is defined as the power request to the motor ( $P_{MG}$ ) divided by the total power request at the wheels ( $P_w$ ).

$$u = \frac{P_{MG}}{P_w} \quad (6.7)$$

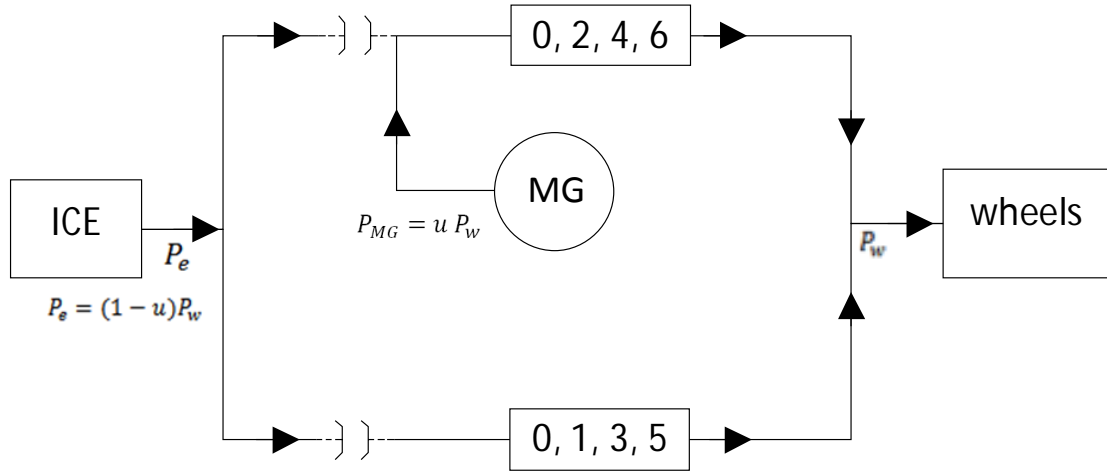


Figure 6.4: Stick model of HDCT design

Therefore,  $u$  times the power request at the wheels has to be delivered by the motor and  $1 - u$  times the power request at the wheels has to be delivered by the ICE ( $P_e$ ).

$$P_e = (1 - u)P_w \quad (6.8)$$

$$P_{MG} = uP_w \quad (6.9)$$

The amount of power split ( $u$ ) and the gear ( $\gamma_i$ ) is decided by the ECMS control at every instant of time. Engine torque ( $T_e$ ), speed ( $w_e$ ), acceleration ( $\dot{w}_e$ ) and power ( $P_e$ ) are given by

$$T_e = \frac{(1 - u)T_w}{\gamma_i \gamma_{diff}}, \quad \forall i = (0, 1, 2, 3, 4, 5, 6) \quad (6.10)$$

$$w_e = w_w \gamma_i \gamma_{diff}, \quad \forall i = (0, 1, 2, 3, 4, 5, 6) \quad (6.11)$$

$$\dot{w}_e = \dot{w}_w \gamma_i \gamma_{diff}, \quad \forall i = (0, 1, 2, 3, 4, 5, 6) \quad (6.12)$$

$$P_e = \frac{T_e w_e}{\eta_{GB} \eta_{diff}} \quad (6.13)$$

Motor-generator torque ( $T_{MG}$ ), speed ( $w_{MG}$ ), acceleration ( $\dot{w}_{MG}$ ) and power ( $P_{MG}$ ) are given by

$$T_{MG} = \frac{uT_w}{\gamma_i \gamma_{diff}}, \quad \forall i = (0, 2, 4, 6) \quad (6.14)$$

$$w_{MG} = w_w \gamma_i \gamma_{diff}, \quad \forall i = (0, 2, 4, 6) \quad (6.15)$$

$$\dot{w}_{MG} = \dot{w}_w \gamma_i \gamma_{diff}, \quad \forall i = (0, 2, 4, 6) \quad (6.16)$$

$$P_{MG} = \frac{T_{MG} w_{MG}}{\eta_{GB} \eta_{diff}} \quad (6.17)$$

Where,  $\eta_{GB}$  and  $\eta_{diff}$  are the efficiency of the gear box and differential respectively. For regenerative braking,

$$P_{MG} = (T_{MG} w_{MG}) \eta_{GB} \eta_{diff} \quad (6.18)$$

The gear ratios ( $\gamma_i$ ) used for the six speed gear box is not given due to confidentiality reasons.

## 6.5 ECVT model (similar to THS-III generation design)

The ECVT THS-III type transmission is modelled as a three shaft configuration as shown in figure 6.5 .The efficiency of each meshing gears are assumed to be 97% and the efficiency of the differential is assumed to be

95%. The characteristic ratio of the first simple planetary gear ( $\rho$ ) is 0.3846 and the fixed gear ratio of the second planetary gear ( $\gamma_1$ ) is 2.636

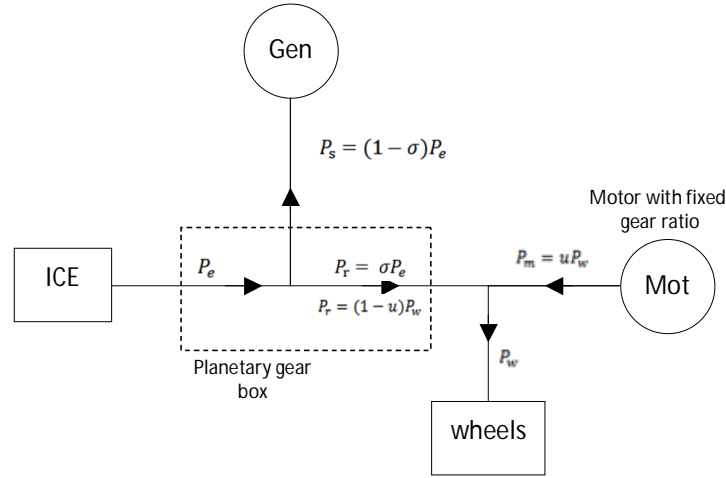


Figure 6.5: Stick model of Ecvt THS-III type design

The power split ratio ( $u$ ) is defined as the power request to the motor ( $P_{MG2}$ ) divided by the total power request at the wheels ( $P_w$ ).

$$u = \frac{P_{MG2}}{P_w} \quad (6.19)$$

Therefore  $u$  times the power request at the wheels has to be delivered by the motor and  $1 - u$  times the power request at the wheels has to be delivered by the 'ring gear' ( $P_r$ ) as indicated in the figure 6.5.

$$P_{MG2} = uP_w \quad (6.20)$$

$$P_r = (1 - u)P_w \quad (6.21)$$

Separation factor,  $\sigma$  (as discussed in chapter 3), determines the amount of power from the engine flowing through mechanical or electrical path. The amount of power split and separation factor is decided by the ECMS control at every instant of time.

$$P_r = \sigma P_e \quad (6.22)$$

$$P_{MG1} = (1 - \sigma)P_e \quad (6.23)$$

Engine torque ( $T_e$ ), speed ( $w_e$ ), acceleration ( $\dot{w}_e$ ) and power ( $P_e$ ) are given by

$$T_e = T_w \frac{(1 + \rho)}{\gamma_{diff}} (1 - u) \quad (6.24)$$

$$w_e = w_w \frac{\gamma_{diff}}{\sigma(1 + \rho)} \quad (6.25)$$

$$\dot{w}_e = \dot{w}_w \frac{\gamma_{diff}}{\sigma(1 + \rho)} \quad (6.26)$$

$$P_e = \frac{T_e w_e}{\eta_{GB} \eta_{diff}} \quad (6.27)$$

MG1 torque ( $T_{MG1}$ ), speed ( $w_{MG1}$ ), acceleration ( $w_{MG1}$ ) and power ( $P_{MG1}$ ) are given by

$$T_{MG1} = T_w \frac{\rho}{\gamma_{diff}} (1 - u) \quad (6.28)$$

$$w_{MG1} = w_w \frac{\gamma_{diff}}{\rho} \left( \frac{1}{\sigma} - 1 \right) \quad (6.29)$$

$$w_{MG1} = \dot{w}_w \frac{\gamma_{diff}}{\rho} \left( \frac{1}{\sigma} - 1 \right) \quad (6.30)$$

$$P_{MG1} = \frac{T_{MG1} w_{MG1}}{\eta_{GB}} \quad (6.31)$$

MG2 torque ( $T_{MG2}$ ), speed ( $w_{MG2}$ ), acceleration ( $w_{MG2}$ ) and power ( $P_{MG2}$ ) are given by

$$T_{MG2} = T_w \frac{u}{\gamma_1 \gamma_{diff}} \quad (6.32)$$

$$w_{MG2} = w_w \gamma_1 \gamma_{diff} \quad (6.33)$$

$$w_{MG2} = \dot{w}_w \gamma_1 \gamma_{diff} \quad (6.34)$$

$$P_{MG2} = \frac{T_{MG2} w_{MG2}}{\eta_{GB} \eta_{diff}} \quad (6.35)$$

## 6.6 Hybrid Power-train control model

Hybrid power-train control working on common principle is used for both HDCT and ECVT THS-III generation type design. The controls used in this thesis work is CDCS controll which uses ECMS in CS mode as described in Chapter 4. The different modes of the control is shown in figure 6.6.

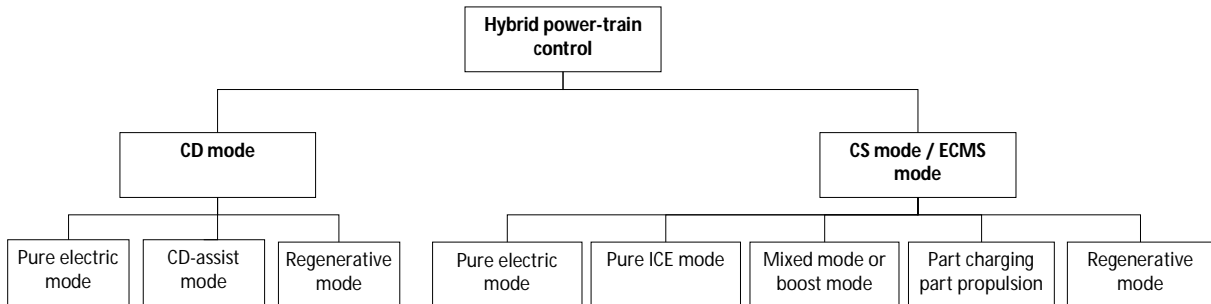


Figure 6.6: *Hybrid power-train control topology*

ECMS control for both HDCT design and ECVT THS-III design is implemented in matlab and then linked to Simulink such that the ECMS control determines the best power split, gear ratio, clutch signal and separation factor without violating the constraints of individual components. The primary goal of the ECMS control is to reduce the total operational cost over the entire driving cycle. For this reason, matlab script is broken down into several smaller functions based on the mode of operation such as Pure Electric mode, CD (charge depletion) assist mode, Pure ICE mode, Mixed mode (or Boost mode), regenerative mode and part charging part propulsion mode. To be on the same page, a brief description of each of these modes and what it actually means in this thesis work is presented below.

- **Pure electric mode:** In this mode, the vehicle is in CD mode and the request at the wheels is supplied only by MG (functioning as a motor) and the engine is turned off.
- **CD assist mode:** In this mode, the vehicle is in CD mode and the power request at the wheels cannot be met by the MG/battery alone. Therefore, MG/battery will provide the maximum tractive effort and the ICE will provide the remaining power required to propel the vehicle.
- **Pure ICE mode:** In this mode the request at the wheels is supplied by ICE alone.

- **Mixed mode or Boost mode:** In this mode the request at the wheels is supplied by both ICE and MG.
- **Part Charging Part propulsion mode:** In this mode, part of the power output of the engine is used to meet the power demand at the wheels while the remaining part is used to charge the battery.
- **Regenerative mode:** In this mode power from the wheels is used to charge the battery via MG during decelerating/braking or driving down a slope.

Apart from the above mentioned basic modes, terms like split path, circulation path and mechanical path is used for ECVT THS-III generation type design. Split path means that the power from the ICE is split into mechanical and electrical path depending on the value of the separation factor. Circulation path is when the separation factor is greater than one, that is, part of the power from the ICE is circulated through MG2 which behaves as a generator and then to the MG1 which behaves as a motor and then to the wheels. Mechanical path is when the power demand at the wheels is supplied by ICE via mechanical path alone.

### 6.6.1 Power-train control flow chart

This section describes the flow chart of the hybrid power-train control built for HDCT and ECVT THS-III type design. Simulation for CD and CS mode are carried out separately.

When the vehicle is switched on, the hybrid power train control first checks the SOC of the battery. If the SOC of the battery is above the minimum SOC limit, then CD mode is selected else the control switches to CS mode (ECMS control) as shown in 6.7. Once the control switches to CS mode it remains in that mode until the end of the driving cycle.

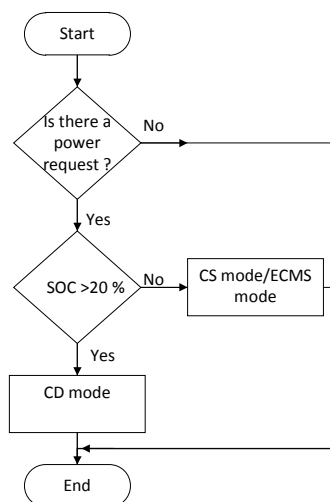


Figure 6.7: First level of supervisory control run at each time step

In CD mode, the hybrid power-train control, first checks the torque request at the wheels. If the torque request is negative, then the control switches to regenerative mode (Refer figure 6.8). If the torque request at the wheel is positive, then, the control checks if the power request at the wheels can be supplied by battery (and MG) only. If yes, then the control calculates the operational cost for all three gear (2nd, 4th and 6th gear) and chooses the one with low operational cost in the case of HDCT power-train, whereas, the control calculates the operational cost for the only fixed ratio in ECVT THS-III type power-train by default. If no, the control switches to 'CD assist' mode where in majority of the power request at the wheels will be supplied by battery (and MG) and the remaining power request will be supplied by ICE. In HDCT power-train, the control divides the power split (ranging from 0 to 1) into smaller segments and within each power-split, operational cost for all 12 gear combinations are computed. The control chooses the power-split and gear combination that will lead to low operational cost. Whereas, in ECVT THS-III type power-train, the control divides the power split (ranging from 0 to 1) into smaller segments and within each power-split, the operational cost for all possible

separation factor is computed. The control chooses the power-split and separation factor that will give low operational cost.

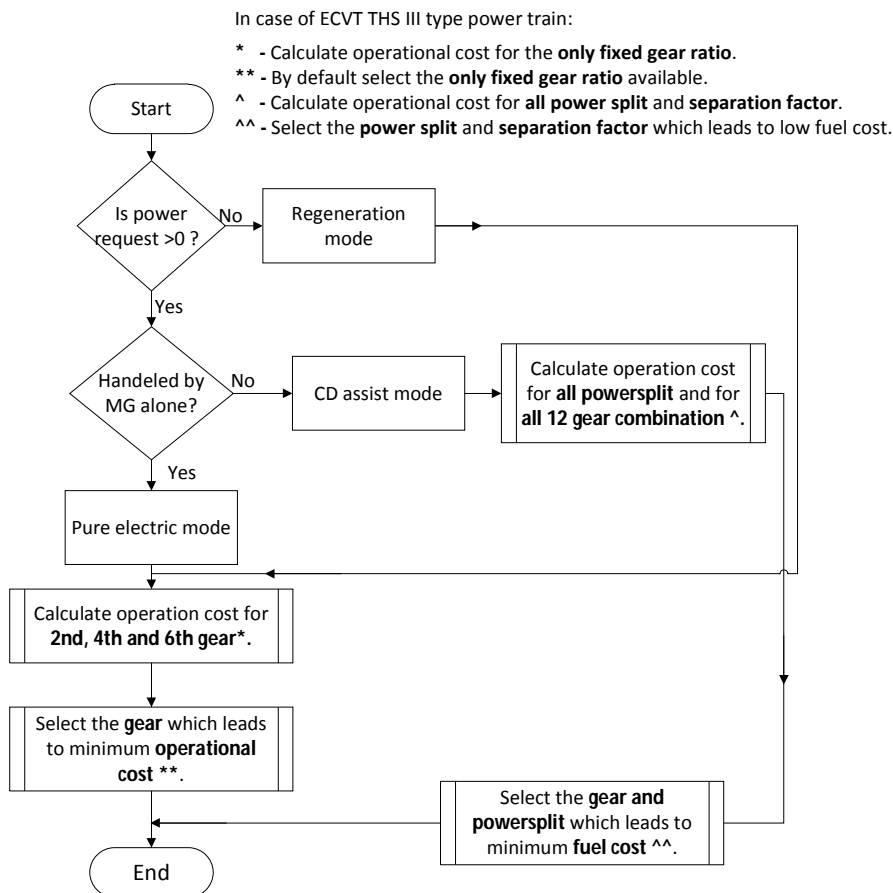


Figure 6.8: CD mode supervisory control run at each time step

Similar to CD mode, in CS mode, the control determines the power-split and gear combinations that will lead to low operational cost in the case of HDCT power-train, whereas, the control determines the power split and separation factor that will lead to low operational cost in the case of ECVT THS-III type power-train. But, in CS mode, the number of sub-modes are greater than in CD mode as shown in figure 6.9. Also, another constraint in CS mode is that the SOC at the end of the driving cycle should be the same as the SOC at the beginning of the ECMS mode. The simulation is iterated for various values of power-split and gear combinations in case of HDCT configuration and power-split and separation factor in case of ECVT configuration until this final constraint is met. This would give optimal control whose result will be similar to dynamic (DP) programming with regards to fuel consumption.

### 6.6.2 Input/Output signals of hybrid power-train control

The hybrid power-train control will compute the total operational cost in all gear ratios, separation factor and power split possible at each instant of time and determines the output signal to be sent to the respective gear box by choosing the control having the least operational cost. Various possible combination of output signals for both HDCT design and ECVT THS-III generation type design is listed in table 6.3 and 6.4.

Note that cranking is not considered in this thesis work. Pure charging at idle is one of the valid signal combinations that are critical during long trip, however it is not considered here in this thesis work.

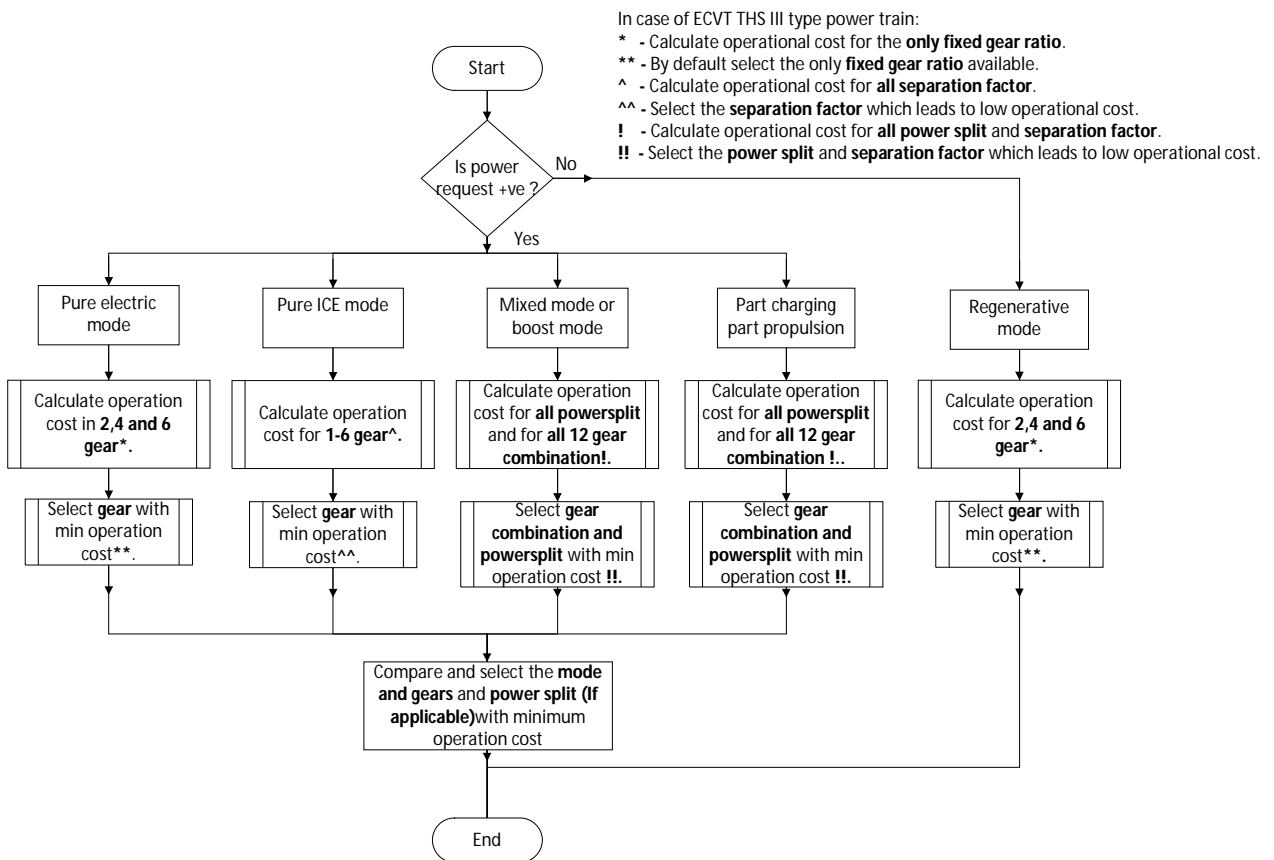


Figure 6.9: CS mode supervisory control run at each time step

Table 6.3: Combination of control output signals possible for HDCT design

	Power Split** ( $u$ )	Odd gear clutch signal* (CL1)	Even gear clutch signal* (CL2)	Comments
Pure electric mode and regenerative mode	1	0	0	Pure electric mode; regeneration mode
	1	1	0	Cranking while vehicle is moving
	1	0	1	Cranking while vehicle is moving or standing still
	1	1	1	Not useful
Pure ICE mode	0	0	0	Idling of ICE; Fuel cut-off
	0	1	0	Pure ICE through odd gears ; Series hybrid functionality at stand still
	0	0	1	Pure ICE through even gears ; Series hybrid functionality at stand still
	0	1	1	Not Allowed
Mixed/Boost mode	$0 < u < 1$	0	0	Not useful as the desired functionality will not be met
	$0 < u < 1$	1	0	mixed/Boost mode
	$0 < u < 1$	0	1	mixed/Boost mode
	$0 < u < 1$	1	1	Not Allowed
Part charging part propulsion	$-1 > u < 0$	0	0	Not useful as the desired functionality will not be met
	$-1 > u < 0$	1	0	part charging part propulsion
	$-1 > u < 0$	0	1	part charging part propulsion
	$-1 > u < 0$	1	1	part charging part propulsion provided gear is neutral on one of the shaft

\*\* - Power split  $-1 > u < 0$  = Part charging part propulsion

\* - clutch signal 0 = open

\* - clutch signal 1 = close

\*\* - power split  $0 < u < 1$  = Mixed/Boost mode

\*\* - power split 1 = Pure electric mode

\*\* - power split 0 = Pure Ice mode

Table 6.4: Combination of output signals possible for ECVT THS-III generation type design

	Power Split ( $u$ )	Separation factor ( $\sigma$ )	Power request battery ( $P_{Bat}$ )	Comments
Pure electric mode	1	inf	$> 0$	Pure electric mode; cranking
	1	inf	$< 0$	Regenerative mode
Pure ICE mode	0	1	-	Pure ICE through mechanical path
	$0 < u < 1$	$0 < \sigma < 1$	0	Pure ICE through split path
	$-1 > u < 0$	$\sigma > 1$	0	Pure ICE through circulation path
Part charging part propulsion	0	$0 < \sigma < 1$	$< 0$	Part charging part propulsion through split path
	$0 < u < 1$	$0 < \sigma < 1$	$< 0$	Part charging part propulsion through split path
	$-1 > u < 0$	$\sigma > 1$	$< 0$	Part charging part propulsion through circulation path
	$-1 > u < 0$	$\sigma = 1$	$< 0$	Part charging part propulsion through mechanical path
Mixed mode/Boost mode	$0 < u < 1$	$0 < \sigma < 1$	$> 0$	Mixed mode/Boost mode through split path
	$0 < u < 1$	$\sigma = 1$	$> 0$	Mixed mode/Boost mode through mechanical path
	$-1 > u < 0$	$\sigma > 1$	$> 0$	Mixed mode/Boost mode through circulation path

## 6.7 Internal combustion engine model

The ICE is modelled as a quasi-static model. Data for a 92 kW, 1.6 litre gasoline direct injection engine, having a maximum torque of 158 Nm at 4000 rpm, is converted into the standard data type and then loaded into matlab workspace as an object file. The ICE map is shown in figure 6.10.

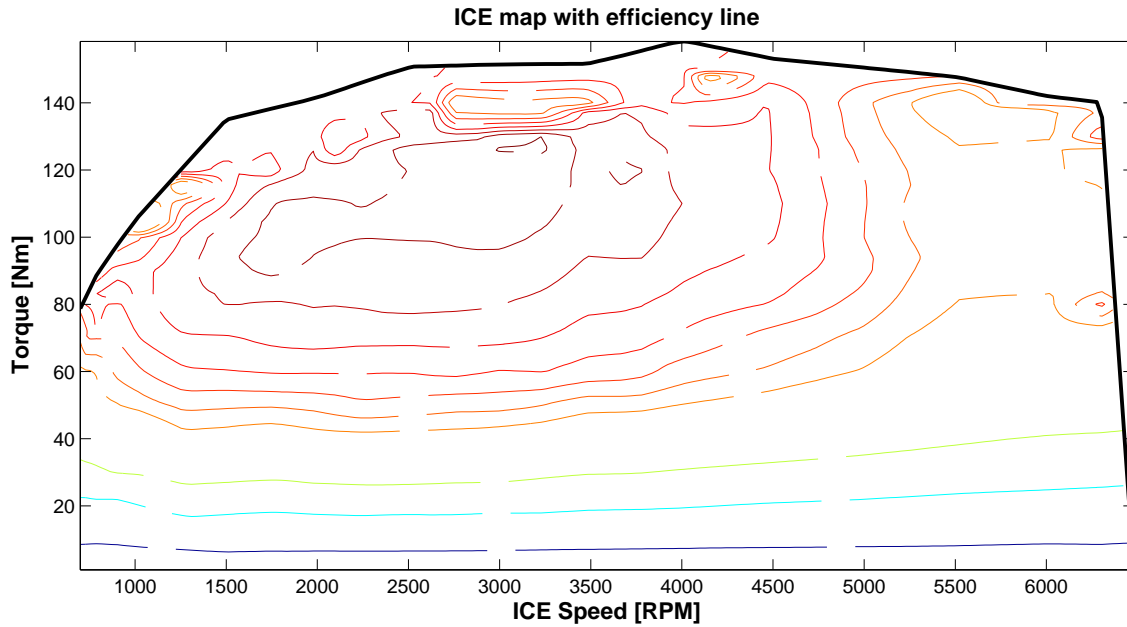


Figure 6.10: ICE map with efficiency line. Efficiency values not shown due to confidentiality reasons

The fuel power ( $P_f$ ) depends on the engine torque ( $T_e$ ), engine speed ( $w_e$ ), engine acceleration ( $\dot{w}_e$ ), inertia of the engine ( $J_e$ ) and power loss ( $P_{loss}$ ). The equation describing the fuel power consumed in the ICE is given by

$$P_f = (T_e + J_e \dot{w}_e) w_e + P_{loss}(T_e, w_e) \quad (6.36)$$

The fuel consumption is then calculated by

$$\text{Fuel consumption} \left[ \frac{l}{100km} \right] = \frac{P_f \rho_f}{Q_{LHV} \text{distance}} \times 10^5 \quad (6.37)$$

Where,  $\rho_f$  is the Density of fuel and  $Q_{LHV}$  is the lower heating value of fuel.

## 6.8 Motor-generator model

Data from the test bench for a permanent magnet synchronous machine is converted into standard type and then loaded into matlab workspace as an object file. The motor-generator map (MG for HDCT and MG2 for ECVT THS-III type design) includes the efficiency of the inverter and is shown in figure 6.11. The highest efficiency is above 95%.

Note that the motor-generator used is not designed for either HDCT power train or ECVT THS-III generation type power-train since the main aim of this thesis work is to compare the conceptual difference between HDCT parallel architecture design and ECVT THS-III generation type series-parallel design by using common power-train components and control.

Due to unavailability of the data for MG1 of the THS-III generation design, a scaled model of figure 6.11 is used which is shown in figure 6.12. The highest efficiency is 90%. Note, the distorted efficiency line along the edges of the torque line at high speed is a numerical error caused by manual sizing of the MG2 map. However

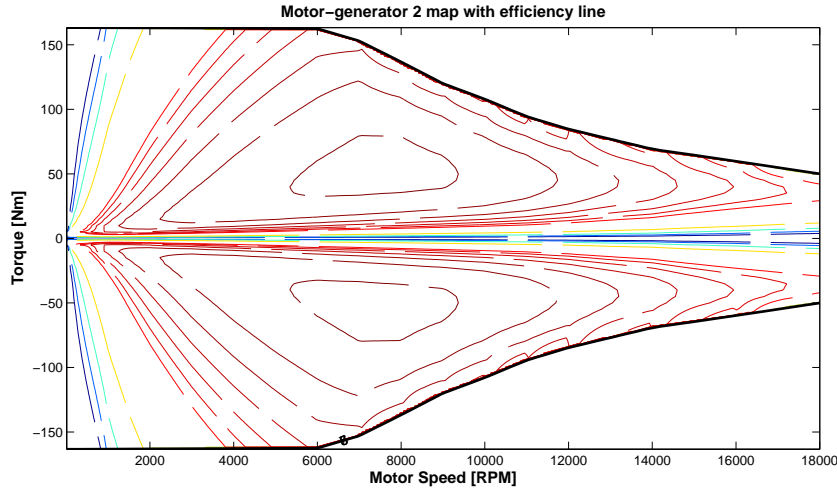


Figure 6.11: *Motor-generator 2 map with efficiency line. Efficiency values not shown due to confidentiality reasons.*

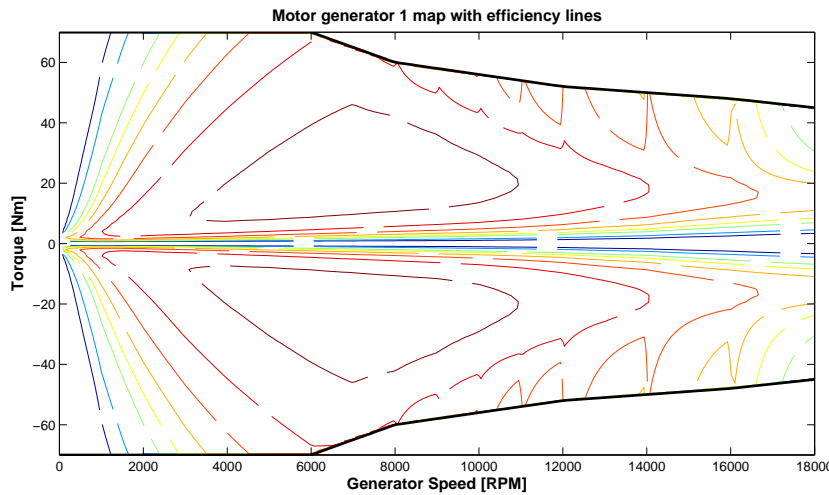


Figure 6.12: *Motor-generator 1 map with efficiency line. Efficiency values not shown due to confidentiality reasons. Note, the distorted efficiency line along the edges of the torque at high speed is a numerical error caused by manual sizing of the MG2 map. However these region in the map is not used in any of the driving cycle and simulation results are not affected.*

these region in the map is not used in any of the driving cycle and simulation results are not affected. The sizing of MG1 in THS-III generation design depends on maximum engine torque given by the equation  $\frac{T_e}{T_{MG1}} = \frac{1+\rho}{\rho}$ .

The power discharged from the battery ( $P_{bat}$ ) depends on the torque of the MG ( $T_{MG}$ ), speed of MG ( $w_{MG}$ ), acceleration of MG ( $w_{MG}$ ), inertia of MG ( $J_{MG}$ ), operating losses of MG ( $P_{Loss, MG}$ ) and auxiliary power ( $P_{aux}$ ). The equation describing the electrical power required from the battery is given by

$$P_{bat} = (T_{MG} + J_{MG}w_{MG})w_{MG} + P_{Loss, MG}(T_{MG}, w_{MG}) + P_{aux} \quad (6.38)$$

## 6.9 Battery

A simple battery model involving constant resistance ( $R_{bat}$ ) is modelled as shown in figure 6.13. Open circuit voltage ( $V_{OC}$ ) is modelled as a function of state of charge of battery (SOC) and is shown in figure 6.14.

The equations governing the operation of the Battery are

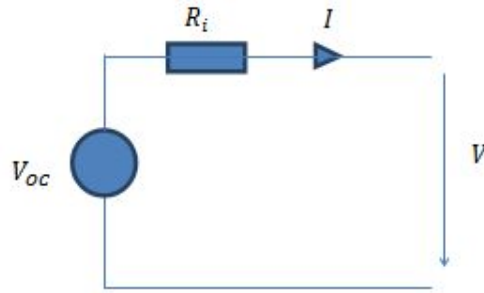


Figure 6.13: Battery model

Table 6.5: Battery parameters

Parameters	Value
Number of cells ( $N$ )	100
Resistance ( $R_{bat}$ )	0.2625 ohm
Battery Capacity ( $Q$ )	30.7 Ah
Nominal voltage ( $V_{nom}$ )	312 V
Maximum discharge current ( $i_{dis}$ )	250 A
Maximum charging current ( $i_{chrg}$ )	-150 A

$$\text{Battery power, } P_{Bat} = [V_{OC}(SOC) - IR_{bat}]IN \quad (6.39)$$

$$\text{Efficiency of the battery, } \eta_{Bat} = 1 - \frac{R_{bat}I}{V_{OC}(SOC)} \quad (6.40)$$

$$\text{SOC of the battery, } SOC_{k+1} = SOC_k - \frac{P_{Bat}\eta_{bat} \Delta t}{E} \quad (6.41)$$

By using equation 6.39, the discharge/charging current can be calculated for a given power request at the battery. Using equation 6.40 and equation 6.41 the SOC of the battery can be calculated at every instant of time.

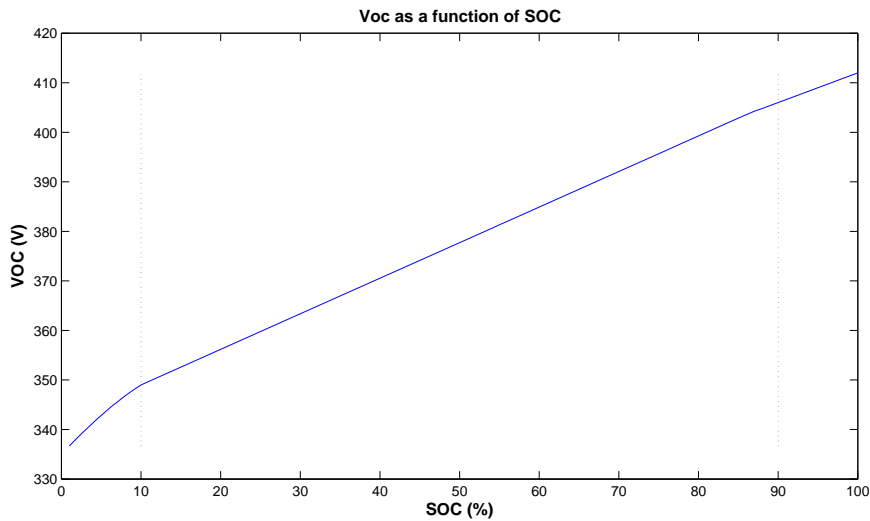


Figure 6.14:  $V_{OC}$  as a function of SOC

## 7 Simulation Result and discussion

In this chapter, efficiency simulation results and discussions are presented first followed by discussion on the performance of both HDCT parallel hybrid design and ECVT THS-III generation type series-parallel hybrid design. Both these architectures are built with the same power train components such as engine, MG and battery. Power-train control is also using the same principle.

Note the word 'type' in the phrase 'ECVT THS-III generation type series-parallel hybrid design'. The word type is used to emphasis on the fact that the power-train components used are not the exact replica of what is used in the real world THS-III generation design and only the architectural design is the same. Here onwards, ECVT THS-III generation type series-parallel hybrid design will be refereed to as ECVT design and HDCT parallel hybrid design will be refereed to as HDCT design.

### 7.1 Efficiency results and discussion

Efficiency simulation results in CD and CS mode are presented separately. Simulations are carried out on three driving cycles namely UDDS, HWFET and NEDC but only the results pertaining to NEDC driving cycle are discussed to limit the pages of this report. Similar graphs for UDDS and HWFET cycles are given in appendix section.

The assumptions and limitations of the results are discussed in section 1.4 and chapter 6

#### 7.1.1 Efficiency of both architectures during CD mode (electric mode)

The efficiency of both power-train design, HDCT and ECVT design, in CD/electric mode is shown in table 7.1. It represents how efficiently the battery energy is utilised by both the architectural designs.

Table 7.1: Efficiency in CD mode for both architectures in NEDC, UDDS and HWFET driving cycle

	NEDC cycle Road load=0.8981 Kw-hr		UDDS cycle Road load=0.7038 Kw-hr		HWFET cycle Road load=1.726 Kw-hr	
	HDCT	ECVT	HDCT	ECVT	HDCT	ECVT
Energy consumed [Kw - hr]	1.221	1.302	1.088	1.256	2.081	2.194
Distance travelled [Km]	10.93	10.93	11.99	11.99	16.51	16.51
Energy consumed per Km [Kw - hr/Km]	<b>0.1117</b>	<b>0.1191</b>	<b>0.0907</b>	<b>0.1046</b>	<b>0.1260</b>	<b>0.1329</b>

Even though both architectural design are coupled with same prime movers and same energy source, the ECVT design shows more losses (0.4045 Kw-hr) when compared to HDCT design (0.3194 Kw-hr) over the entire NEDC cycle. Figure 7.1 shows the losses in each component accrued over the entire NEDC cycle in CD/electric mode.

More losses encountered in the ECVT design can be explained as follows:

1. **'No-load' losses in MG1:** By rotating one of the shafts, either sun or ring or carrier shaft, a simple planetary gear box can be made to rotate. In CD/electric mode, in ECVT design, ICE is off and MG2 is the only prime mover supplying the power demand at the wheel. To maintain the torque equilibrium on the planetary gear set, MG1 is just spinning without generating any current which will lead to 'no-load' losses in MG1. 'No-load' losses are the losses encountered in motor-generator unit when it is just spinning without producing any power. Therefore, in ECVT deign, in addition to the operating losses in MG2, there are 'no-load' losses in MG1. Whereas, in HDCT design there is only operating losses in MG. The 'no-load' power losses in MG1 for ECVT design as a function of time over the NEDC cycle is shown in figure 7.2. The energy losses encountered in MG1 amounts to 11% of the total energy loss.

### Energy Loss in CD mode for both architectures [Kw-hr]

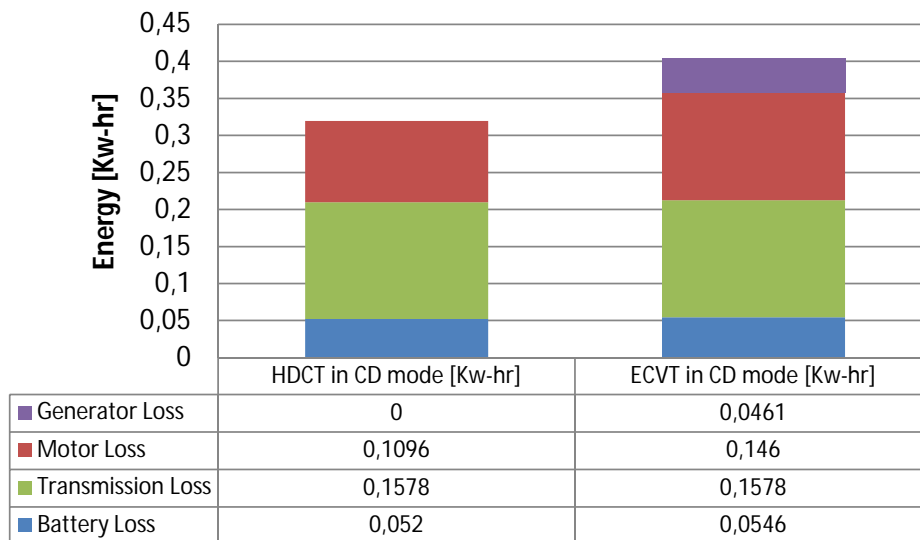


Figure 7.1: Energy loss accrued in each component in NEDC cycle for both architectures in CD/electric mode

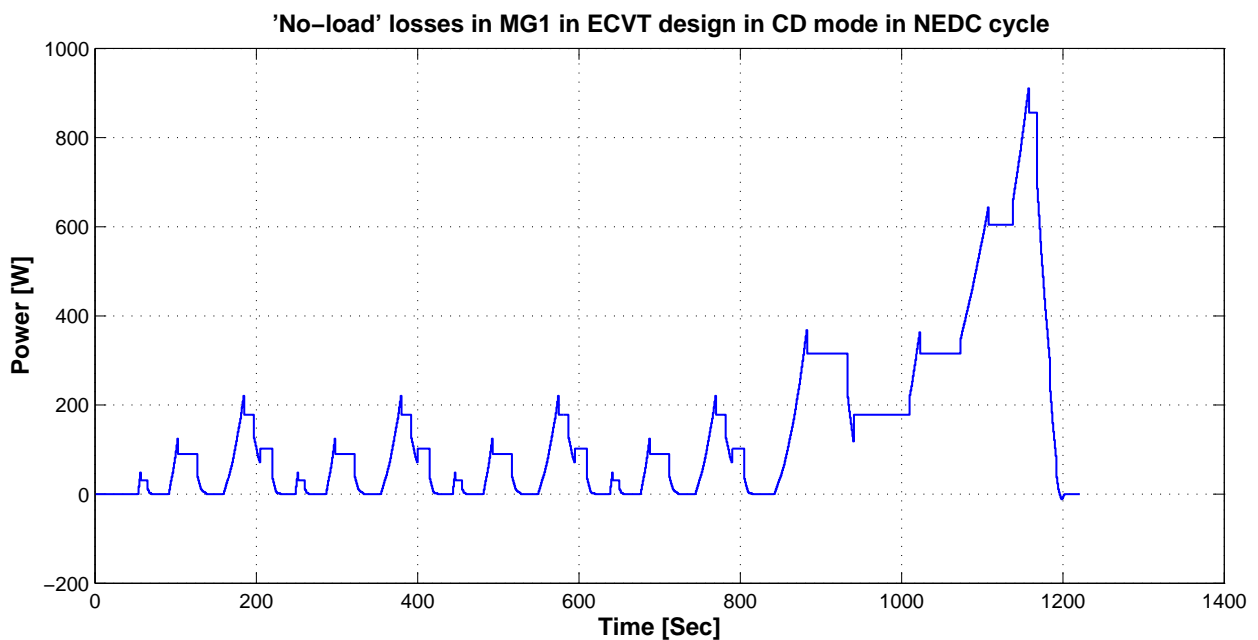


Figure 7.2: 'No-load' losses in MG1 in ECVT design in CD mode in NEDC cycle

2. **Operating losses in MG2:** In HDCT design, the hybrid power-train controller can select between three different gears depending on the operating point that gives the best efficiency. However, for ECVT design, the controller cannot influence the operating point since the ECVT design allows for one fixed gear ratio. The operating points for both the architectures are shown in figure 7.3, 7.4 and 7.5.

From figure 7.3, 7.4 and 7.5 it is seen that the MG unit (functioning as motor) in HDCT design in general operates at slightly better efficient operating points and it avoids high torque at low speeds. As mentioned earlier, the MG1 in ECVT design is just spinning and is not producing any current which will lead to no-load losses.

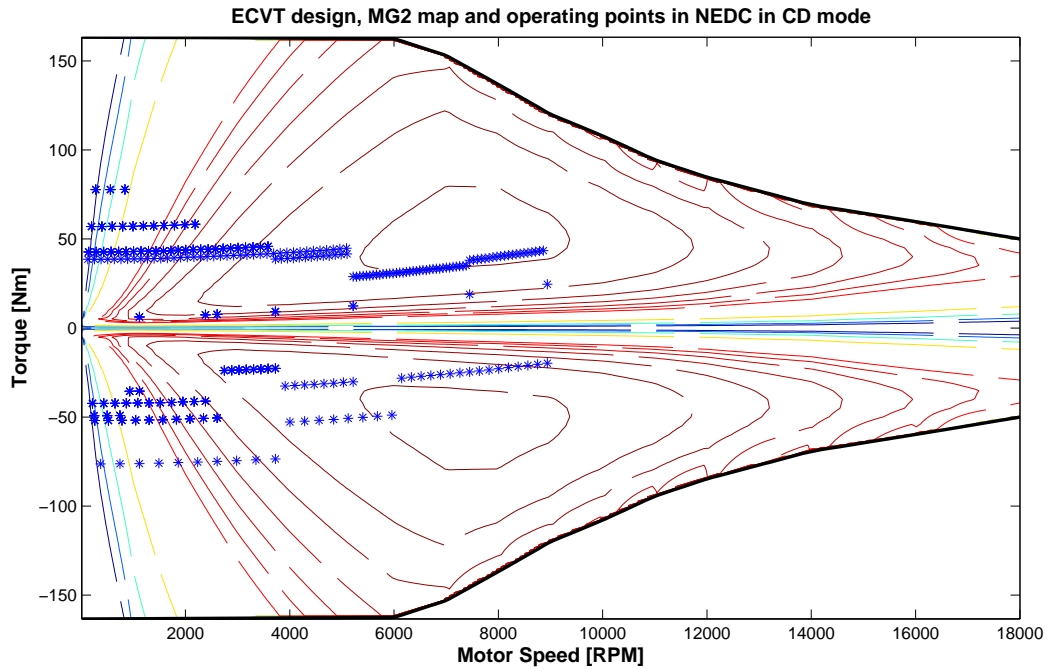


Figure 7.3: *ECVT design, MG2 map and operating points in CD mode in NEDC*

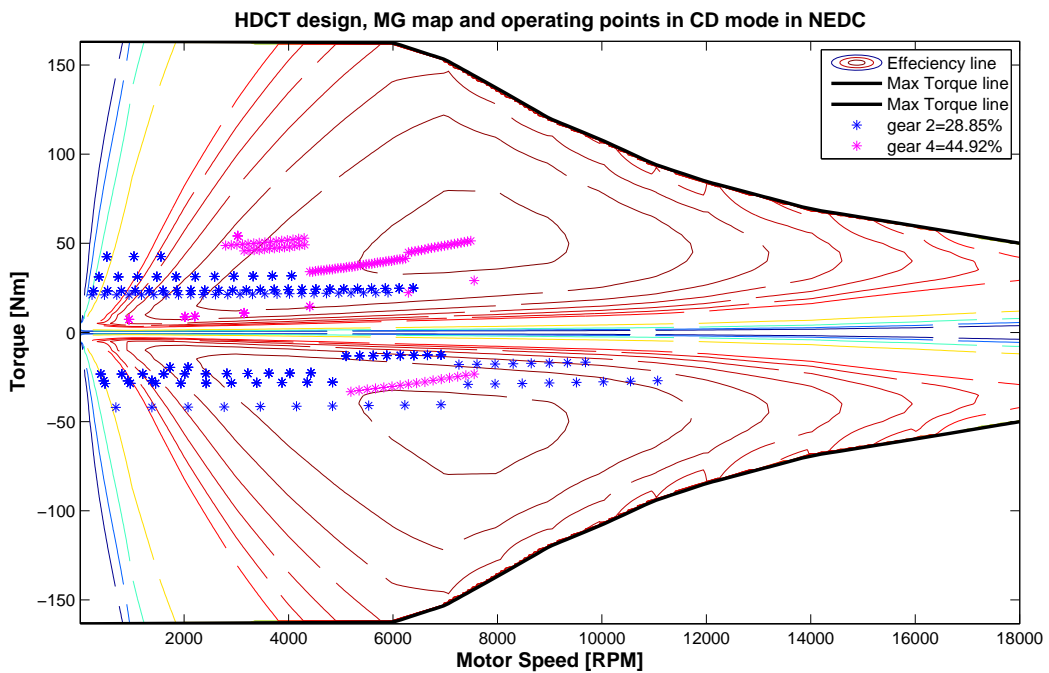


Figure 7.4: *HDCT design, MG map and operating points in CD mode in NEDC*

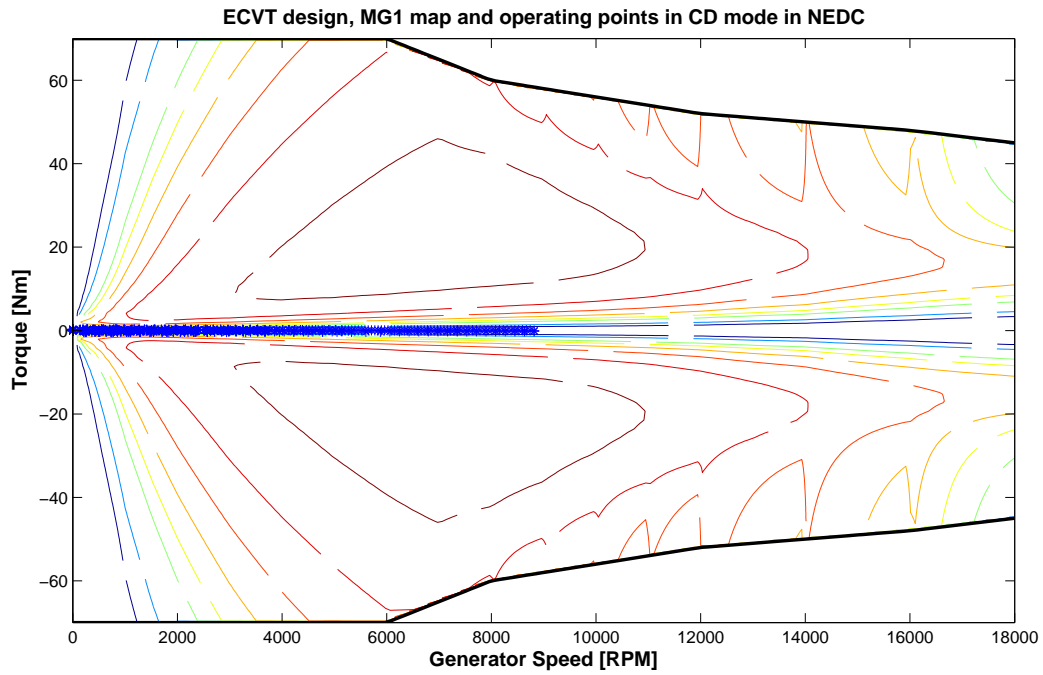


Figure 7.5: *ECVT design, MG1 map and operating points in CD mode in NEDC*

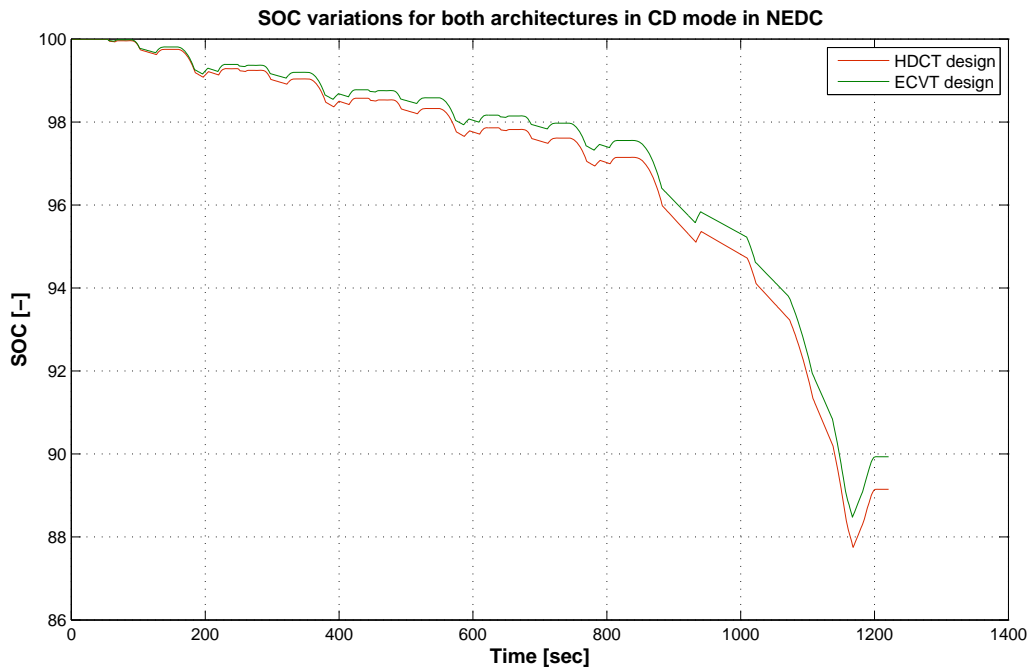


Figure 7.6: *SOC variations for both architectures in CD mode in NEDC*

3. **Battery losses:** Slightly more losses in battery in ECVT design can be attributed to the fact that the battery discharges current to suffice the road load, inertia requirements and losses of *two* electric machine where as in HDCT design the battery discharges current only to suffice the road load, inertia requirement and losses of *one* electric machine. Losses in the battery are directly proportional to square of the current ( $P_{Loss} \propto i^2$ ). Therefore, more current discharged will result in more losses.

From the discussion above for CS mode it can be concluded that HDCT design is more efficient than ECVT design in CD mode. This is mainly because of the inherent losses in the ECVT architectural design such as, no load loss in MG 1 in ECVT design. Due to these losses, the current discharged from the battery is high which will lead to poor utilization of the battery energy when compared to that of HDCT design. Therefore the SOC of the battery in ECVT design depletes more rapidly when compared to HDCT design, which is shown in figure 7.6. In addition to this, the power-train control in HDCT design has the possibilities for choosing between three gear ratios while it is not possible in the current ECVT design considered. Reference [19] shows the need and benefit of multi speed gearbox for mixed city and highway driving for electric vehicles.

However, this advantage in efficiency for HDCT design over the ECVT design might be offset due to energy loss during clutch-less gear shifting in HDCT design which is inevitable (see section 3.4.2). Although the frequency of gear shifting in CD mode in HDCT design can be minimized, it forms an area of interest for future research to investigate the time and quality of gear shift (due to higher gear steps in electric mode; 2<sup>nd</sup> to 4<sup>th</sup> and 4<sup>th</sup> to 6<sup>th</sup> gear) and also the wear and tear induced in the synchronizers.

### 7.1.2 Efficiency of both architectures during CS mode (ECMS mode)

The efficiency of the both designs, HDCT and ECVT design, in CS mode or ECMS mode is shown in table 7.2. The HDCT design uses approximately 3.1 L/100km on UDDS, 3.8 L/100km on NEDC and 4.5 L/100km on HWFET cycle. There is a variation of 0.7L/100km from one driving cycle to another. The ECVT design uses approximately 4.0 L/100km on UDDS, 4.4 L/100km on NEDC and 4.9L/100km on HWFET cycle. There is a variation of 0.4 L/100 km from one driving cycle to another. However, the HDCT design is still more fuel efficient than the ECVT design on all the three driving cycle.

Table 7.2: Efficiency in CS mode for both architectures in NEDC, UDDS and HWFET driving cycle

	NEDC cycle Road load=0.8981 Kw-hr		UDDS cycle Road load=0.7038 Kw-hr		HWFET cycle Road load=1.726 Kw-hr	
	HDCT	ECVT	HDCT	ECVT	HDCT	ECVT
Fuel Energy consumed [Kw - hr]	3.261	3.743	2.926	3.735	5.676	6.323
Distance travelled [Km]	10.93	10.93	11.99	11.99	16.51	16.51
Liter per 100 Km [L/100Km]	<b>3.882</b>	<b>4.456</b>	<b>3.176</b>	<b>4.054</b>	<b>4.475</b>	<b>4.985</b>

Figure 7.7 shows the energy losses accrued in each component in CS/ECMS mode over the entire NEDC cycle. The total energy loss in HDCT design is 2.3538 Kw-hr while that in ECVT design is 2.8363 Kw-hr.

The reason for more losses in ECVT design in spite of having same prime mover and energy source and same control principle are explained below.

1. **'No-load losses and No-spin losses' in MG :** In ECVT design, in addition to the operating losses, 'no-load' and 'no-spin' losses are encountered in the motor-generator units. 'No-spin' losses are the losses encountered in motor-generator unit when the machine generates torque without spinning, that is , there is no energy conversion. In ECVT design, 'no-load' losses are encountered in MG1 when the vehicle is in pure electric mode and in MG2 when the power to the wheel is supplied by ICE only. 'No-spin' losses are encountered in MG1 only, when the power to the wheels is supplied by ICE only through mechanical path. 'No-load losses and No-spin losses' encountered in MG1 during the NEDC cycle is shown in figure 7.8. Although the energy losses at every instant of time is low, it depreciates the overall efficiency of the ECVT design over the complete driving cycle.

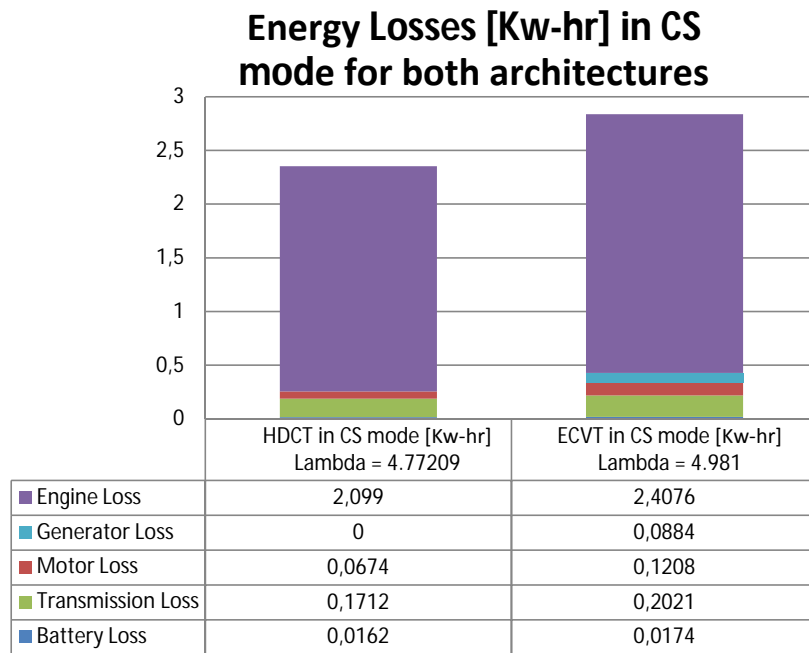


Figure 7.7: Energy loss accrued in each component in NEDC cycle for both architectures in CS/ECMS mode

While in HDCT design, there are *no* 'no-spin' losses encountered. No-load losses in MG is encountered when the power to the wheels comes from ICE alone via the even gears only.

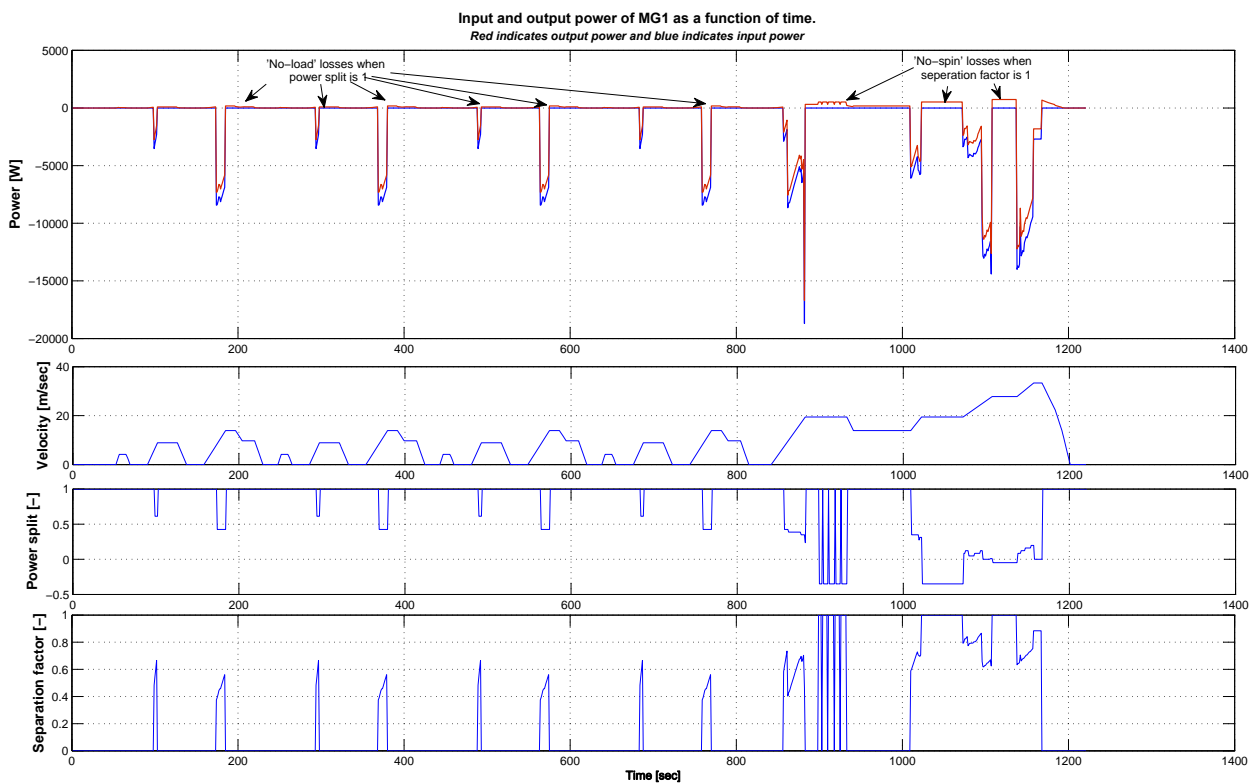


Figure 7.8: No-load and No-spin losses in ECVT design in MG1 in CS mode in NEDC

2. **Operating losses in MG:** Figure 7.9 shows the ICE output for both architectures with road load in

CS mode in NEDC cycle.

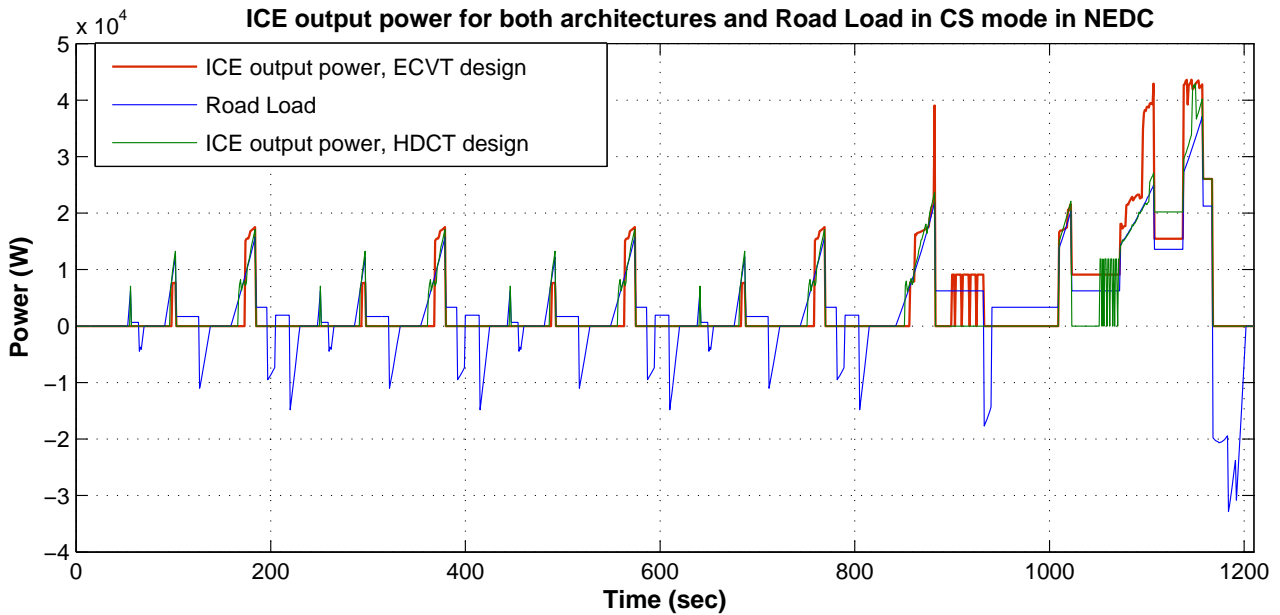


Figure 7.9: ICE power output for both architectures in CS mode in NEDC

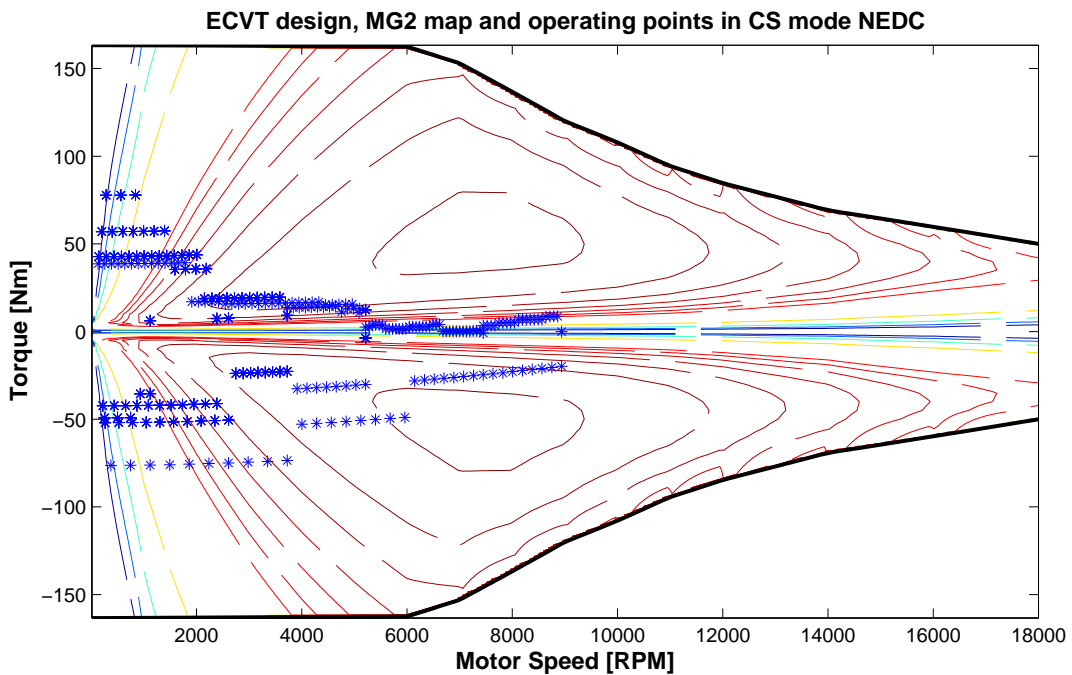


Figure 7.10: ECVT design, MG2 map and operating points in CS mode in NEDC

From figure 7.9 it is seen that the ICE kicks in much earlier in HDCT design than that in the ECVT design, which means the amount of time the vehicle runs with electricity (Partially or fully) is more in ECVT design when compared to HDCT design in CS mode in NEDC cycle.

As discussed earlier, in HDCT design, the power-train controller has the ability to select from three different gear ratios while it is not possible in ECVT design. The operating points in the motor generator units in CS mode in NEDC cycle for both architectures are shown in figure 7.10, 7.11 and 7.12, . From figures 7.10, 7.11 and 7.12 it is inferred that the gear ratios in HDCT and the only gear ratio in ECVT

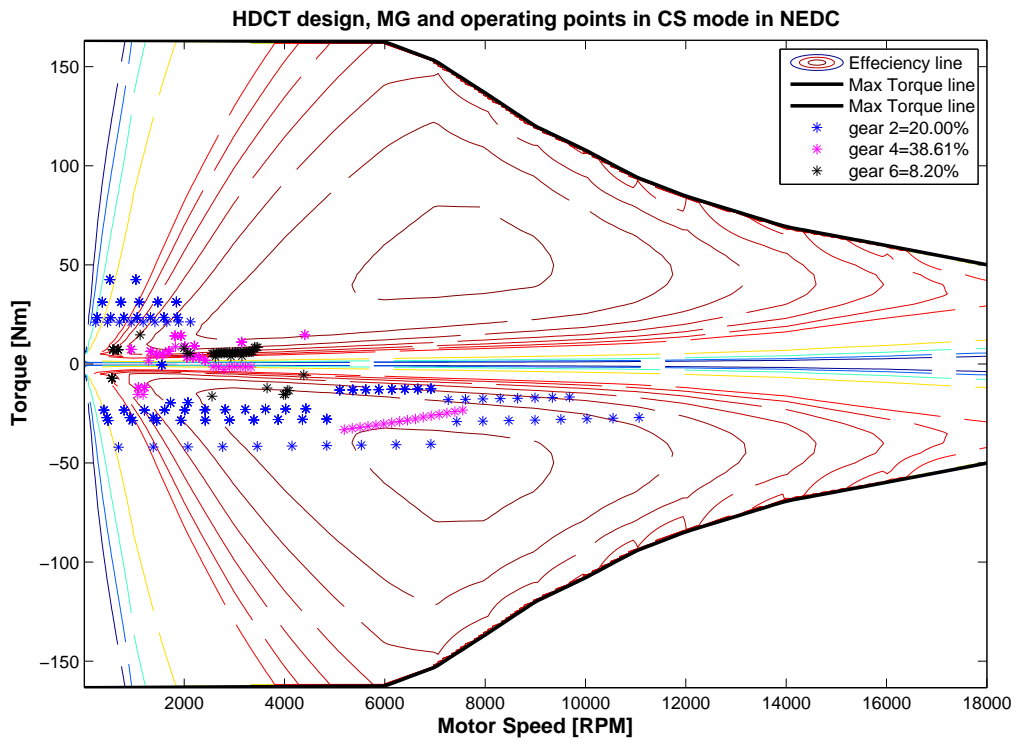


Figure 7.11: HDCT design, MG map and operating points in CS mode in NEDC

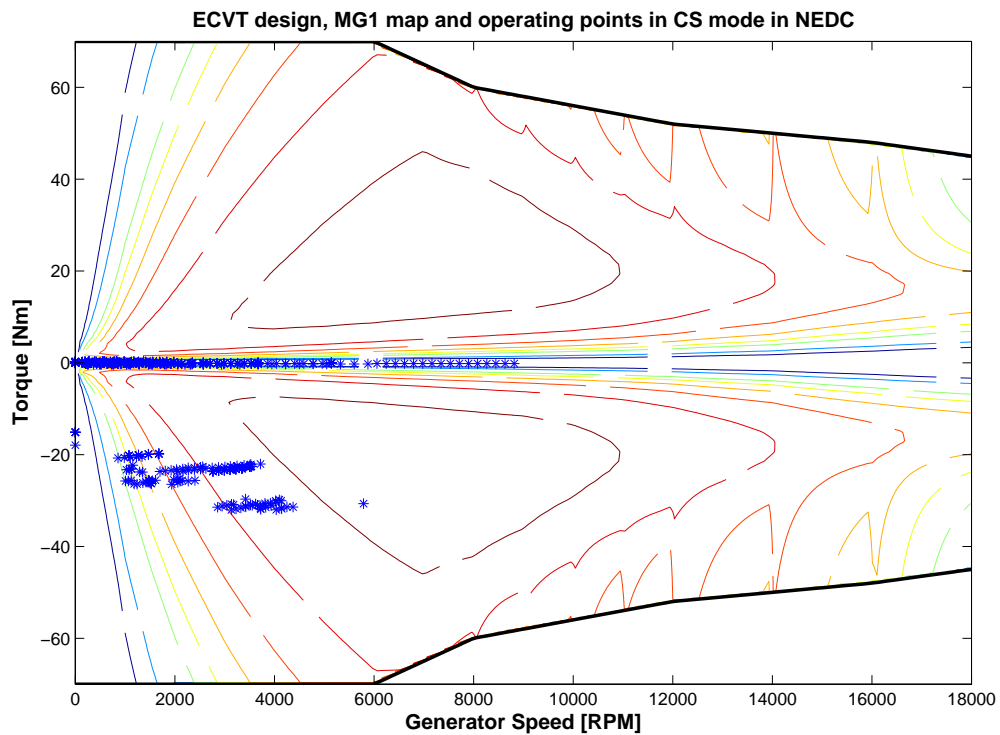


Figure 7.12: ECVT design, MG1 map and operating points in CS mode in NEDC

design are not optimised for CS mode. More losses in MG units in ECVT design than in HDCT design as implicit from figure 7.7 is due to the amount of time the vehicle runs with electricity (partially or fully) as discussed in figure 7.9.

- Battery loss:** The battery in ECVT design has to supply for the additional losses, as a result the SOC of the battery in ECVT design depletes more quickly than in the HDCT design as shown in figure 7.13.

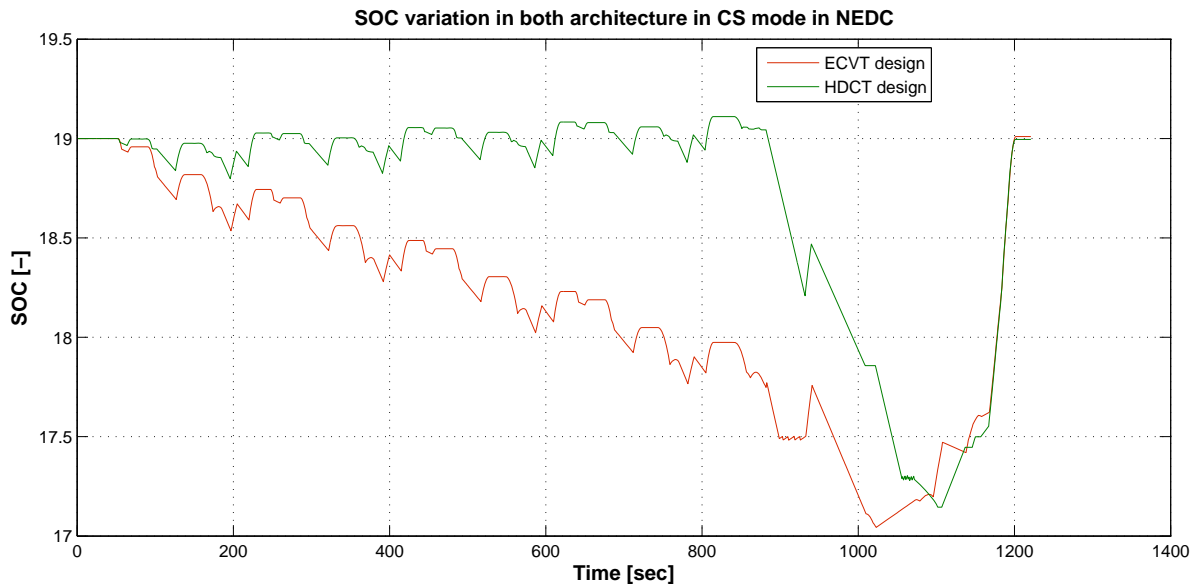


Figure 7.13: SOC variation in both architectures in CS mode in NEDC

- Engine losses:** Figure 7.14 and 7.15 shows the operating points on the ICE map for both architectures. The operating points on the ICE map in ECVT design is concentrated at highest efficiency points, whereas, the operating points on the ICE map of HDCT is more spread out. This is due to the fact that there is flexibility in choosing the ICE speed independent of the vehicle speed in ECVT design, whereas, the ICE speed is dependent on the vehicle speed by the gear ratio in HDCT design. However, the engine efficiency in HDCT design is very close to that of ECVT design with deviations typically less than 1%.

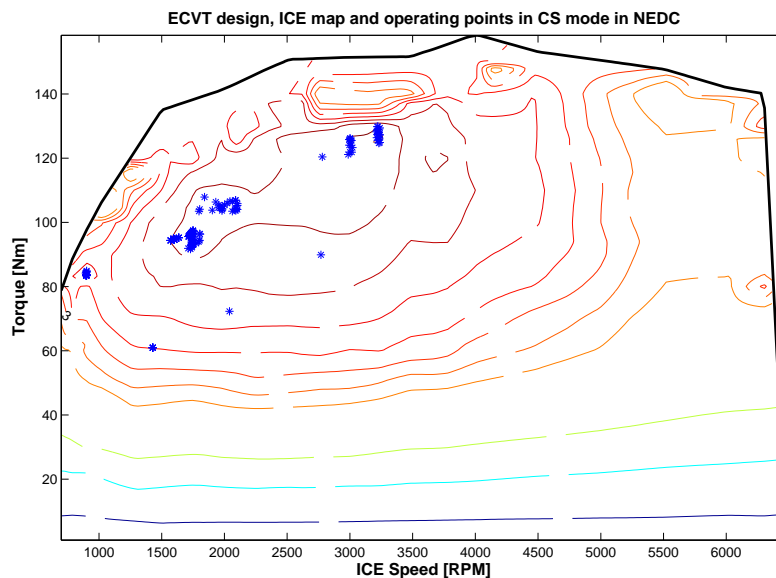


Figure 7.14: ECVT design, ICE map and operating points in CS mode in NEDC

The ICE in ECVT architecture although operating at the sweet points (Highest efficiency points), it

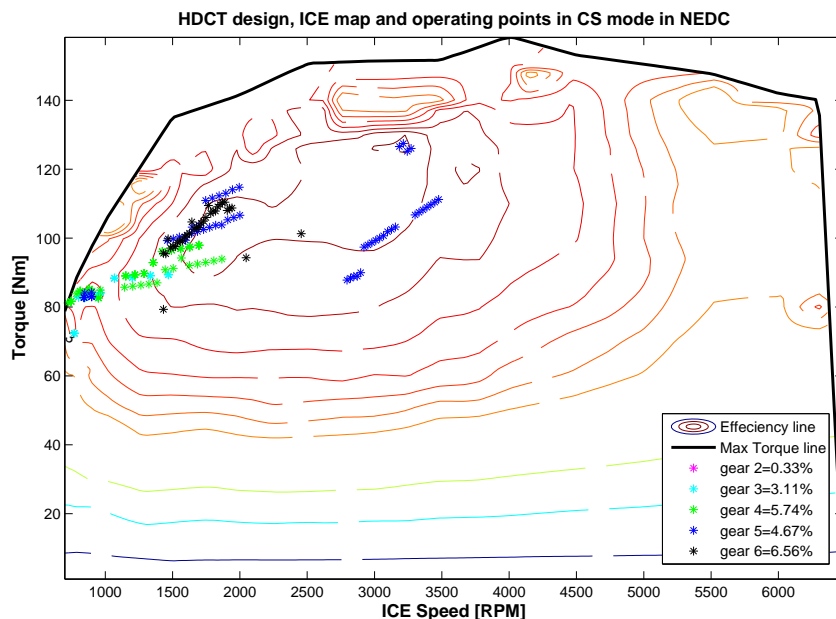


Figure 7.15: HDCT design, ICE map and operating points in CS mode in NEDC

delivers more power than road load when compared to that with HDCT design as shown in figure 7.9. An alternate way of showing the difference in operating points is shown in 7.16

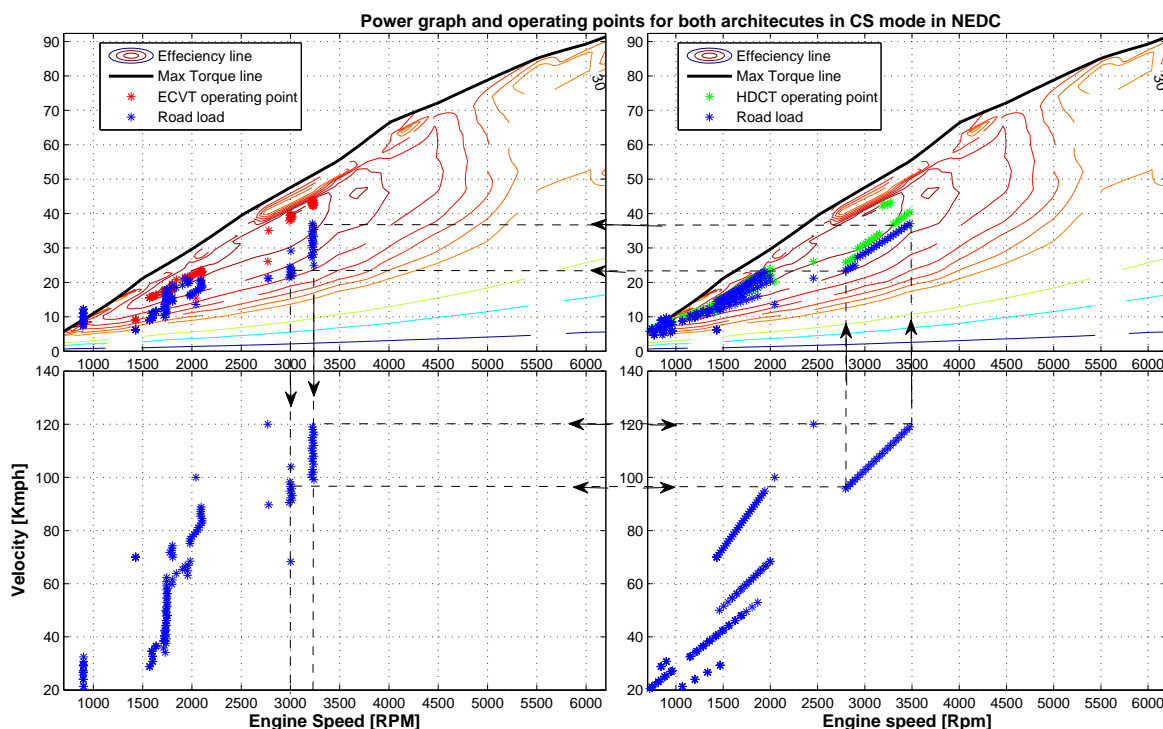


Figure 7.16: Power map for both architecture with operating points and road load

**Reading figure 7.16:** Bottom right graph shows the engine speed for a particular vehicle speed in NEDC cycle for HDCT design as chosen by the power-train control. At 120 Km/h, the operating engine speed for HDCT design is around 3500 rpm. At this point, the road load is determined by extrapolating

the line to top right graph which shows the operating point and road load at 120 kmph in NEDC for HDCT design. The road load is around 37 kW and the ICE output is around 40 kW. Since the road load for both HDCT and ECVT design experienced during NEDC is the same, a line can be extrapolated to the left which shows the operating point and road load on ICE map in ECVT design. The ICE in ECVT design produces around 42 kW which is slightly more than that produced by ICE in HDCT design. Further, extrapolating the line to bottom left graph gives the engine speed at 120 kmph in ECVT design which is around 3200 rpm. This figure can be used to compare the engine speed for both architectures at particular vehicle velocity and road load. Also, it gives an idea about how ECVT design tends to produce more power than the HDCT design for particular velocity.

For example, at around 90 kmph, the ICE in HDCT design operates at approximately 2800 rpm. At this particular vehicle velocity of 90 kmph, the road load is around 24 kW obtained by extrapolating a line to the top right graph. The ICE produces approximately 27 kW in HDCT design to suffice the transmission losses. Extrapolating the road load point to the left gives the ICE output for ECVT design which is around 42 kW. Further extrapolating the line to the bottom left graph gives the ICE speed for ECVT design which is around 3000 rpm. Therefore from the above two example and figure 7.9 it is clear that the ICE in ECVT design tends to produce more power than the ICE in HDCT design. This extra power produced by ICE in ECVT design is lost partially or fully through electric path while trying to supply for double energy conversion losses.

Assuming the transmission efficiency to be 100% ,the best fuel economy can be obtained by shifting the operating point to the best efficiency point on the engine map along the '*constant power line*'. The ECVT design tends to shifts the operating point to the best efficiency point on the engine map by trying to reduce or increase the engine speed. In doing so it doesn't operate along the '*constant power line*' and produces more power than that is produced in conventional design. This, extra power produced by ICE in ECVT design is lost partially or fully through electric path while trying to supply for the losses inherent in the architectural design which is briefly explained in section 7.1.3.

From the discussion above for CS mode, it can be concluded that HDCT design is more efficient than ECVT design even in CS mode. The ECVT design although improves the efficiency of the ICE, it deteriorates the overall efficiency of the power-train itself. This is mainly because of the inherent losses in the ECVT architectural design such as, no load losses in MG1 and MG2, no-spin loss in MG1, double energy conversion loss, and loss due to circulation of energy. No-load loss in MG1 is encountered when the vehicle is in pure electric mode. No-spin loss in MG1 and no-load loss in MG2 is encountered when the power demand at the wheel is met by ICE alone via the mechanical path. The power flow path leading to double energy conversion loss is one of the most prominent and often used paths in order to obtain the ECVT action. The energy circulation path leads to least power-train efficiency. These losses in the architectural design have to be supplied either by fuel energy or electric energy thus leading to more fuel consumption or electricity consumption.

Therefore, irrespective of the mode chosen there are additional losses in the ECVT architectural design which leads to lower efficiency when compared to HDCT architectural design.

### 7.1.3 Summary of additional losses in ECVT design

In this section, the summary of the additional losses in the ECVT design excluding the common losses in both designs are presented. Common losses includes ICE losses , transmission losses, battery losses, electric machine operating loss. Note that, Common losses refer to losses which are common in both the designs but the degree of losses need not be same. Note that in figure 7.19, 7.18 and 7.20 the losses are assumed to be supplied by the battery, however in general, it could be supplied by ICE also.

1. **'No-load' loss:** When the vehicle is in pure electric mode (power split = 1), ICE is off and MG2 is the only prime mover supplying the power demand at the wheel. To maintain the torque equilibrium on the planetary gear set, MG1 is just spinning without generating any current which will lead to 'no-load' losses in MG1 as shown in figure 7.17.
2. **Double energy conversion loss:** When the power request at the wheels is met by ICE only, the power flowing through electrical path will experience double energy conversion loss as shown in figure 7.18. This is when the separation factor is greater than zero but less than 1. This power flow path in

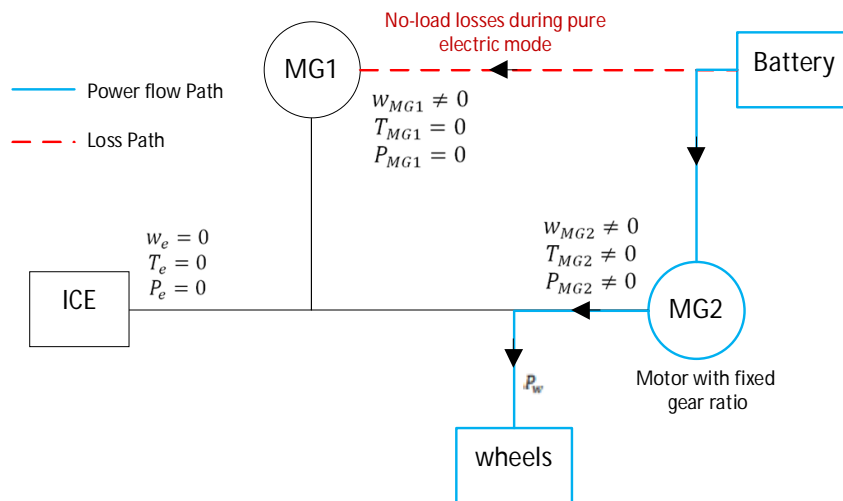


Figure 7.17: No-load loss in MG1 in ECVT design when the vehicle is in pure electric mode

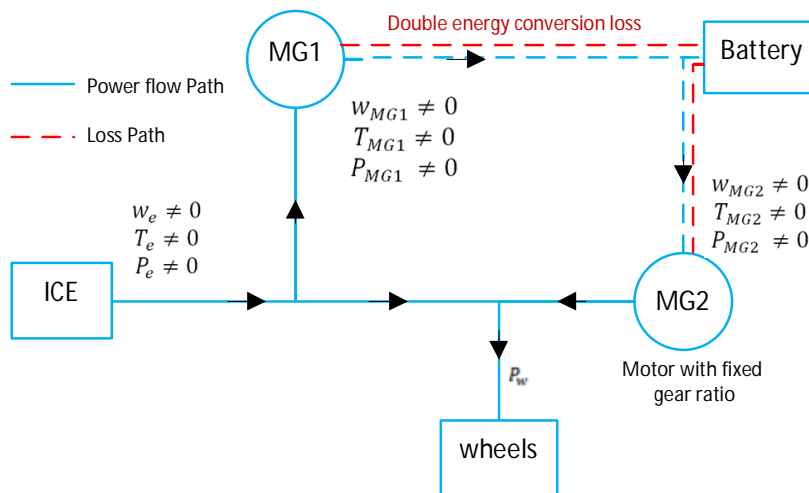


Figure 7.18: Double energy conversion loss in ECVT design when the separation factor is greater than zero but lesser than one. Note, in this figure the losses are assumed to be supplied by the battery

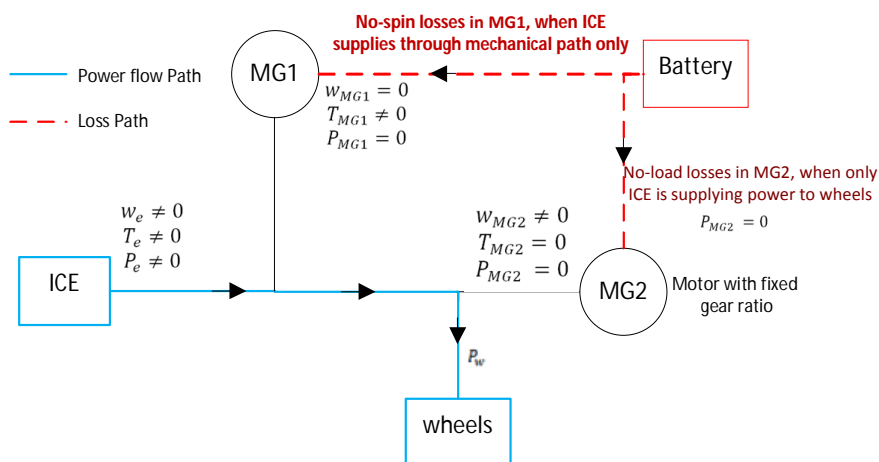


Figure 7.19: No-load and No-spin loss in MG2 and MG1 respectively in ECVT design when the power request at the wheels is met by ICE only via mechanical path. Note, in this figure the losses are assumed to be supplied by the battery

ECVT design is one of the most prominent path and most often used in order to achieve the ECVT action of the architecture.

3. **'No-spin' loss:** There are no-load losses in MG2 and no-spin losses in MG1, when the power request at the wheels is met by ICE alone via mechanical path as shown in figure 7.19. This is when the separation factor is 1 and power split is zero. In this mode the ICE speed is dependent on the vehicle speed and ECVT action of the design is hindered.
4. **Loss due to circulation of energy:** When the separation factor is greater than one, the function of MG2 and MG1 reverses. MG2 acts as a generator sending power to MG1 which functions as a motor. During this mode there is energy loss due to double energy conversion. In addition to double energy conversion loss, there is losses due to circulation of energy caused due to efficiency of the meshing gear as shown in figure 7.20.

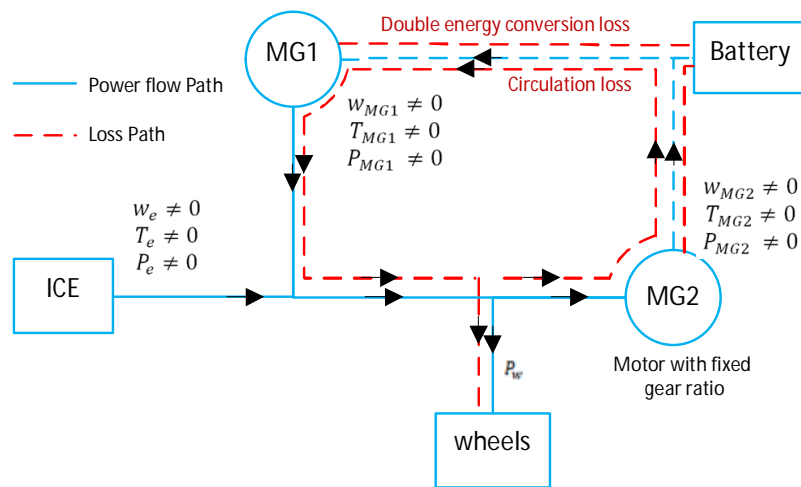


Figure 7.20: Double energy conversion loss and loss due to circulation of energy when separation factor is greater than one. Note, in this figure the losses are assumed to be supplied by the battery

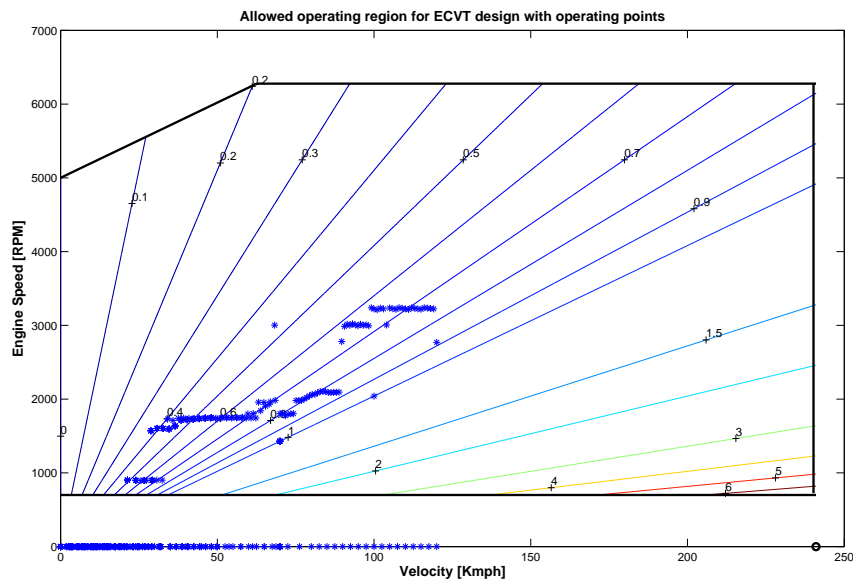


Figure 7.21: Separation factor chosen by power-train control in CS mode in NEDC in ECVT design

Therefore, these inherent losses within the power-train architecture decreases the benefit of fuel economy of the continuously variable transmission irrespective of the mode chosen. The power-train control determines the

best possible power split and separation factor taking these inherent losses into consideration. The separation factor chosen by the power-train control is shown in figure 7.21.

### 7.1.4 Summary of additional losses in HDCT design

This section will explain the additional losses in HDCT architecture excluding the common losses in both architectures. Common losses includes ICE losses inclusive of inertia, transmission losses, battery losses, electric machine operating loss, inertia of electric machines and other common losses. Note that, Common losses refer to losses which are common in both the designs but the degree of losses might need not be same.

1. **No-load loss:** When the request at the wheels is met by ICE alone via the even gears there are no-load losses in MG as shown in figure 7.22 since it is located on the common shaft. Note that, when the request at the wheels is met by ICE alone via the odd gear there are *no* no-load losses encountered in the MG.

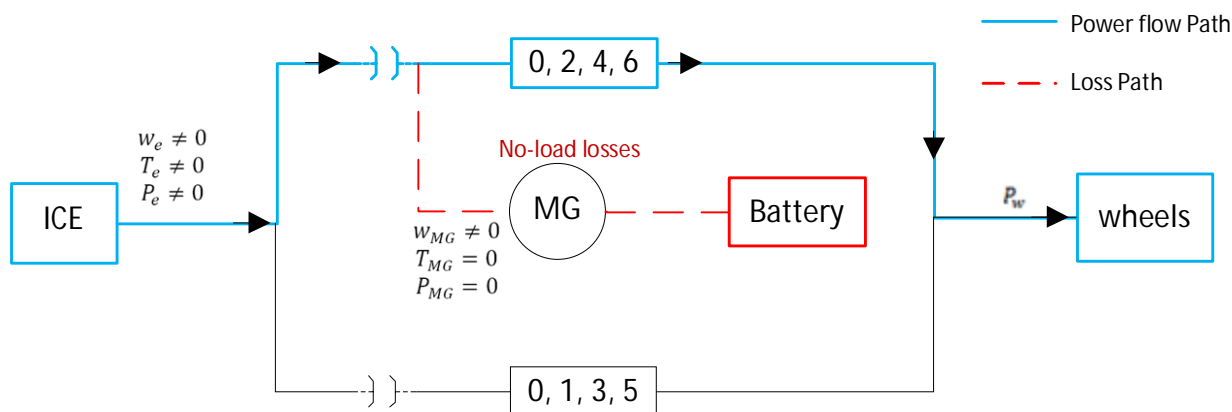


Figure 7.22: No-load losses in HDCT design when the power request at the wheels is supplied by ICE alone via the even gears

2. **Energy loss during charging via odd gear:** When the ICE is used to meet the power request at the wheels via the odd gears and some part of it is transmitted through the final drive to the motor via the even gears to charge the battery, the power flow to the battery will encounter transmission loss twice as shown in figure 7.23. However, this transmission loss is quite small when compared to the MG efficiency advantages gained by using one of the three even gears.

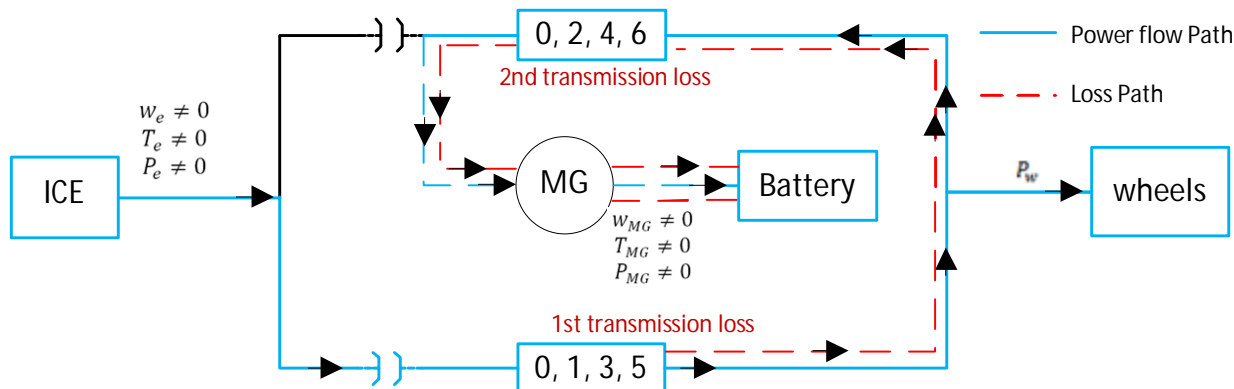


Figure 7.23: Energy loss during charging via the odd gear in HDCT design

3. **Power loss while shifting gear during CD mode:** As discussed in section 3.4.2, there will be battery energy loss during clutch-less gear shifting while the vehicle is in CD mode. However, it must be

noted that due to high rated motor-generator speed, the frequency of gear shifting while in electric mode can be minimised.

- 4. **Other losses:** In addition to the losses explained above, there are clutch activation, gear shifting and losses in hydraulics (due to controlling the pre selection of the gear). Since, analysing these losses will require detailed models of the gear box, they are not included in the simulation in this thesis work.

The power-train control determines the best possible power split and gear ratio at every instant of time with the main aim of reducing the operational cost over the entire NEDC cycle. The operating point on graph of engine speed vs vehicle velocity and MG speed vs Engine speed for HDCT design as chosen by the power-train control is shown in figure 7.24 and 7.25.

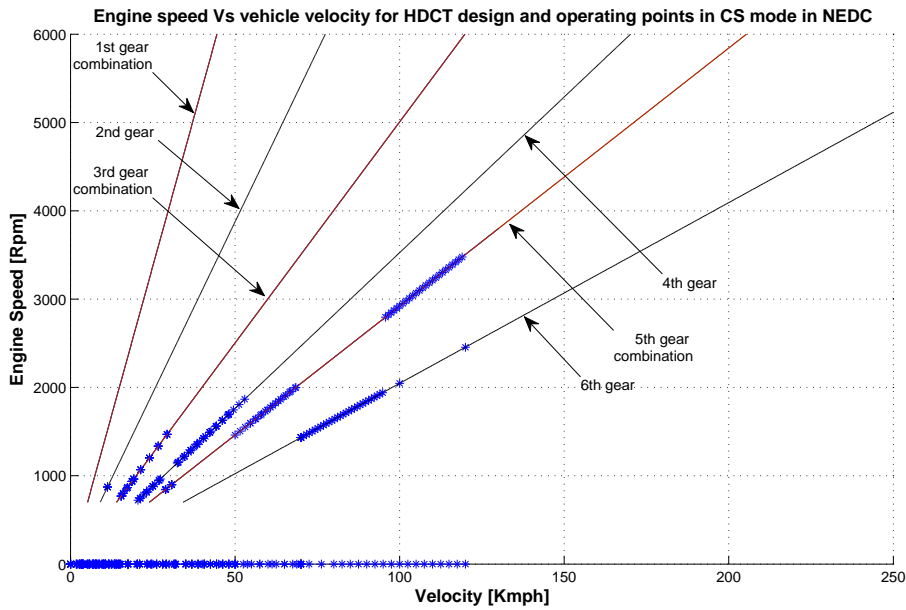


Figure 7.24: Engine speed vs vehicle velocity and operating points in CS mode in NEDC in HDCT design

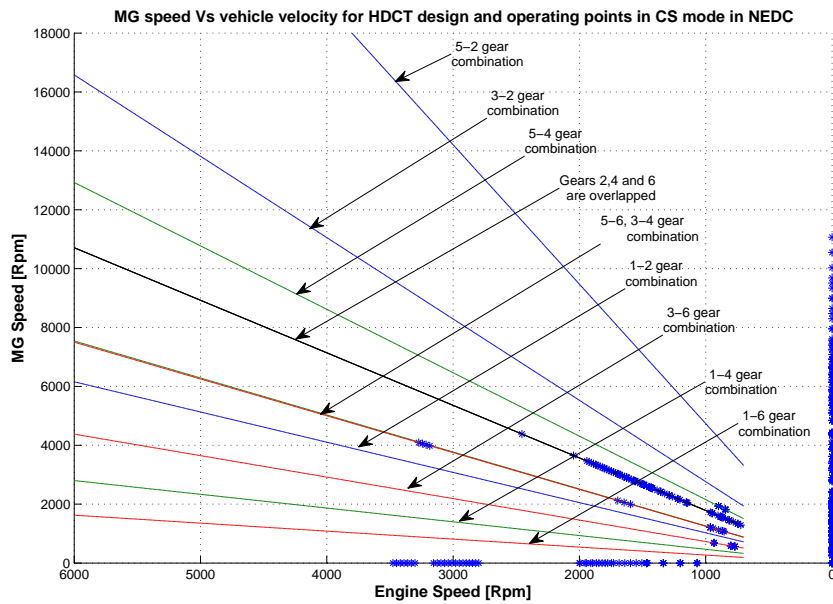


Figure 7.25: MG speed vs vehicle velocity and operating points in CS mode in NEDC in HDCT design

### 7.1.5 Comparison of additional losses within both the architectures

Table 7.3 lists out the losses encountered in both designs excluding the common losses. Losses common to both design includes ICE losses inclusive of inertia, transmission losses, battery losses, MG operating loss and other common losses.

Table 7.3: Comparison of additional losses within both the architectures

Operating mode	Losses in the ECVT design excluding common loss to both architecture	Losses in the HDCT design excluding common loss to both architecture
Electric mode	<ol style="list-style-type: none"> <li>1. No-load losses in MG1</li> <li>2. Inertia of two electric machines during acceleration phase.</li> </ol>	<ol style="list-style-type: none"> <li>1. Gear shifting losses.</li> <li>2. Inertia of one electric machines during acceleration phase.</li> </ol>
ICE mode	<ol style="list-style-type: none"> <li>1. Double energy conversion loss. (when <math>1 &gt; \sigma &gt; 0</math> and <math>1 &lt; \sigma \leq \sigma_{max}(v)</math>)</li> <li>2. Battery loss.</li> <li>3. Inertia of two MG unit during acceleration phase.</li> <li>4. No-load losses in MG2. (When <math>\sigma = 1</math>).</li> <li>5. No-spin losses in MG1 (When <math>\sigma = 1</math>).</li> </ol>	<ol style="list-style-type: none"> <li>1. Clutch losses.</li> <li>2. Gear shifting losses.</li> <li>3. Inertia of one MG unit only when even gear is selected for ICE to supply the power to the wheels.</li> <li>4. No-load losses in MG only when even gear is selected for ICE.</li> </ol>
Boost mode	<ol style="list-style-type: none"> <li>1. Double energy conversion loss (when <math>1 &gt; \sigma &gt; 0</math> and <math>1 &lt; \sigma \leq \sigma_{max}(v)</math>).</li> <li>2. Inertia of two MG unit during acceleration phase.</li> <li>3. Battery energy loss due to controlling the speed of MG1.</li> <li>4. No-spin losses in MG1 (when <math>\sigma = 1</math>).</li> </ol>	<ol style="list-style-type: none"> <li>1. Clutch loss.</li> <li>2. Inertia of one MG unit during acceleration phase.</li> <li>3. Gear shifting losses.</li> </ol>

## 7.2 Performance capability of both architectures

In this section the performance capability of the ECVT architecture and HDCT architecture are presented.

### 7.2.1 Performance capability of both architectures in pure electric mode

The MG in HDCT design, can use either second or fourth or sixth gear. In addition to these three gear ratio there is one gear ratio specific to the MG unit. In ECVT design, MG can use one fixed gear ratio. The acceleration capability of both the architectures is shown in figure 7.26. Note that, figure 7.26 shows the hardware capability of the architectural design and top speed could be limited by the power rating of MG unit. HDCT design has the capability of having different top speed specific to electric mode depending on the rated speed of MG. From figure 7.26 it is clear that HDCT design has better acceleration capability in CD/electric mode.

### 7.2.2 Performance capability of both architectures in ICE mode when battery power is zero

Figure 7.27 shows the acceleration capability of both architectures in pure ICE mode when battery power is zero. Acceleration capability of HDCT design follows a six speed conventional transmission whereas acceleration capability of ECVT design is intricate and is explained in section 7.2.4.

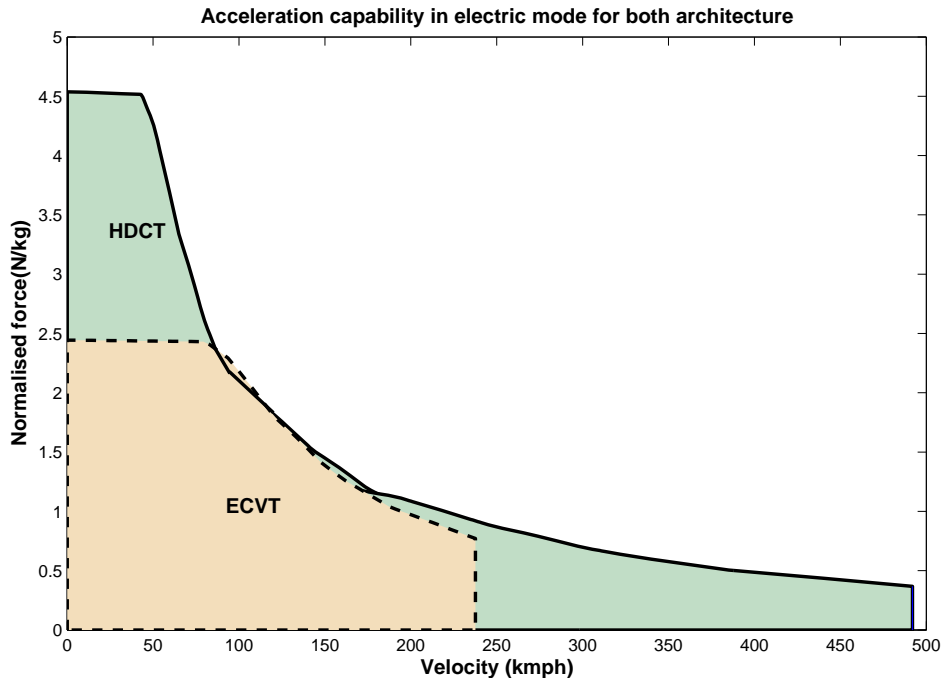


Figure 7.26: Acceleration capability of both architectures in pure electric mode

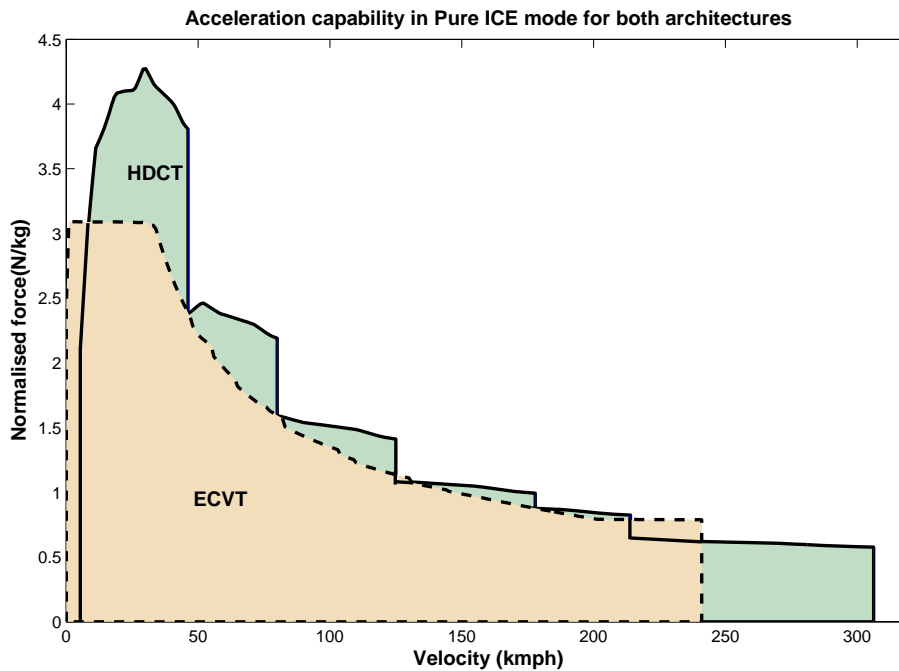


Figure 7.27: Acceleration capability of both architectures in ICE mode when power from the battery is zero

### 7.2.3 Performance capability of both architectures in Boost mode when battery power is positive

In ECVT architecture the power-train control selects the separation factor such that the maximum torque region of the engine is utilised. Note that the engine is not assisted by any fixed gear ratio other than the ECVT transmission itself. Part of the power flowing electrically from the ICE is added up with the battery power such that the maximum torque of the MG2 is utilised. Note that MG2 uses one fixed gear ratio. Figure 7.28 shows the acceleration capability of both designs in boost mode when maximum power from the battery is

utilised. An alternate figure specific to the acceleration capability of HDCT design in boost mode showing different gear combinations possible is shown in figure 7.29. From figure 7.28, it is clear that HDCT design has excellent acceleration capability in boost mode when compared to ECVT design.

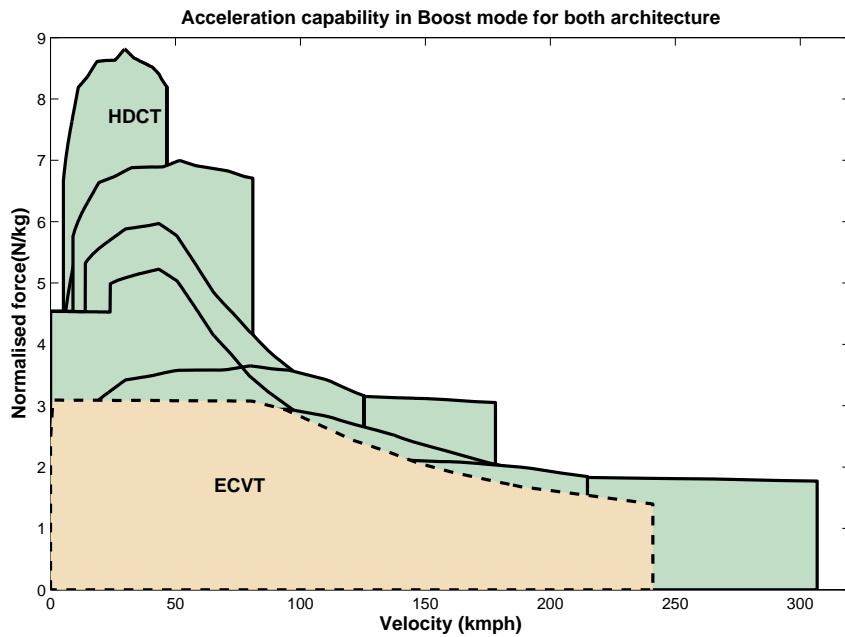


Figure 7.28: Acceleration capability of both architectures in Boost mode when power from the battery is positive

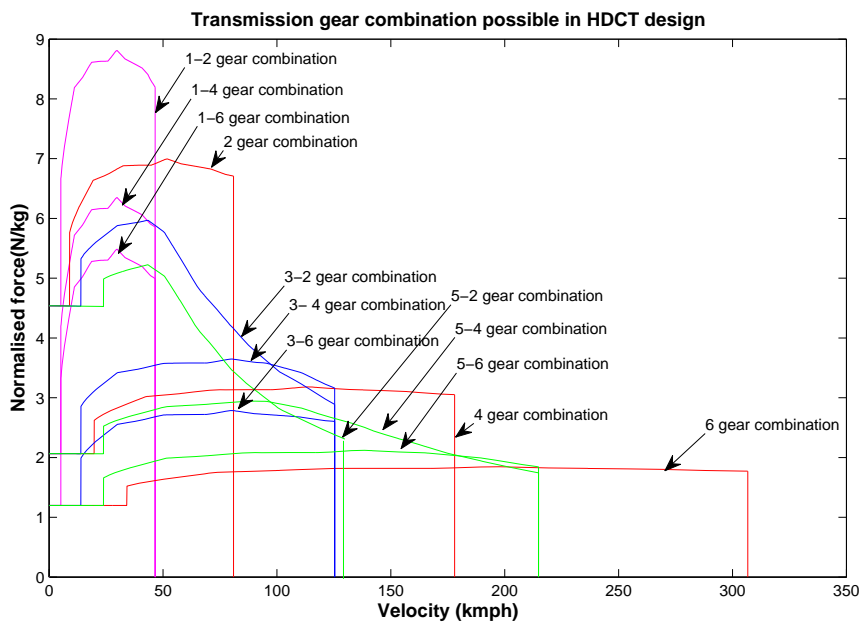


Figure 7.29: Transmission gear combinations possible in HDCT design

#### 7.2.4 Performance capability of ECVT architecture in ICE mode when battery power is zero (reference figure 7.27)

In conventional vehicle, the acceleration depends on the torque rating of the engine/MG and gear ratio. However in ECVT design it is difficult to say which is the best for acceleration. There are three possible ways to attain maximum acceleration in ECVT design in pure ICE mode. They are

1. Choose the separation factor such that the engine revs for maximum engine torque.
2. Choose the separation factor such that the engine revs maximum and maximum power flows through MG1 and then finally to MG2. However, MG2 has a limit on how much power it can use which vary with vehicle velocity.
3. Or a mix of above both.

The separation factor chosen by power-train control for maximum acceleration in ICE mode is shown in figure 7.30. MG1 speed for that particular separation factor is shown in figure 7.31.

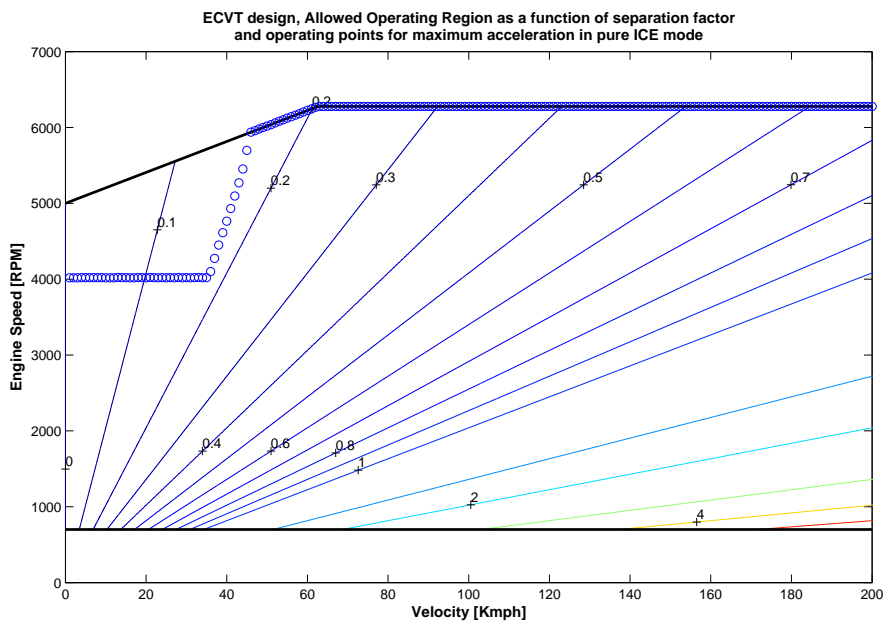


Figure 7.30: Separation factor chosen by power-train control for maximum acceleration in pure ICE mode in ECVT design

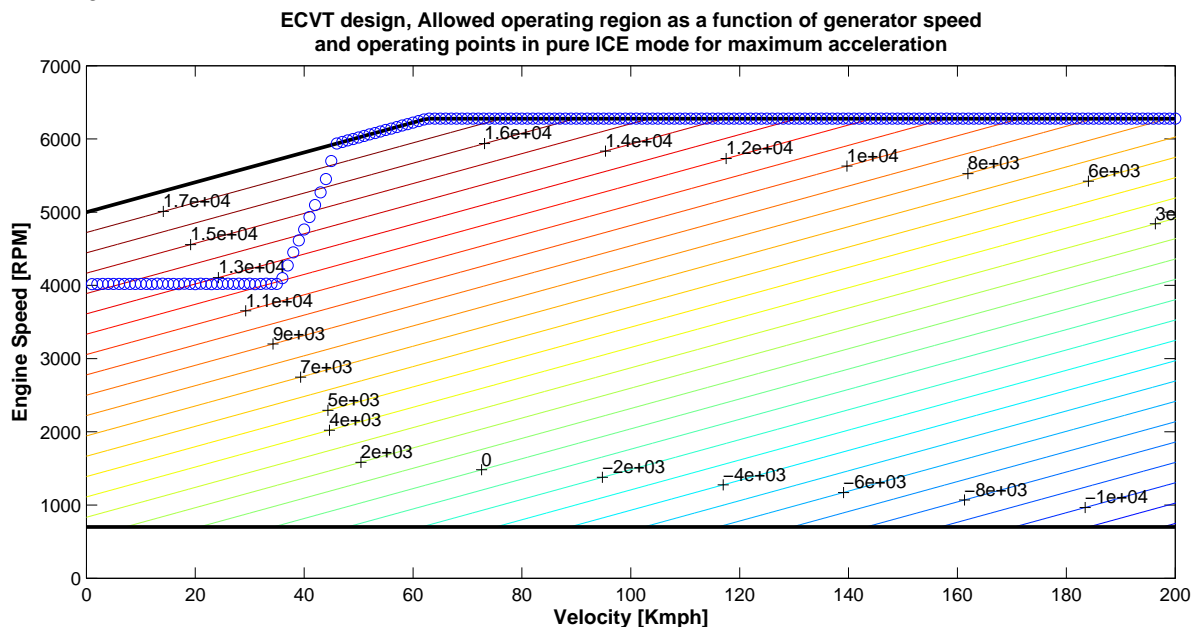


Figure 7.31: MG1 speed for maximum acceleration in ICE mode in ECVT design

1. At low vehicle velocity (below 40 kmph), the power-train control chooses the separation factor such that maximum torque region of the engine is utilized which is 158 NM at 4000 rpm. Revving the engine

at much higher speed will result in lesser torque from engine but higher power to MG2 through MG1. But, since the MG2 speed is related to the vehicle velocity, the amount of power transmitted electrically through MG1 during this low velocity period is sufficiently high enough for the MG2 to produce maximum torque. This extra power generated by the engine must be therefore anyway be sent to the battery.

2. At higher velocity (greater than 40 kmph), the power-train control chooses the separation factor such that more power from the engine is transmitted electrically through MG1 while compromising on the torque from the engine. Also it must be noted that MG2 utilizes a fixed gear ratio. Therefore it is beneficial to rev the engine maximum so that more power is sent through the motor. (It must be noted here that the engine doesn't use the fixed gear ratio) At a velocity greater than 200 kmph, power is transmitted to the wheels via circulation path where in the separation factor is chosen such that more power is transmitted electrically through MG1.

Figure 7.32, 7.33 and 7.34 shows the utilisation of prime movers for maximum acceleration in ICE mode. Note, the MG1 (generator map) used here is different than what is used in chapter 6 in figure 6.12, mainly because the operating points for maximum acceleration here utilises the efficiency point along the edges of the torque line which is distorted in figure 6.12. It must also be noted that bigger size of MG1 does not implicitly mean better for acceleration. The maximum MG1 torque depends on the maximum engine torque given by equation 3.5.

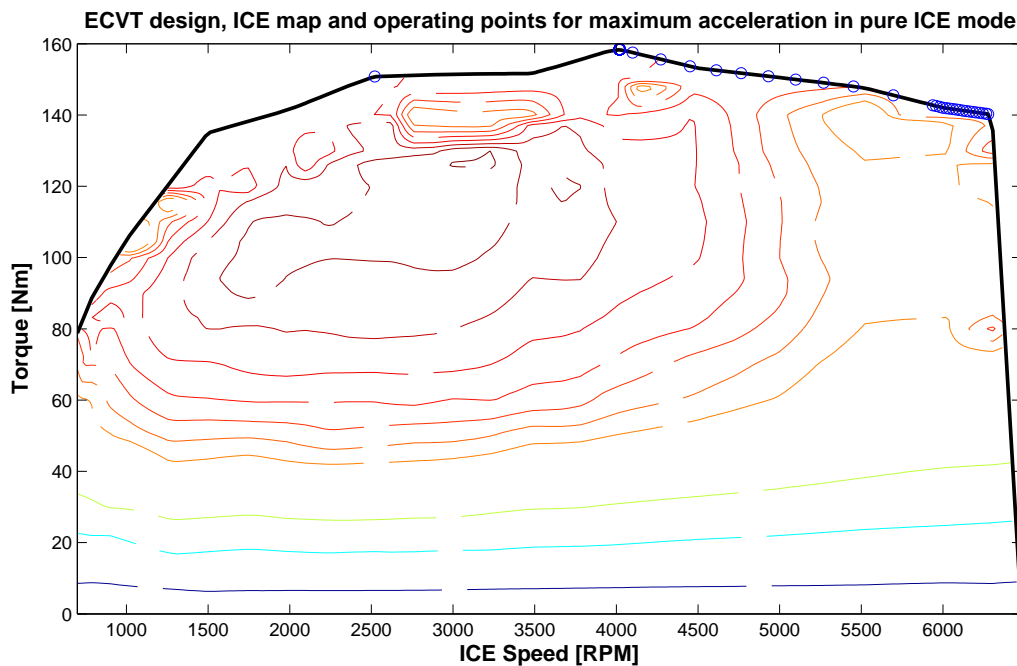


Figure 7.32: Operating points on ICE map for maximum acceleration in ICE mode for ECVT design

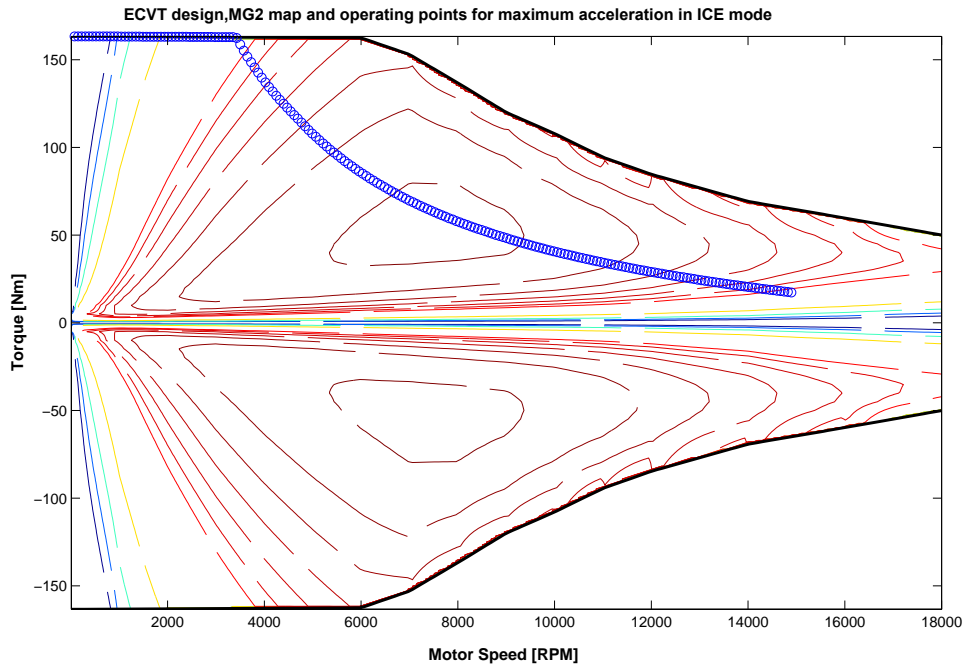


Figure 7.33: Operating points on MG2 map for maximum acceleration in ICE mode for ECVT design

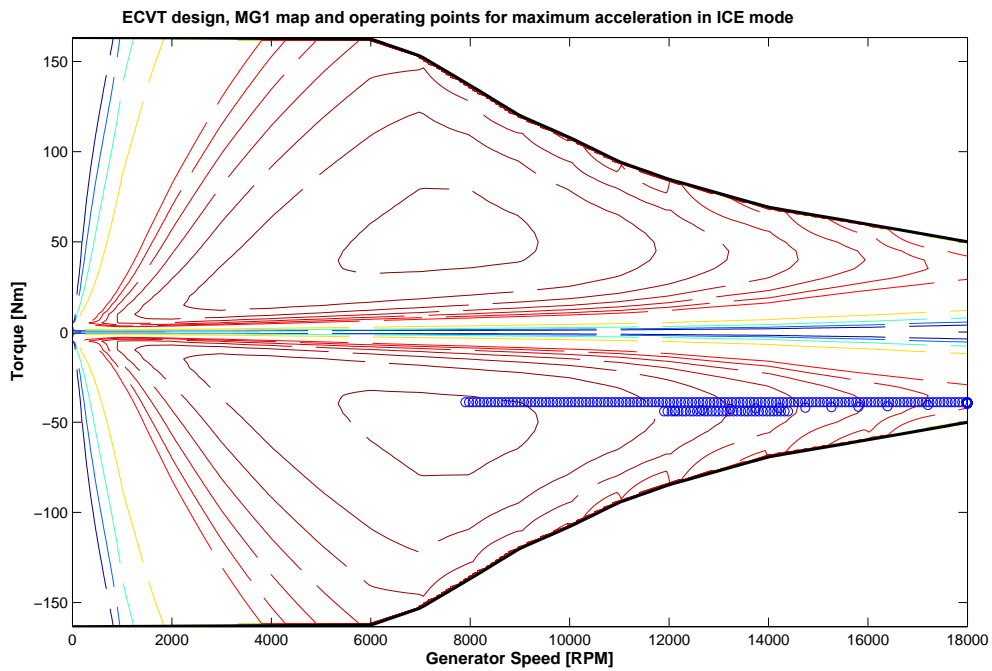


Figure 7.34: Operating points on MG1 map for maximum acceleration in ICE mode for ECVT design. Note, the MG1 (generator map) used here is different than what is used in chapter 6 in figure 6.12

## 8 Conclusion and future work

### 8.1 Conclusion

The HDCT in general is found better regarding all the compared properties. The differences may depend on some assumptions. However, for many vehicles the HDCTs are expected to be a better solution than the ECVT. This conclusion is based on the following

- Simulation results showed that HDCT design is more efficient than ECVT design in both CD and CS mode.
  - In CD mode the efficiency advantage of the HDCT design over ECVT design might be offset due to inevitable clutch-less gear shifting required in HDCT design. The quality of the clutch-less gear shifts in CD mode depends on the gear step and precise control of MG speed. On the other hand the frequency of clutch-less gear shifts can be minimised due to excellent torque-speed characteristics of the MG unit. However, further investigation might be required in-terms of quality of gear shift and life of the synchronisers inside the transmission.
  - Simulations results for CS mode showed that HDCT design outperforms the ECVT design on all three driving cycle namely UDDS, HWFET and NEDC regarding fuel consumption. It must be noted that the simulation results doesn't involve the gear shift dynamics, clutch loss and loss in hydraulics (or electro-mechanical) device for pre-selection of the gear in HDCT design. Dynamics involved in controlling the MG1 speed for both HDCT and ECVT design are not taken into consideration in this thesis work.
- Simulation results show HDCT design has better performance capability than ECVT design in all the modes. However, as mentioned earlier gear shift dynamics is not considered in this thesis work. But, on the other hand, DCTs are known to have excellent fuel efficiency, responsiveness, shift and launch control without the requirement of a torque converter.
- Basic functionality and cost comparison showed that HDCT are cheaper and can offer all the customer functionalities as that of the other three power-trains (Voltec 4ET50, GM 2MT70 and THS-III).
- **Design modularity:** HDCT design can be easily adapted to conventional or hybrid vehicles, light or heavy vehicles, SUVs or luxury vehicles with little modifications. Whereas, in ECVT design, the specifications of MG1 and ICE are related and cannot be sized independently.
- **Change in production plant:** Migrating to ECVT design requires major changes in production line. Whereas, little modification is required for HDCT design.

### 8.2 Future work

Clutch-less gear shifting in HDCT design in CD mode is inevitable and since the gear step is high, experimental validation might be interesting to investigate the time and quality of the gear shift and also the wear and tear induced on the synchronisers.

The simulations similar to that performed in this thesis work with the combination of CDCS and ECMS control strategy can be tested on a number of driving cycles. The power split and the gear ratios used at every instant of time for different driving cycle can be noted down which can then be used to develop a rule based control for specific vehicle.

Detailed modelling of losses in HDCT including the clutch control, lubrication, cooling and the axillary losses (like hydraulic losses during pre selection of gear) and re-simulating with these losses to see its influence on the overall fuel economy would be interesting.

## References

- [1] *Autonomie Light duty vehicles*. [http://www.autonomie.net/docs/6-Papers/Lightduty/cost\\_benefit\\_analysis.pdf](http://www.autonomie.net/docs/6-Papers/Lightduty/cost_benefit_analysis.pdf).
- [2] Jonathan L Breen and Glenn Bower. *Clutchless Shifting of an Automated Manual Transmission in a Hybrid Powertrain*. Sept. 2011. DOI: 10.4271/2011-01-2194. URL: <http://dx.doi.org/10.4271/2011-01-2194>.
- [3] *Environmental protection agency*. <http://www.epa.gov/otaq/climate/documents/420r11015.pdf>. Accessed: 2013-11-02.
- [4] *Environmental protection agency*. <http://www.epa.gov/otaq/climate/420r10010.pdf>. Accessed: 2013-11-02.
- [5] *Getrag Hybrid Drive*. <http://www.getrag.com/en/products/hybriddrive/hybriddrive.html>. Accessed: 2013-11-02.
- [6] Tim M. Grewe, Brendan M. Conlon, and Alan G. Holmes. *Defining the General Motors 2-Mode Hybrid Transmission*. Apr. 2007. DOI: 10.4271/2007-01-0273. URL: <http://dx.doi.org/10.4271/2007-01-0273>.
- [7] James Hendrickson, Alan Holmes, and David Freiman. *General Motors Front Wheel Drive Two-Mode Hybrid Transmission*. Apr. 2009. DOI: 10.4271/2009-01-0508. URL: <http://dx.doi.org/10.4271/2009-01-0508>.
- [8] Iqbal Husain. "Introduction to alternate vehicles". In: *Electric and hybrid vehicles : design fundamentals*. CRC Press: Boca Raton : CRC Press, cop. 2011, 2011.
- [9] Masatoshi Ito et al. *Hybrid Transmission Development for AWD Luxury Cars*. Oct. 2007. DOI: 10.4271/2007-01-4122. URL: <http://dx.doi.org/10.4271/2007-01-4122>.
- [10] Antonio Sciarretta Lino Guzzella. "Supervisory Control Algorithms". In: *Vehicle propulsion systems*. Springer-Verlag Berlin Heidelberg 2005: Springer, 2005.
- [11] Hongbo Liu et al. *Gear-Shift Strategy for a Clutchless Automated Manual Transmission in Battery Electric Vehicles*. Apr. 2012. DOI: 10.4271/2012-01-0115. URL: <http://dx.doi.org/10.4271/2012-01-0115>.
- [12] Bernd Matthes. *Dual Clutch Transmissions - Lessons Learned and Future Potential*. Apr. 2005. DOI: 10.4271/2005-01-1021. URL: <http://dx.doi.org/10.4271/2005-01-1021>.
- [13] Jerome Meisel. *An Analytic Foundation for the Toyota Prius THS-II Powertrain with a Comparison to a Strong Parallel Hybrid-Electric Powertrain*. Apr. 2006. DOI: 10.4271/2006-01-0666. URL: <http://dx.doi.org/10.4271/2006-01-0666>.
- [14] Jerome Meisel. *An Analytic Foundation for the Two-Mode Hybrid-Electric Powertrain with a Comparison to the Single-Mode Toyota Prius THS-II Powertrain*. Apr. 2009. DOI: 10.4271/2009-01-1321. URL: <http://dx.doi.org/10.4271/2009-01-1321>.
- [15] Jerome Meisel. *Kinematic Study of the GM Front-Wheel Drive Two-Mode Transmission and the Toyota Hybrid System THS-II Transmission*. Apr. 2011. DOI: 10.4271/2011-01-0876. URL: <http://dx.doi.org/10.4271/2011-01-0876>.
- [16] Michael A. Miller et al. *The GM "Voltec" 4ET50 Multi-Mode Electric Transaxle*. Apr. 2011. DOI: 10.4271/2011-01-0887. URL: <http://dx.doi.org/10.4271/2011-01-0887>.
- [17] Yota Mizuno et al. *Development of New Hybrid Transmission for Compact-Class Vehicles*. Apr. 2009. DOI: 10.4271/2009-01-0726. URL: <http://dx.doi.org/10.4271/2009-01-0726>.
- [18] Koichiro Muta, Makoto Yamazaki, and Junji Tokieda. *Development of New-Generation Hybrid System THS II - Drastic Improvement of Power Performance and Fuel Economy*. Mar. 2004. DOI: 10.4271/2004-01-0064. URL: <http://dx.doi.org/10.4271/2004-01-0064>.
- [19] Guang Wu, Xing Zhang, and Zuomin Dong. *Impacts of Two-Speed Gearbox on Electric Vehicle's Fuel Economy and Performance*. Apr. 2013. DOI: 10.4271/2013-01-0349. URL: <http://dx.doi.org/10.4271/2013-01-0349>.
- [20] Z. Zhong et al. "Shifting control of an automated mechanical transmission without using the clutch". English. In: *International Journal of Automotive Technology* 13.3 (Apr. 2012), pp. 487-496.

## Appendices

## A THS-III generatoin power-train parameters used for drawing graph shown in figure 3.5 and 3.6

Table A.1: THS-III generation power-train parameters used for drawing the graph shown in figure 3.5 and 3.6

Parameters	Values
Wheel radius	0.3067 m
Characteristic ratio of simple planetary gear	30/78
Engine Speed range	600 - 6000 rpm
Generator speed range	-13500 to 13500 rpm
Motor speed range	-13500 to 13500 rpm
Final gear ratio	3.267
Fixed gear ratio	2.636

## B GM 2MT70 power-train parameters used for drawing graph shown in figure 3.10 and 3.11

Table B.1: GM 2MT70 power-train parameters used for drawing graph shown in figure 3.10 and 3.11

Parameters	Values
Wheel Radius	0.351
Characterisitic ratio of compound planetary gear	44/104
Charactersitic ratio of simple planetary gear	37/83
Engine speed range	600 to 6000 rpm
Generator speed range	-7500 to 7500 rpm
Motor speed range	-9000 to 9000 rpm
Maximum pinion gear speed	14000 rpm
First gear ratio	3.243
Second gear ratio	1.871
Third gear ratio	1
Fourth gear ratio	0.612
Final gear ratio	3.02

## C Voltec 4ET50 power-train parameters used for drawing graph shown in figure 3.14 and 3.15

Table C.1: Voltec 4ET50 power-train parameters used for drawing graph shown in figure 3.14 and 3.15

Parameters	Values
Wheel radius	0.351 m
Characteristic ratio of simple planetary gear	0.5909
Engine Speed range	600 - 4800 rpm
Generator speed range	-4800 to 4800 rpm
Motor speed range	-10000 to 10000 rpm
Final gear ratio	2.6

## D Graphs relating to NEDC driving cycle

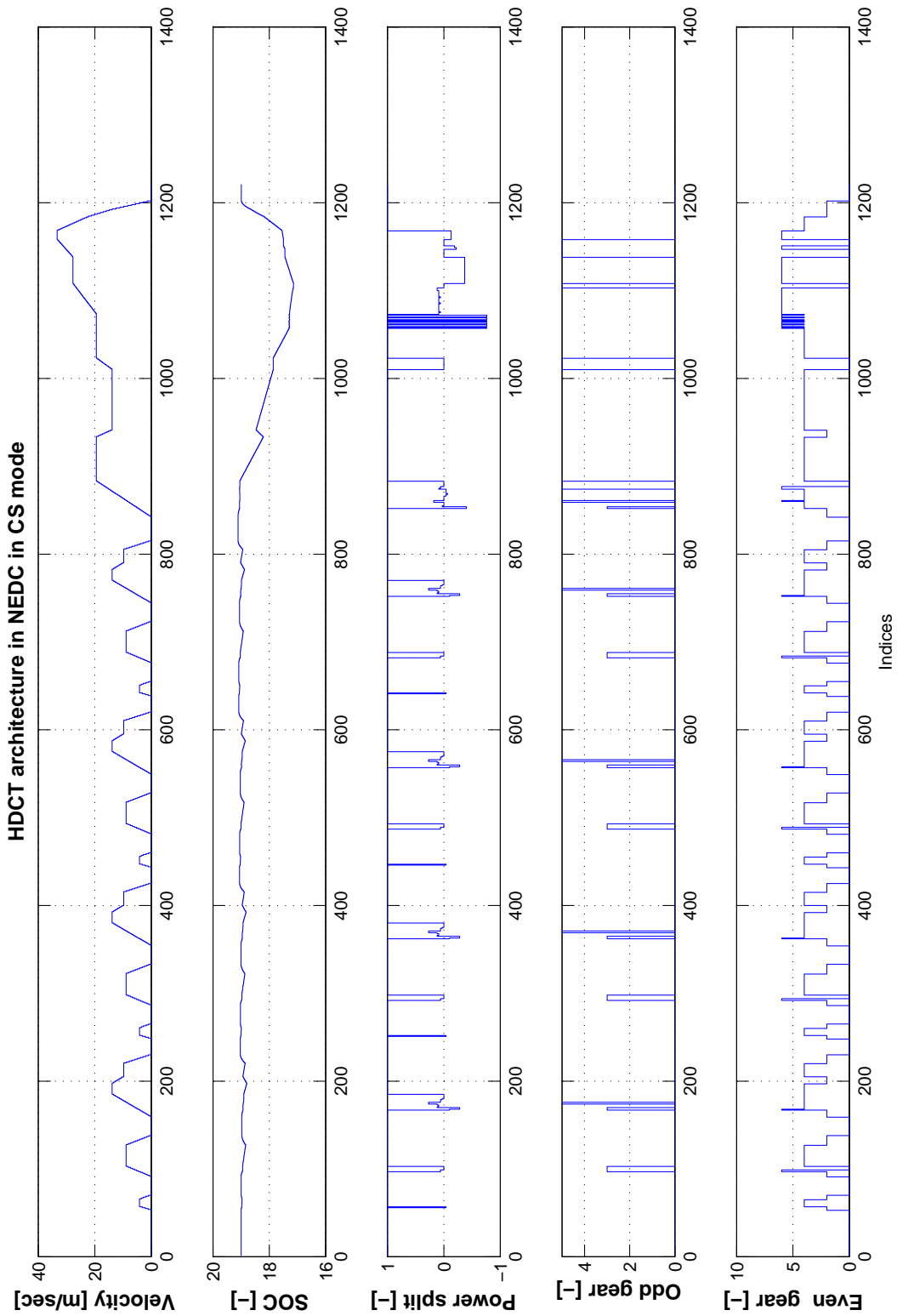


Figure D.1: HDCT architecture, power-train control signals in NEDC in CS mode

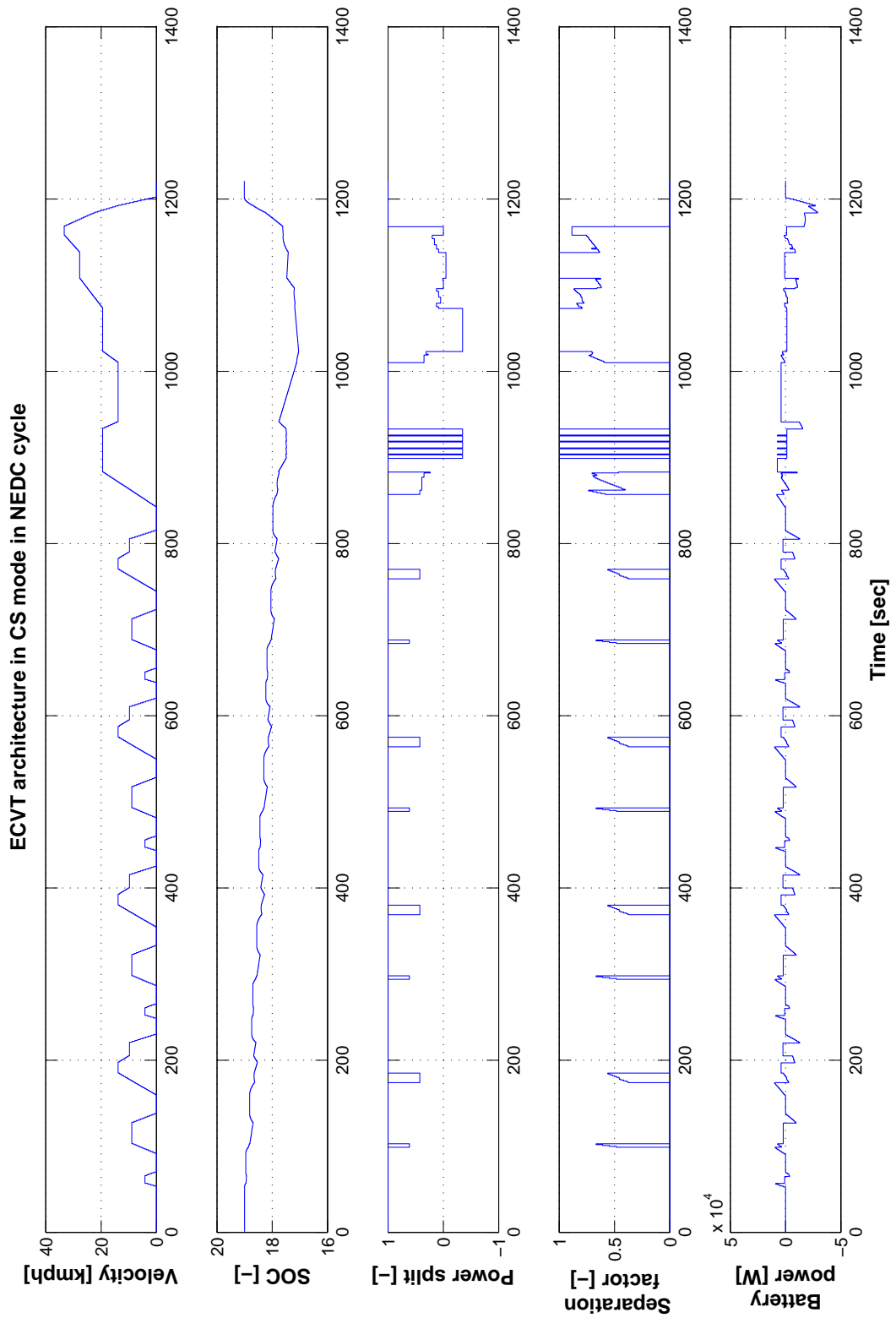


Figure D.2: *ECVT architecture, power-train control signals in NEDC in CS mode*

## E Efficiency simulation results for both architectures in UDDS driving cycle

### E.1 Efficiency of both architectures during CD mode (electric mode) in UDDS

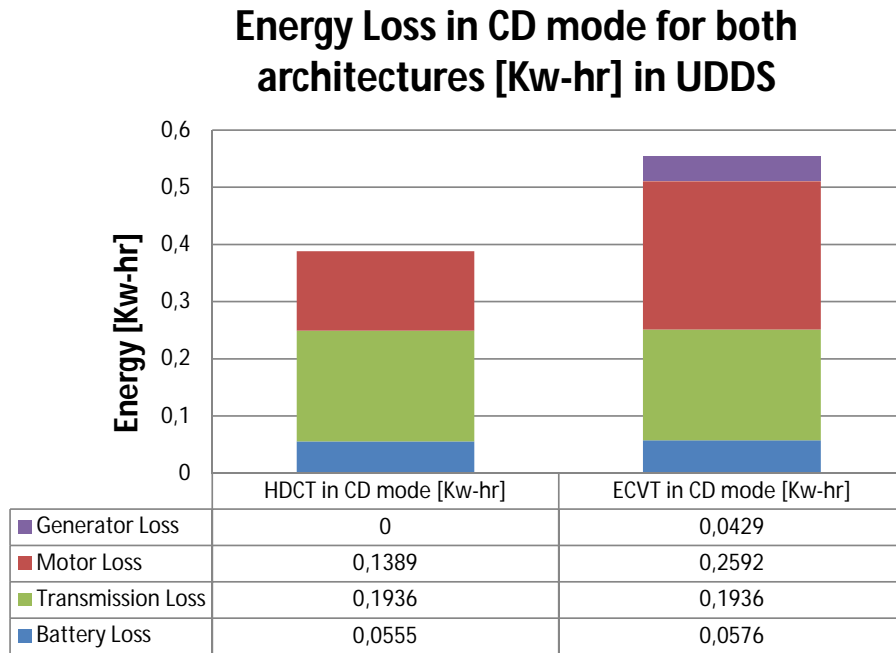


Figure E.1: Energy loss accrued in each component in UDDS cycle for both architectures in CD/electric mode

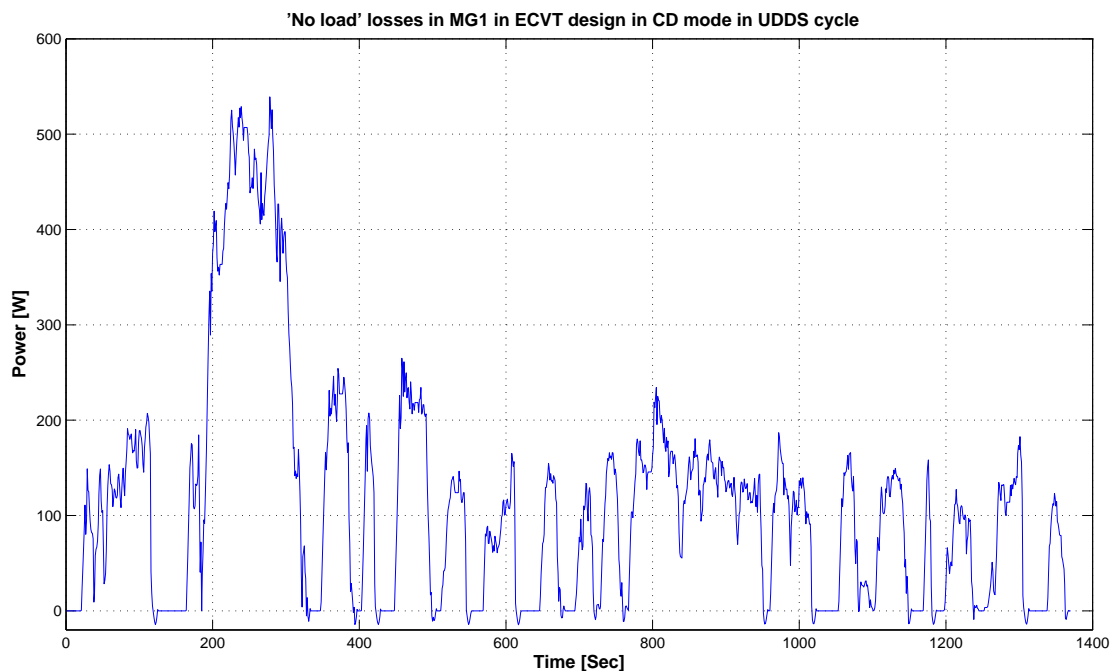


Figure E.2: 'No-load' losses in MG1 in ECVT design in CD mode in UDDS cycle

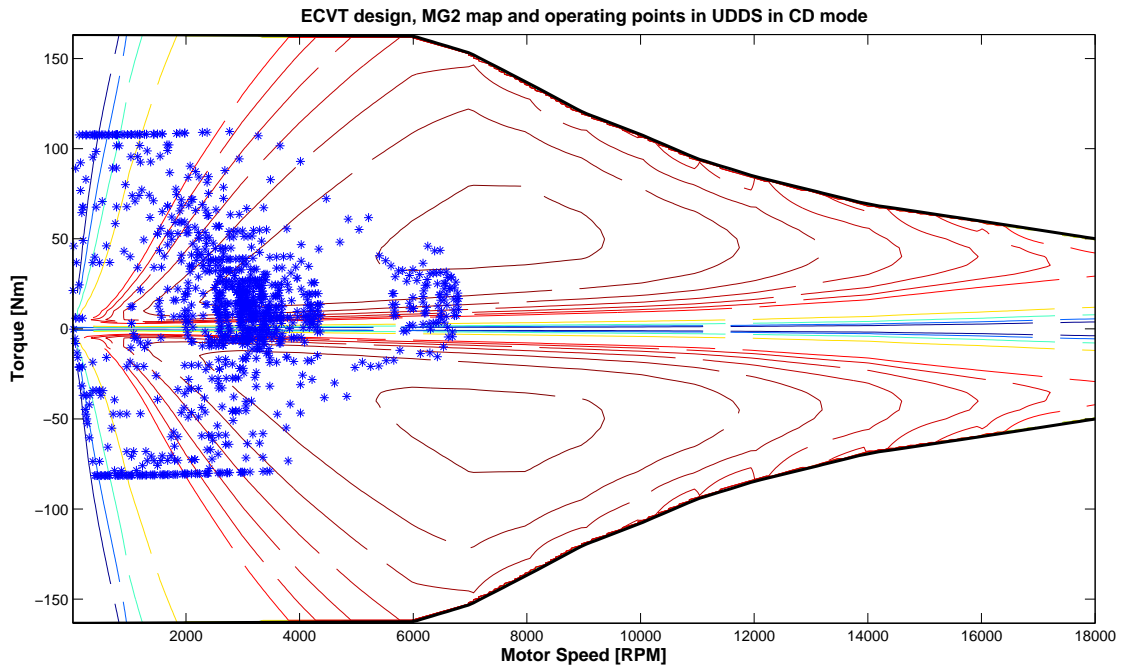


Figure E.3: *ECVT design, MG2 map and operating points in CD mode in UDDS*

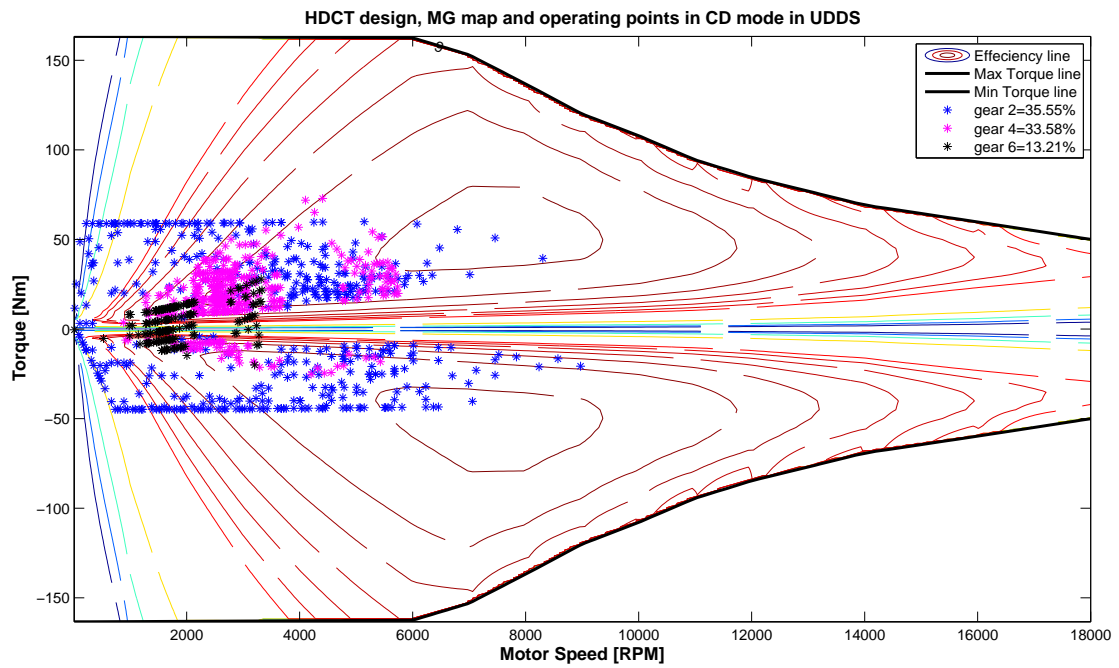


Figure E.4: *HDCT design, MG map and operating points in CD mode in UDDS*

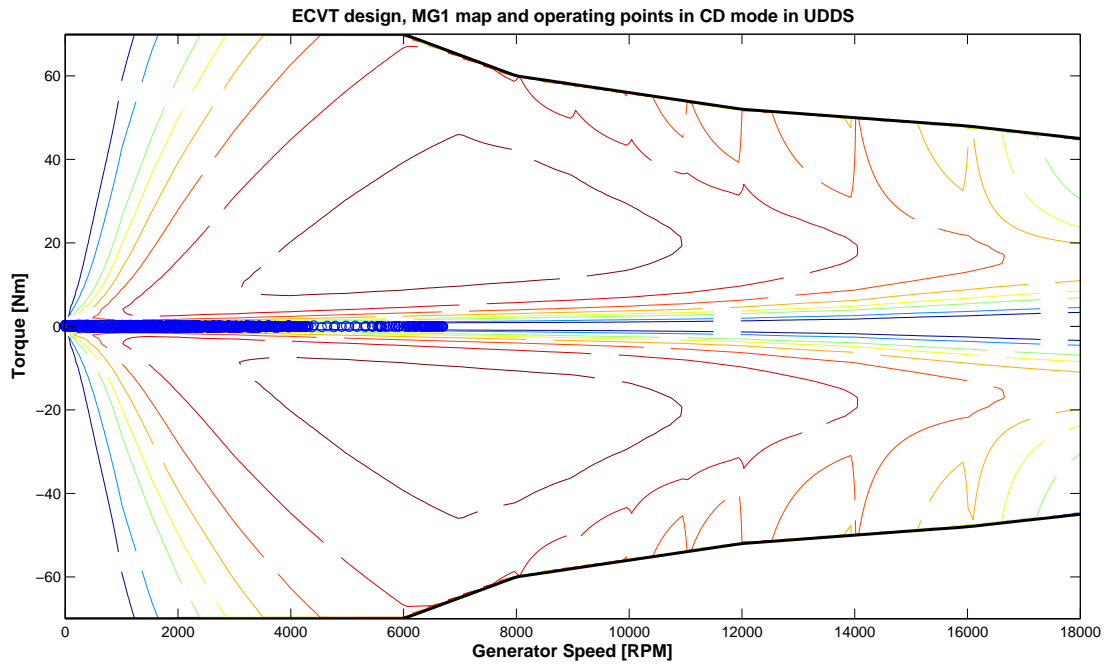


Figure E.5: ECVT design, MG1 map and operating points in CD mode in UDDS

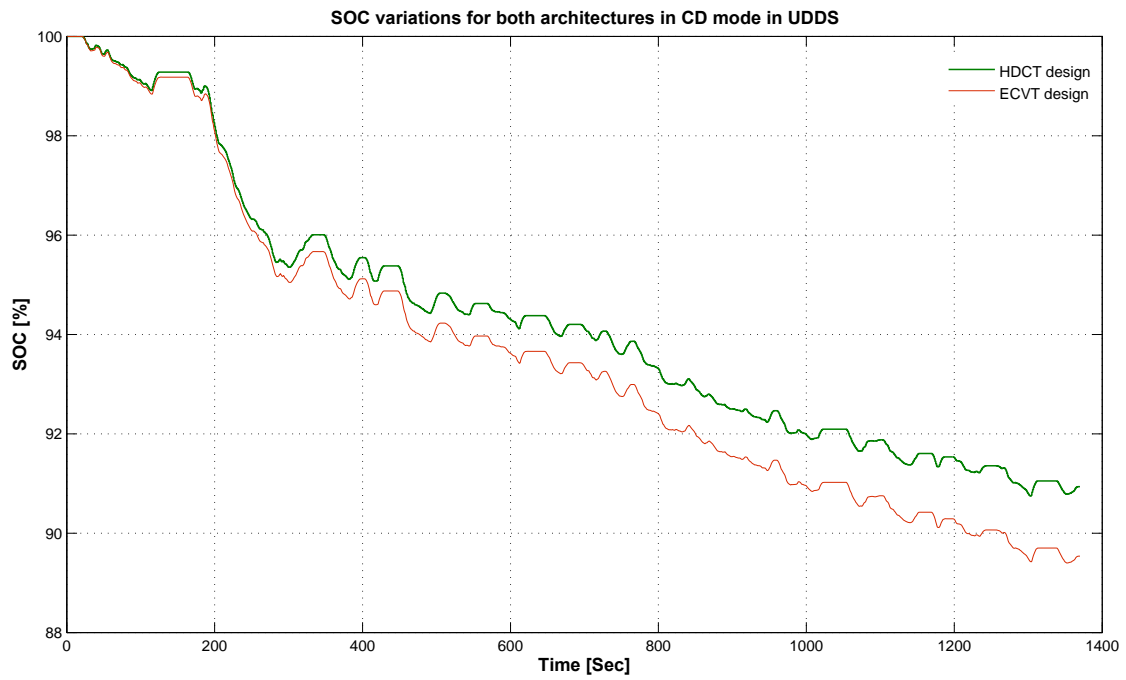


Figure E.6: SOC variations for both architectures in CD mode in UDDS

## E.2 Efficiency of both architectures during CS mode (ECMS mode) in UDDS

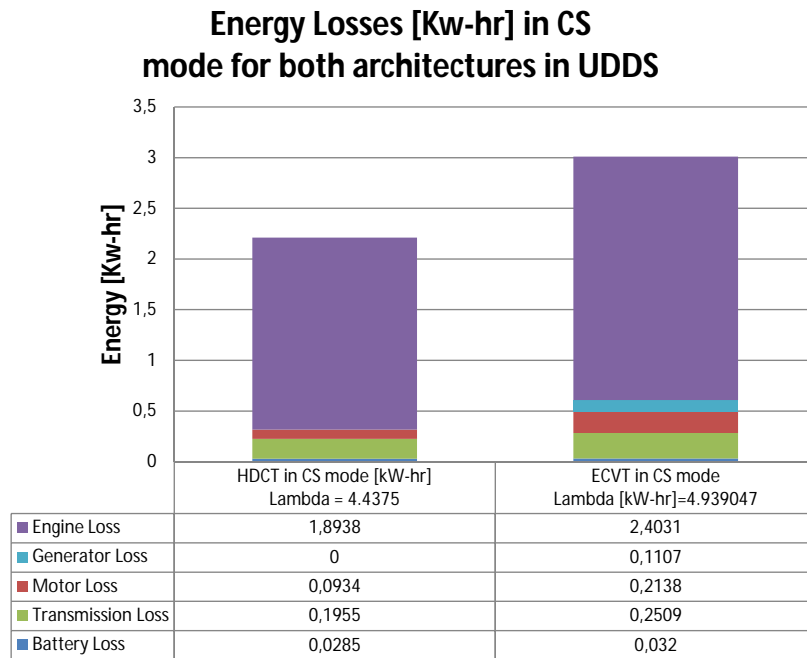


Figure E.7: Energy loss accrued in each component in UDDS cycle for both architectures in CS/ECMS mode

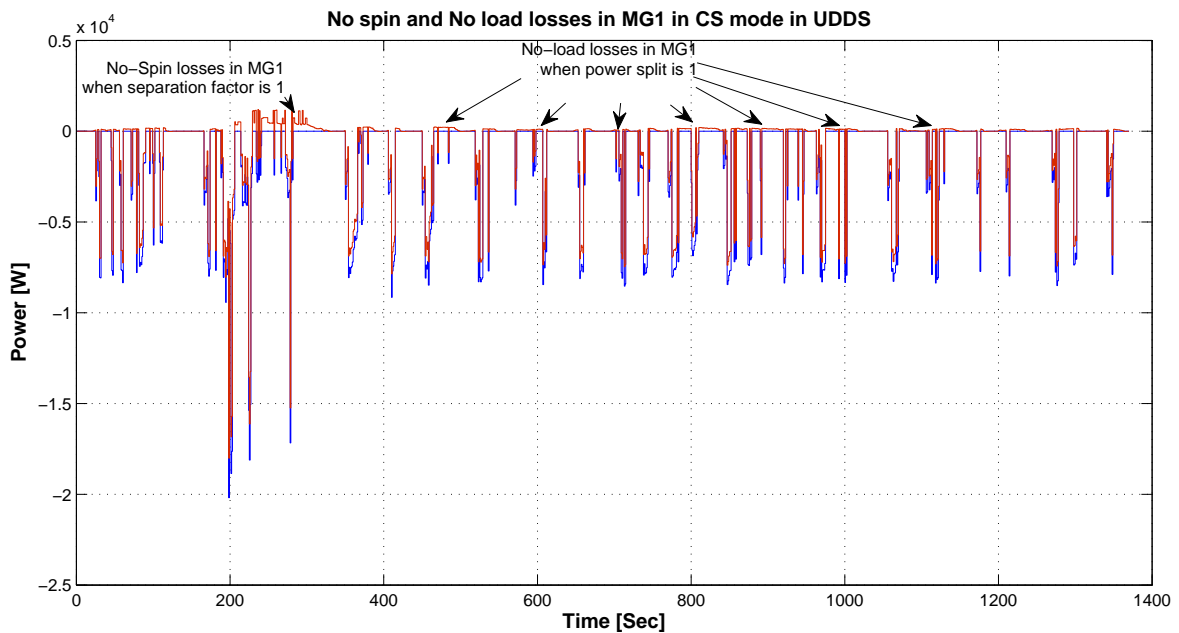


Figure E.8: No-load and No-spin losses in ECVT design in MG1 in CS mode in UDDS

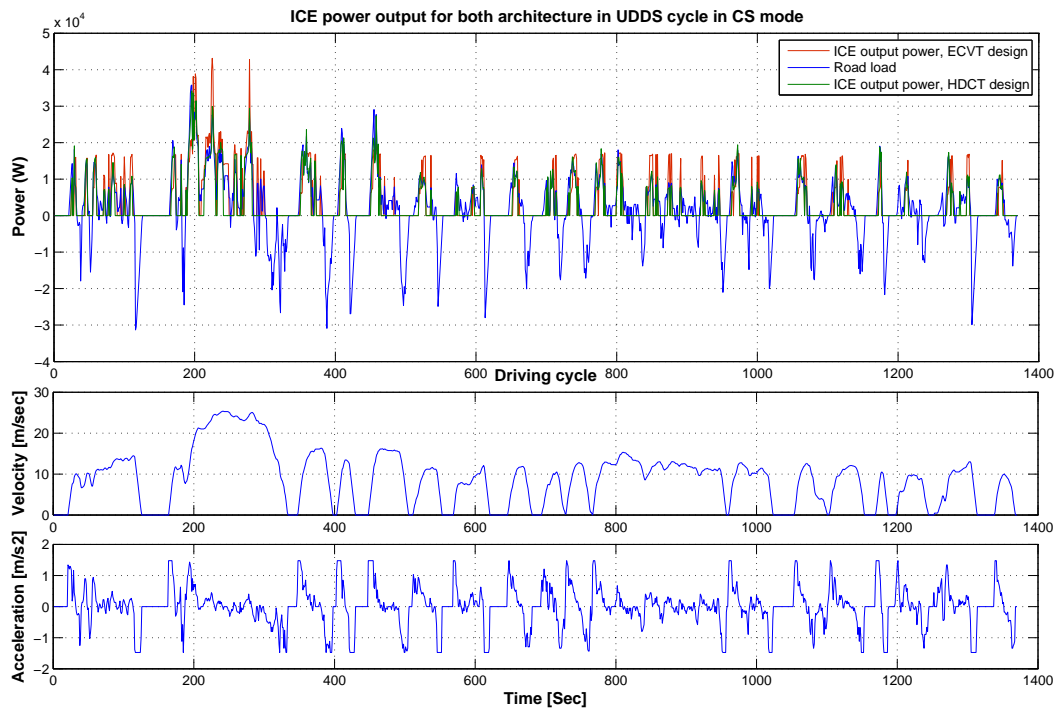


Figure E.9: ICE power output for both architectures in CS mode in UDDS

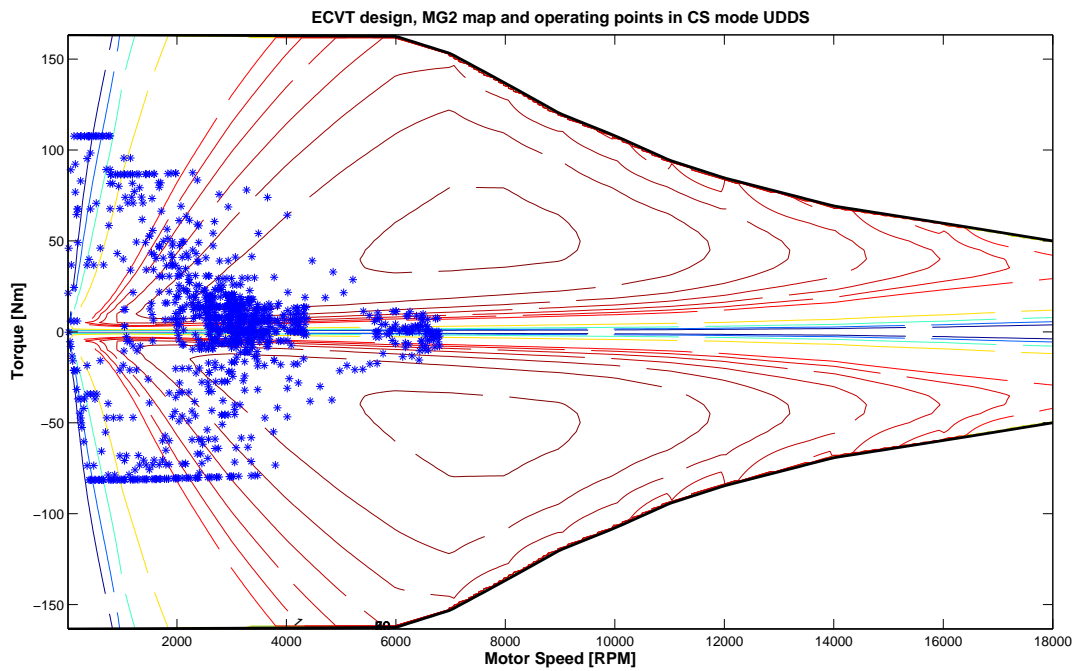


Figure E.10: ECVT design, MG2 map and operating points in CS mode UDDS

## F Efficiency simulation results for both architectures in HWFET driving cycle

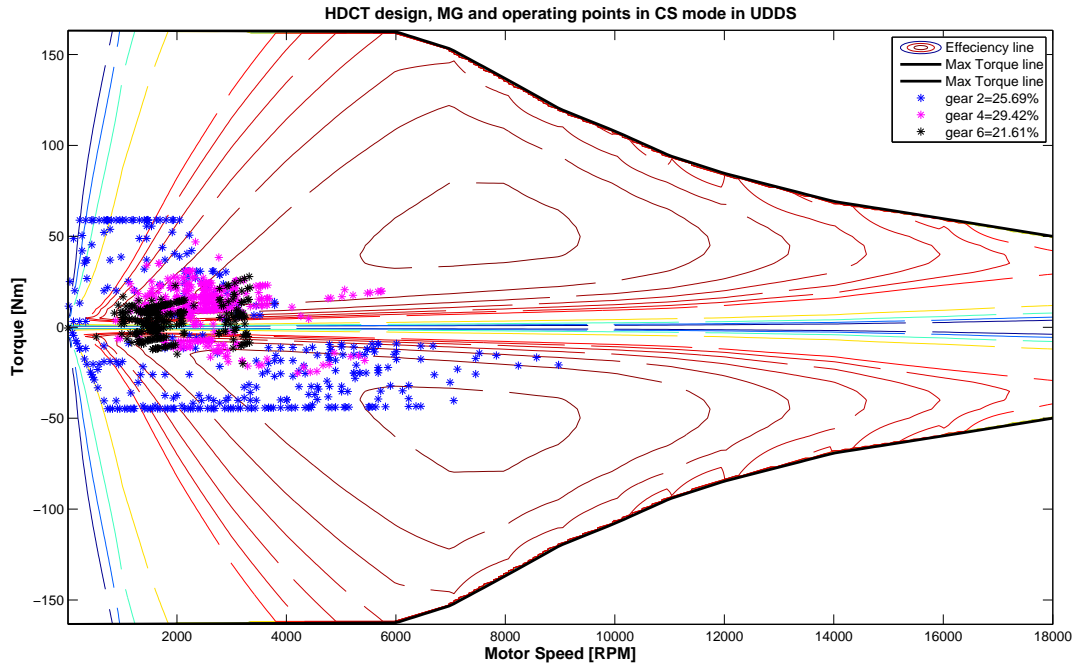


Figure E.11: HDCT design, MG map and operating points in CS mode in UDDS

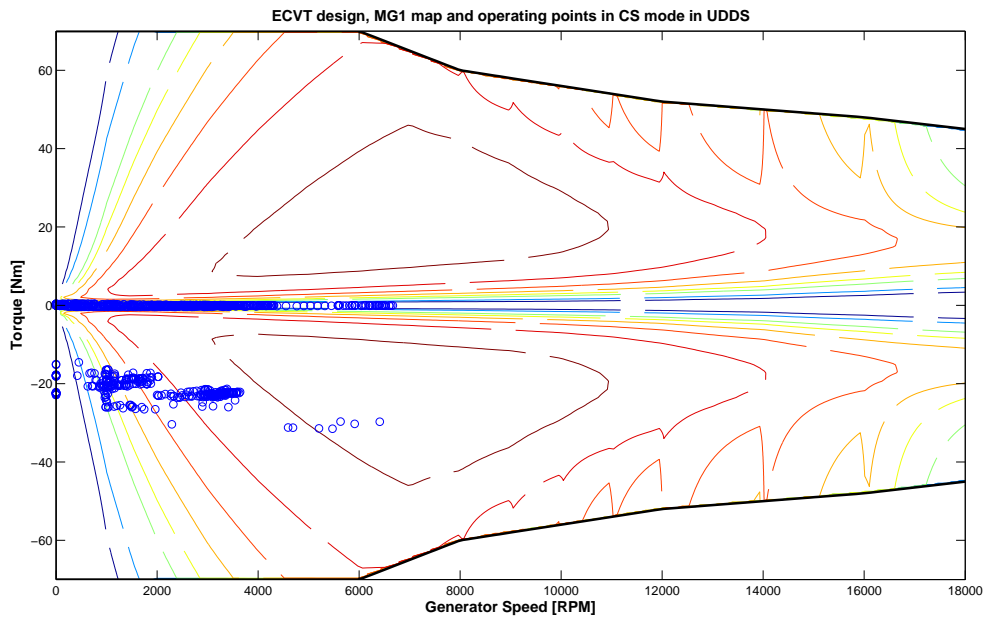


Figure E.12: ECVT design, MG1 map and operating points in CS mode in UDDS

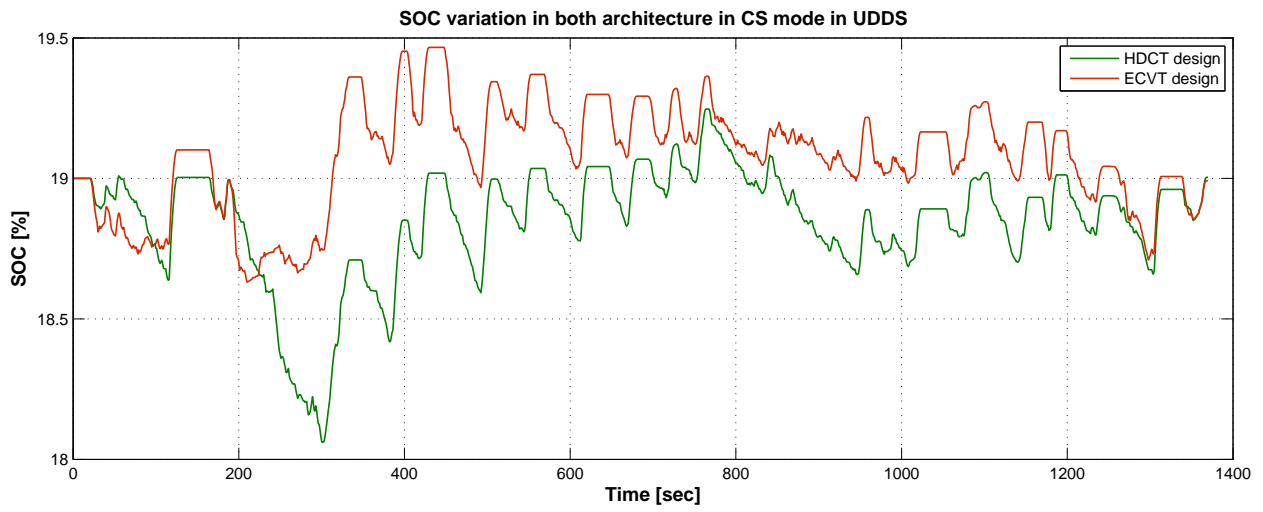


Figure E.13: SOC variation in both architectures in CS mode in UDDS

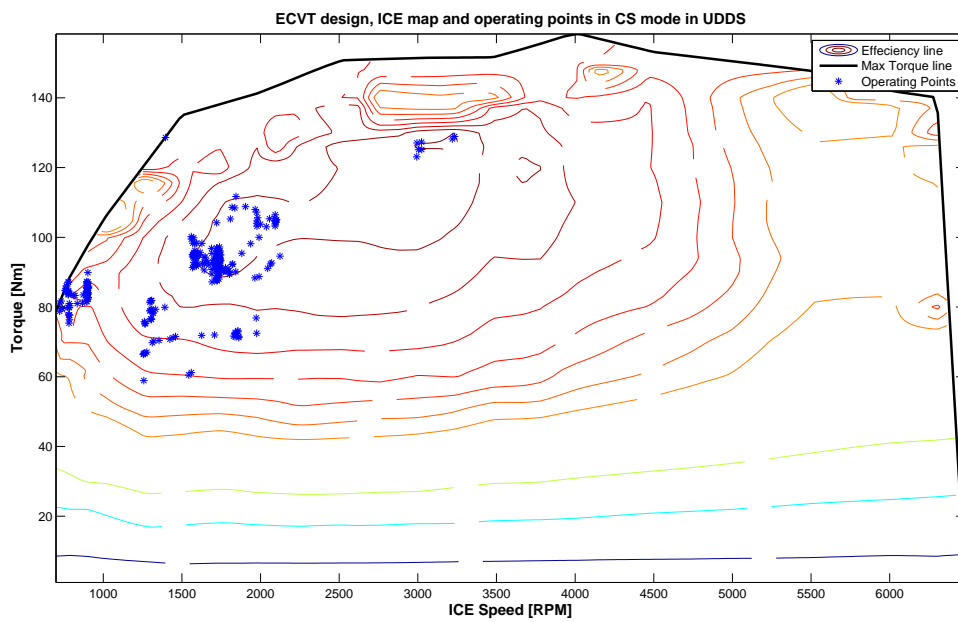


Figure E.14: ECVT design, ICE map and operating points in CS mode in UDDS

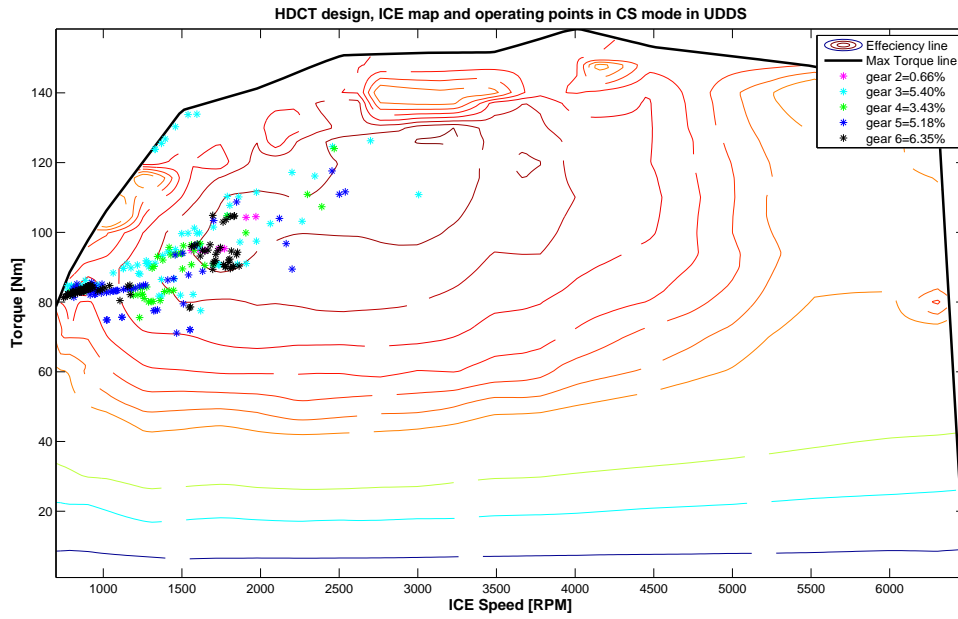


Figure E.15: HDCT design, ICE map and operating points in CS mode in UDDS

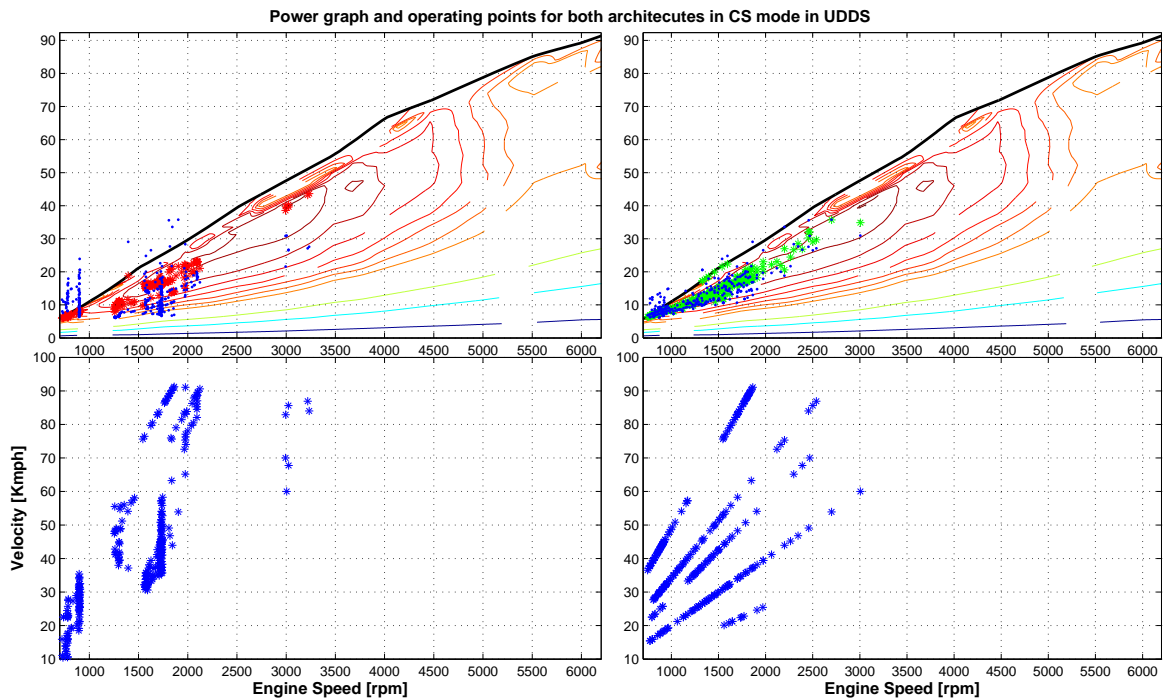


Figure E.16: Power map for both architecture with operating points and road load in UDDS

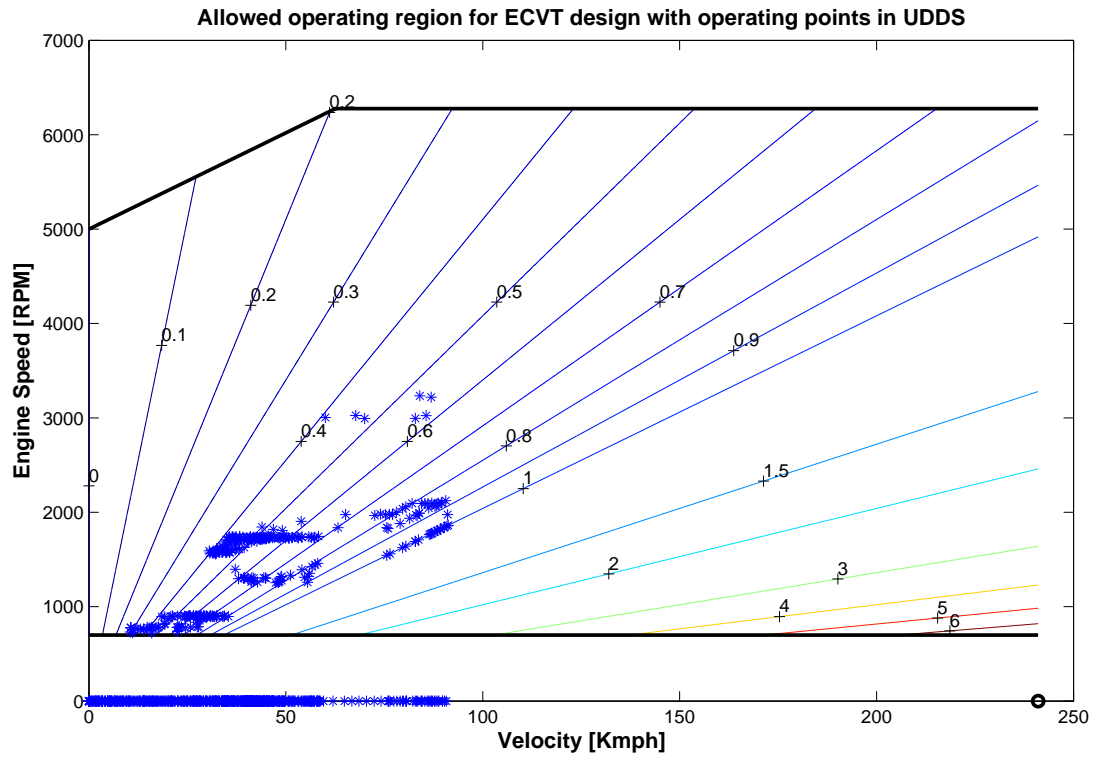


Figure E.17: Separation factor chosen by power-train control in CS mode in UDDS in ECVT design

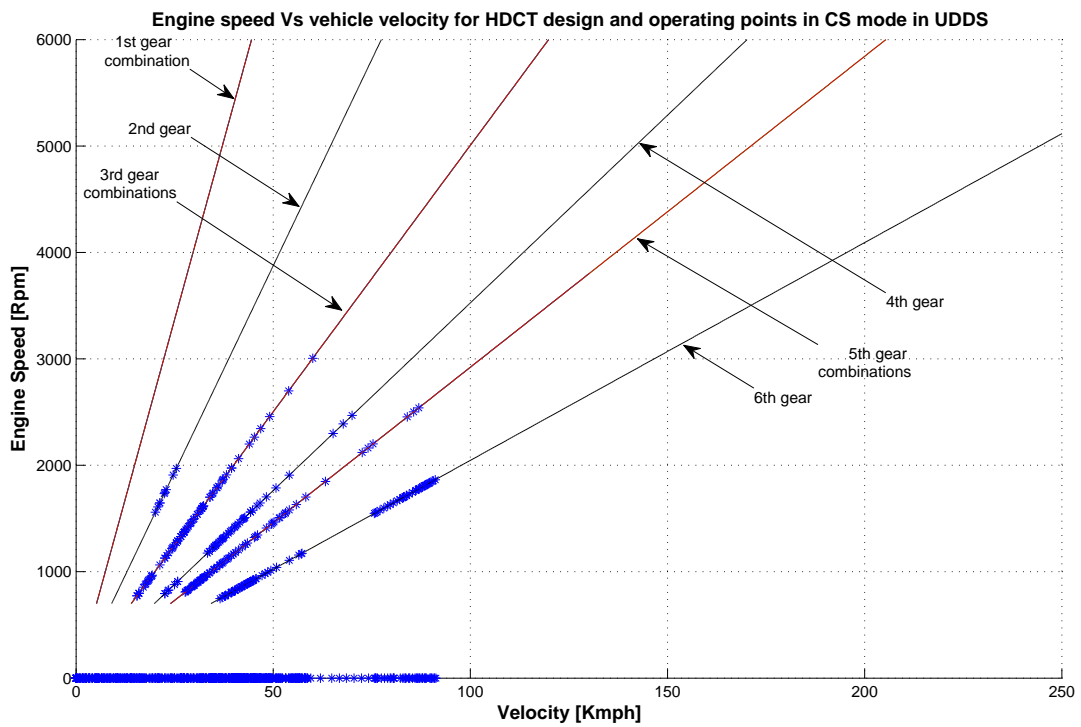


Figure E.18: Engine speed vs vehicle velocity and operating points in CS mode in UDDS in HDCT design

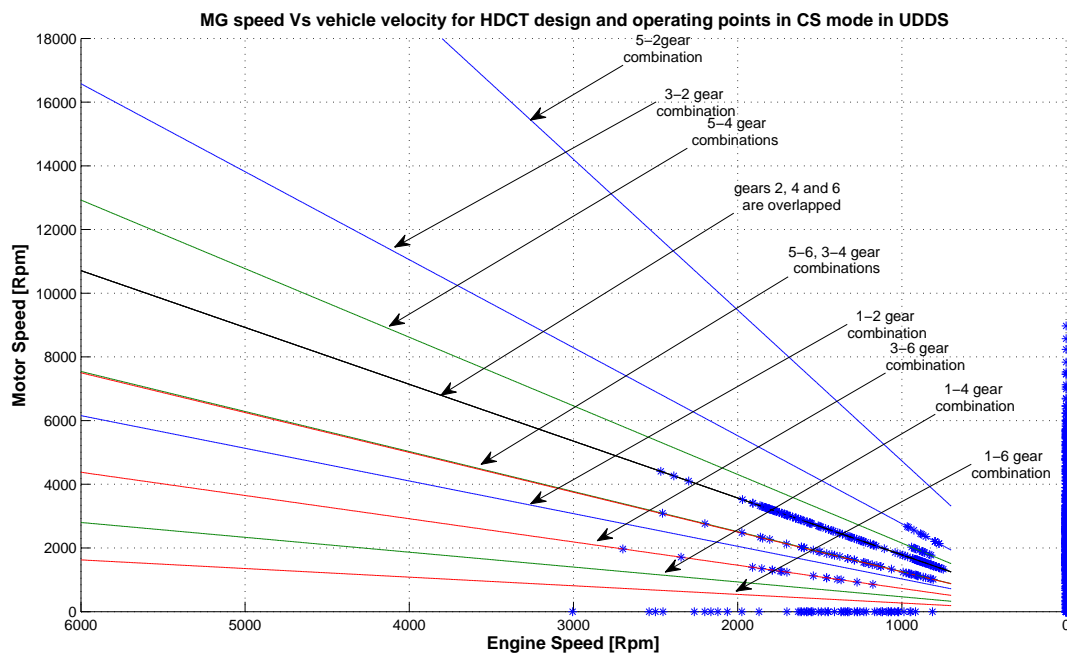


Figure E.19: MG speed vs vehicle velocity and operating points in CS mode in UDDS in HDCT design

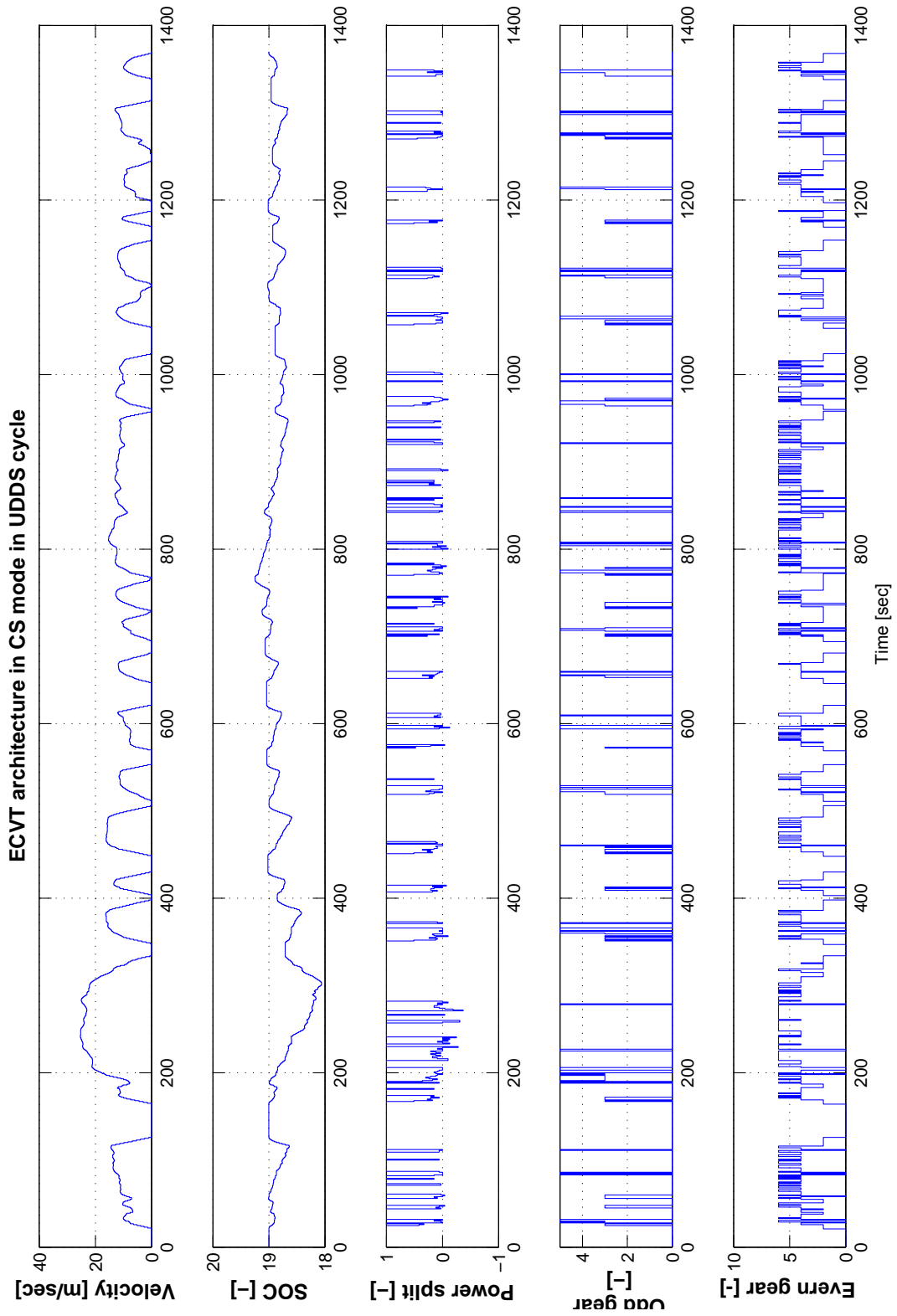


Figure E.20: HDCT architecture, power-train control signals in UDDS in CS mode

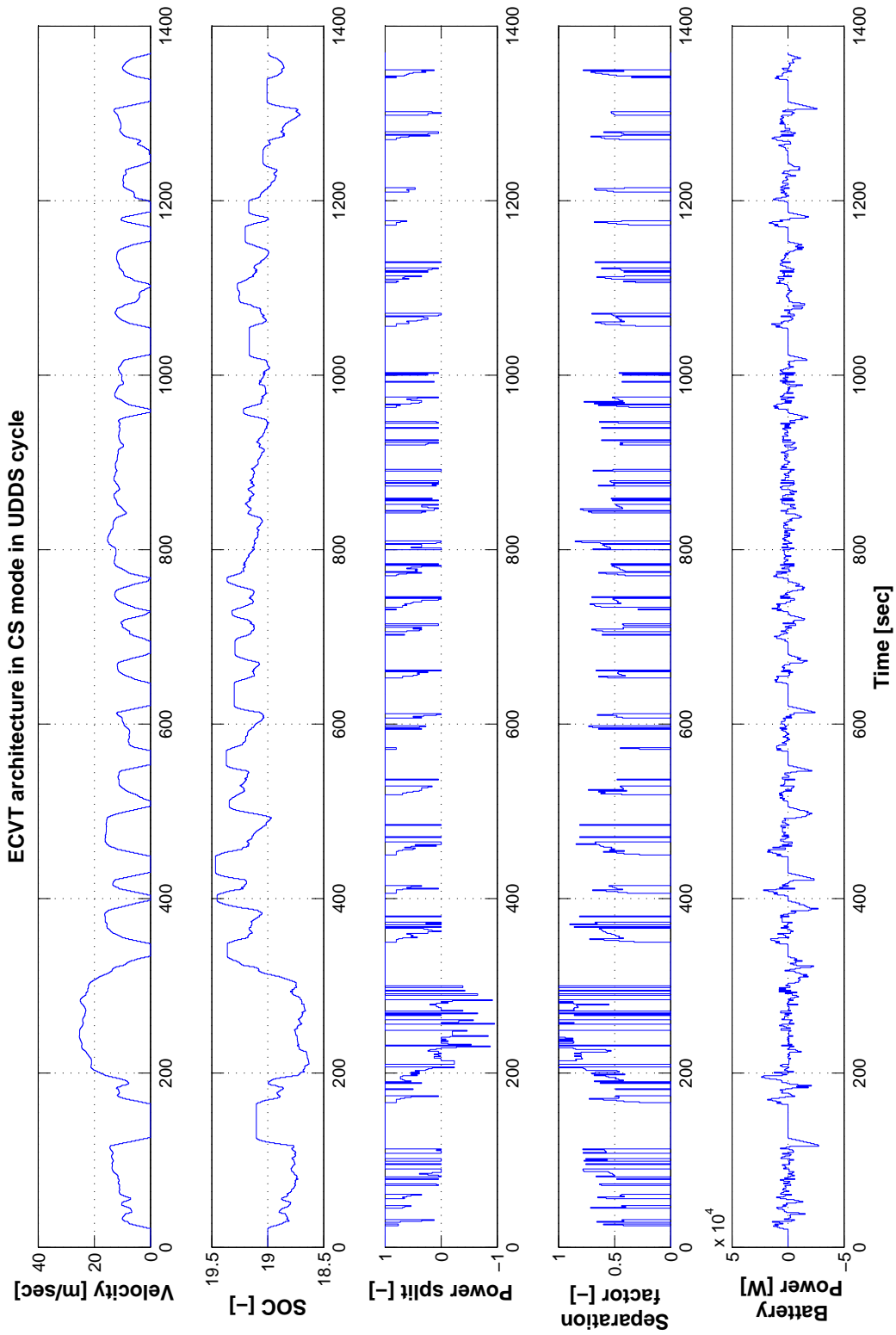


Figure E.21: *ECVT architecture, power-train control signals in UDDS in CS mode*

F.1 Efficiency of both architectures during CD mode (electric mode) in HWFET

Energy Loss in CD mode for both architectures [Kw-hr]

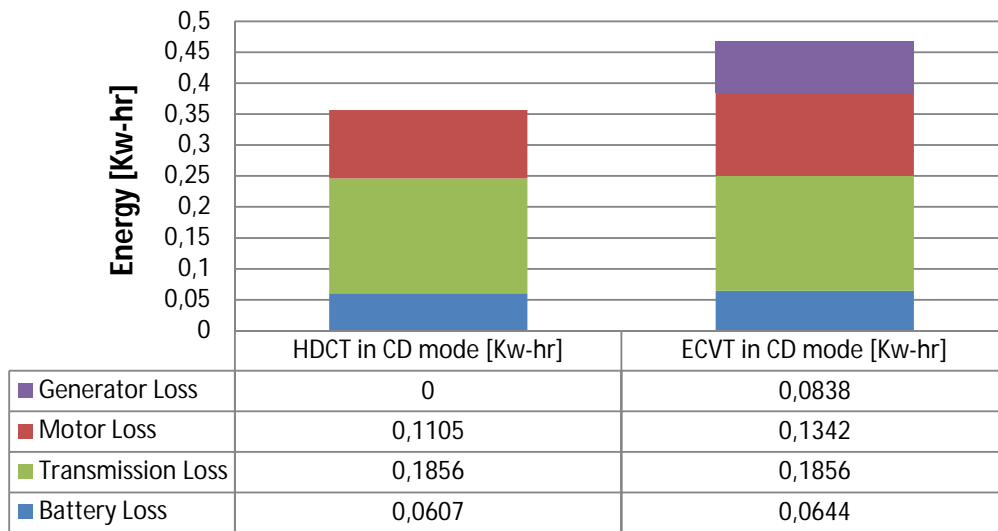


Figure F.1: Energy loss accrued in each component in HWFET cycle for both architectures in CD/electric mode

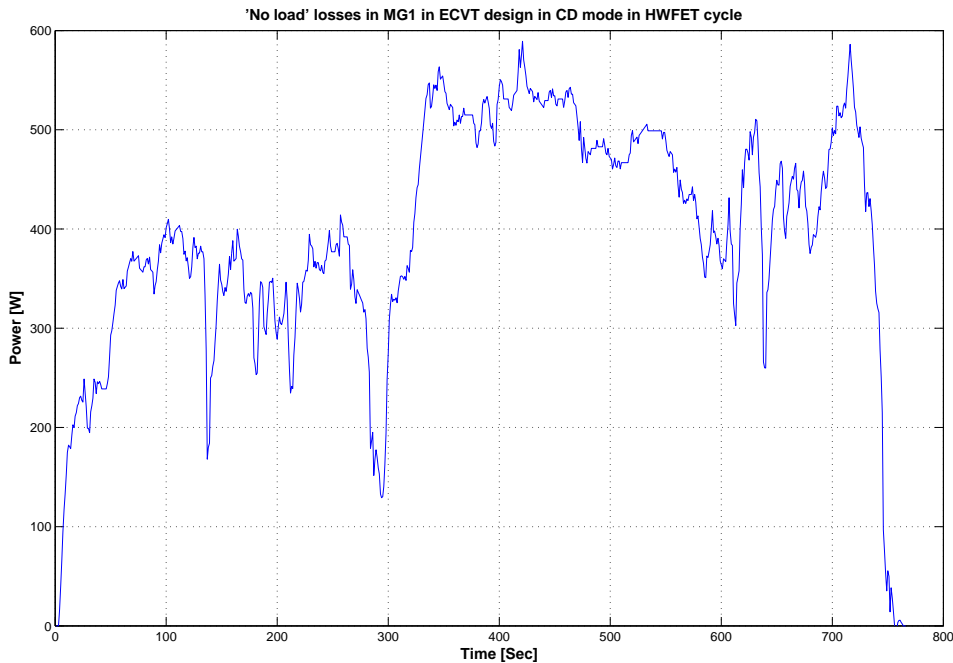


Figure F.2: 'No-load' losses in MG1 in ECVT design in CD mode in HWFET cycle

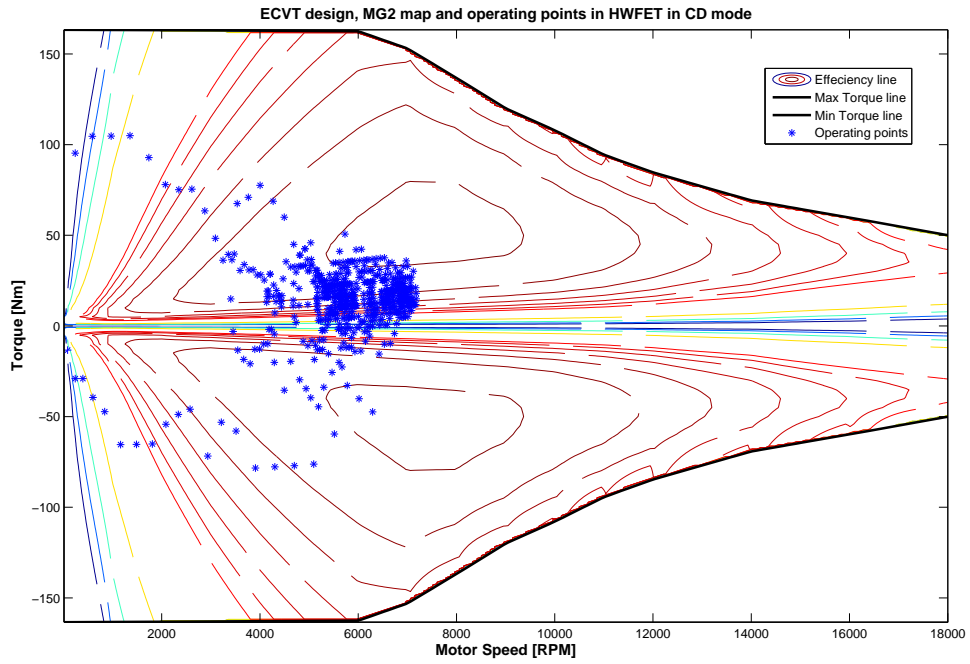


Figure F.3: *ECVT design, MG2 map and operating points in CD mode in HWFET*

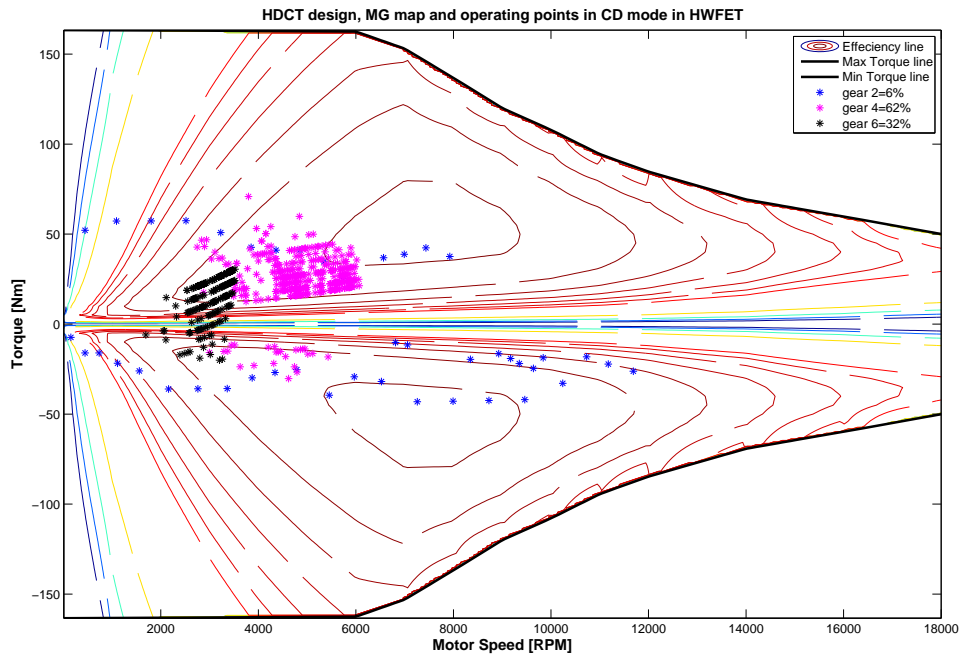


Figure F.4: *HDCT design, MG map and operating points in CD mode in HWFET*

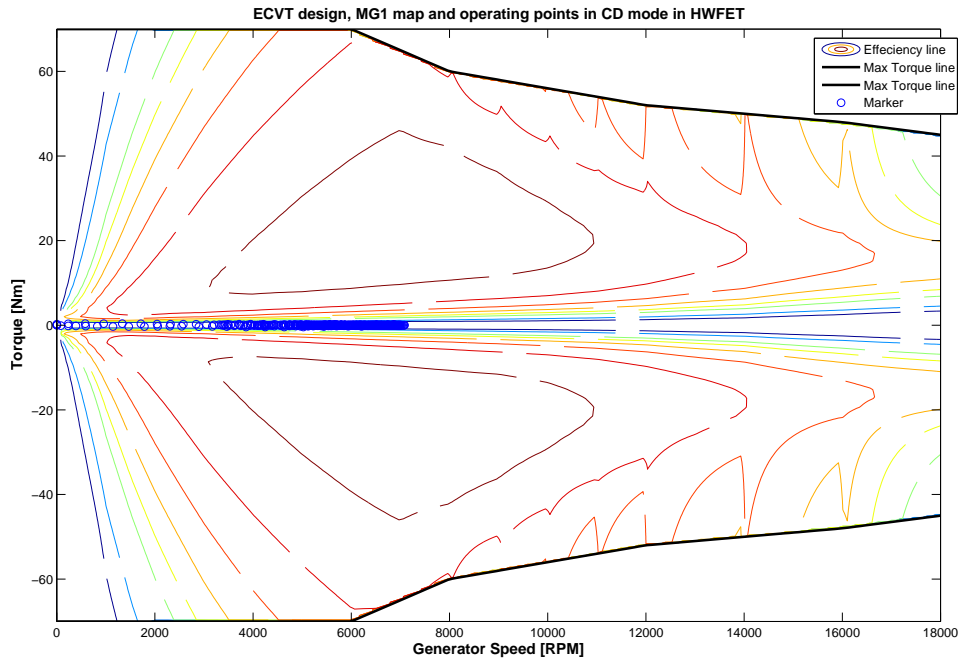


Figure F.5: *ECVT design, MG1 map and operating points in CD mode in HWFET*

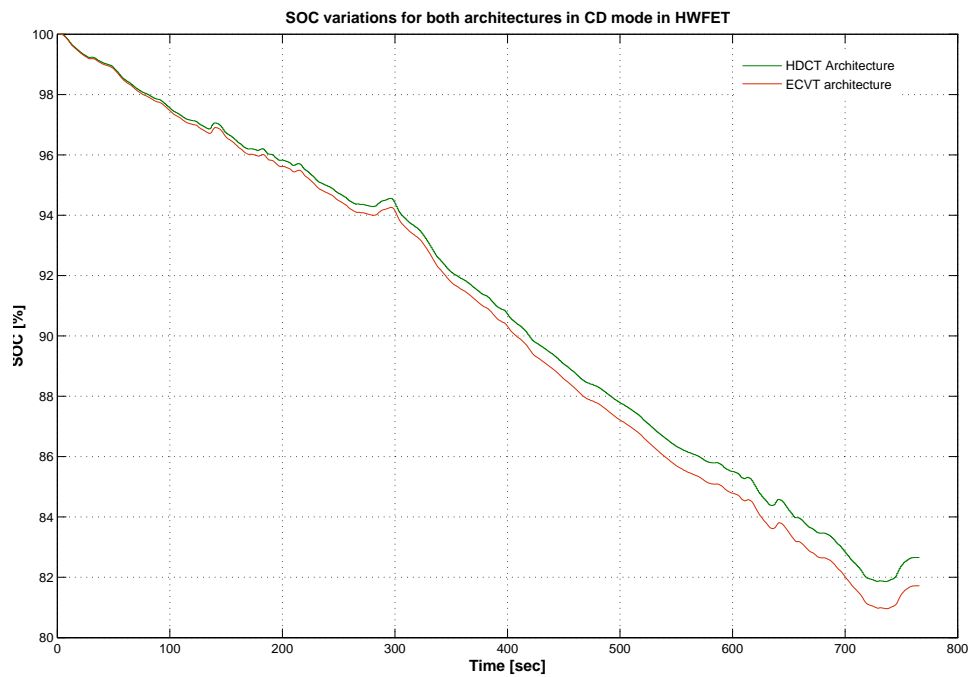


Figure F.6: *SOC variations for both architectures in CD mode in HWFET*

**F.2 Efficiency of both architectures during CS mode (electric mode) in HWFET**

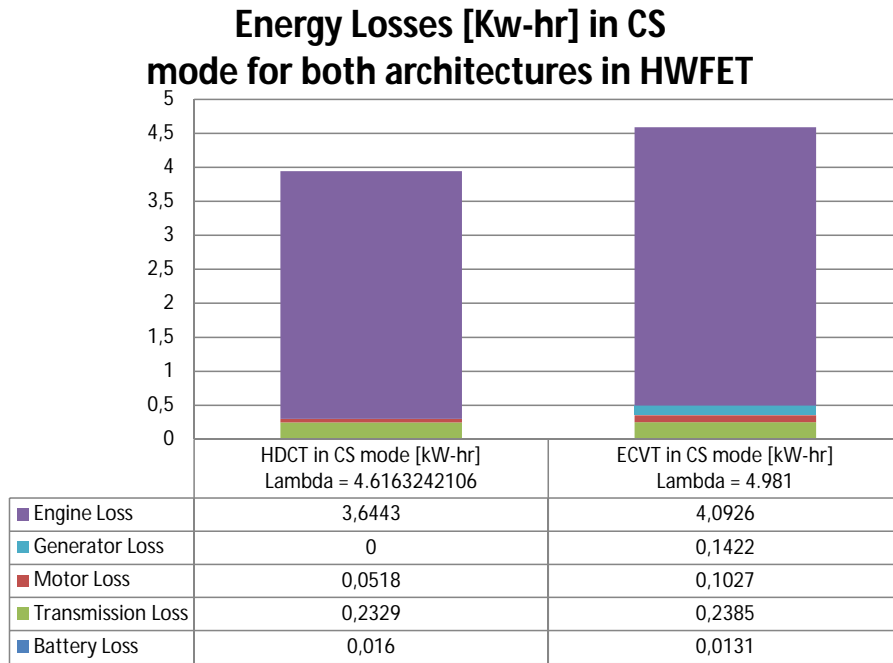


Figure F.7: Energy loss accrued in each component in HWFET cycle for both architectures in CS/ECMS mode

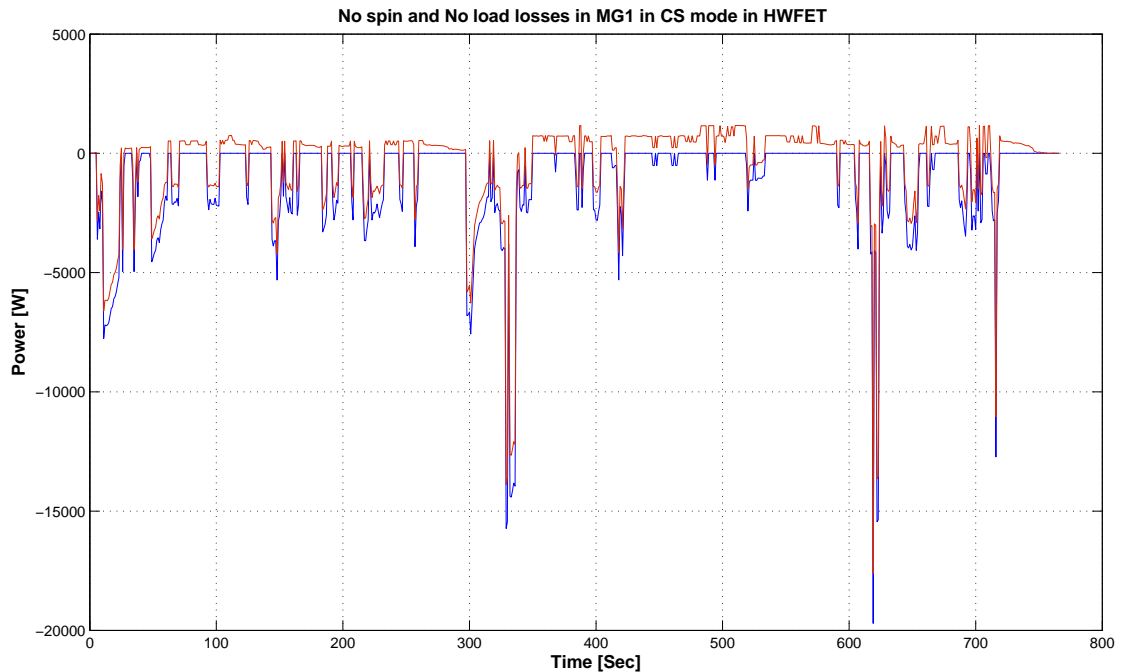


Figure F.8: No-load and No-spin losses in ECVT design in MG1 in CS mode in HWFET

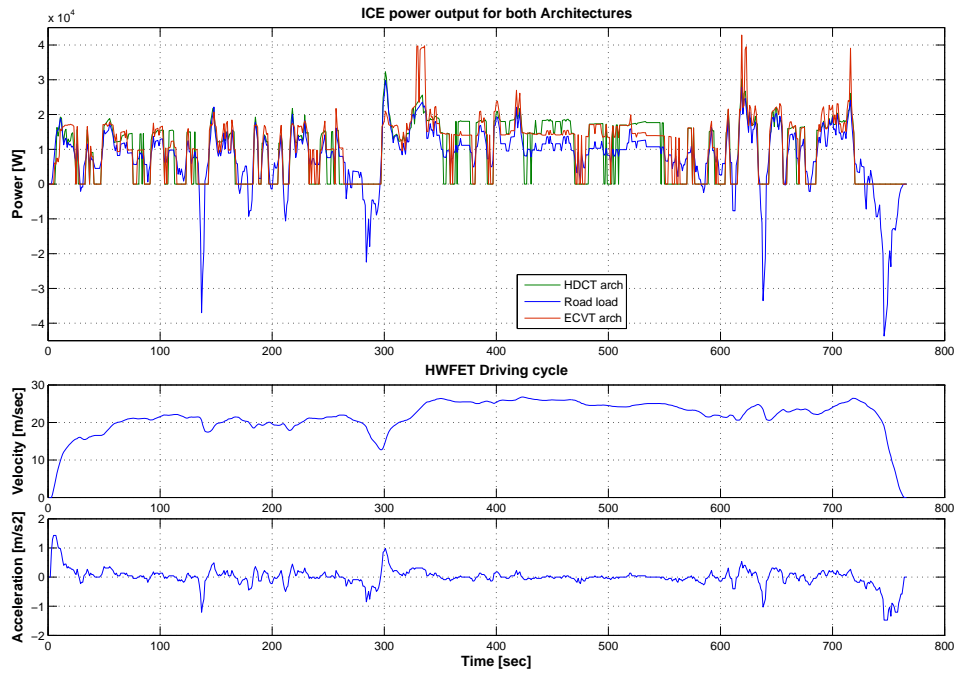


Figure F.9: ICE power output for both architectures in CS mode in HWFET

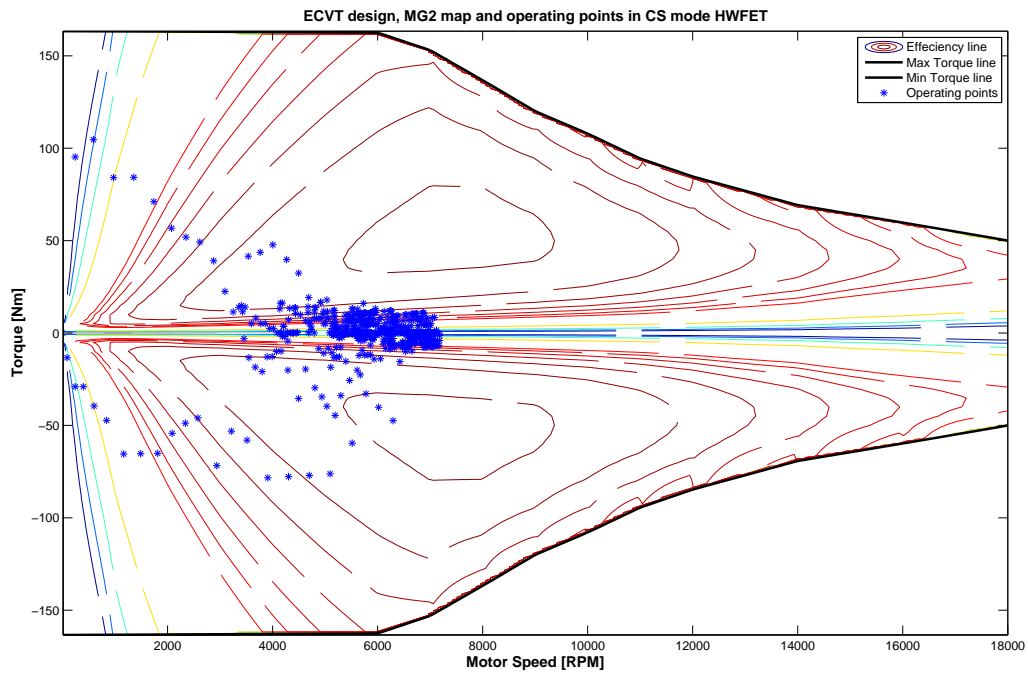


Figure F.10: ECVT design, MG2 map and operating points in CS mode HWFET

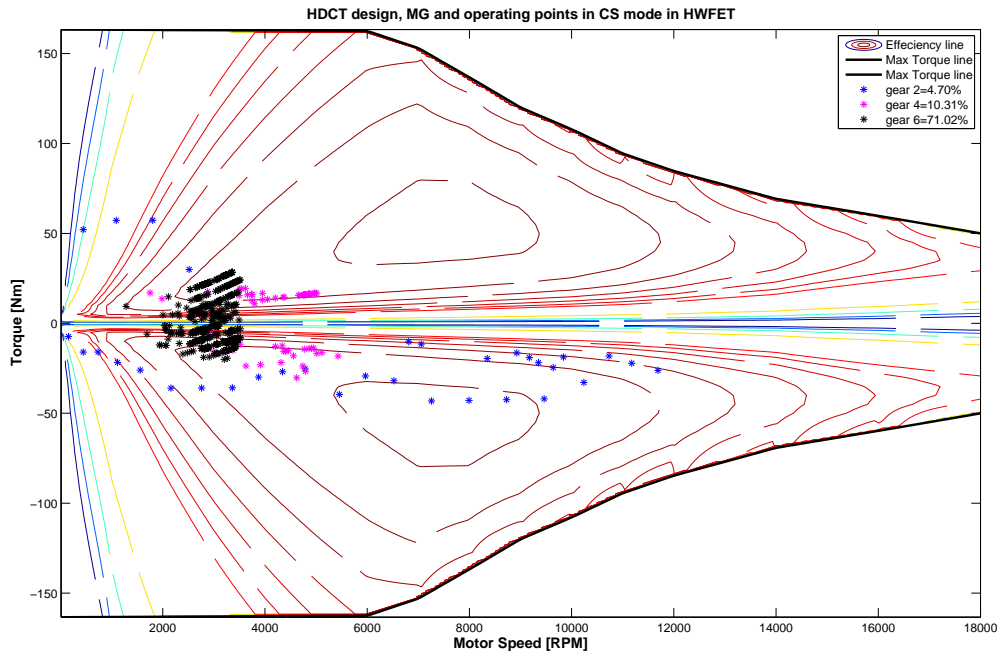


Figure F.11: HDCT design, MG map and operating points in CS mode in HWFET

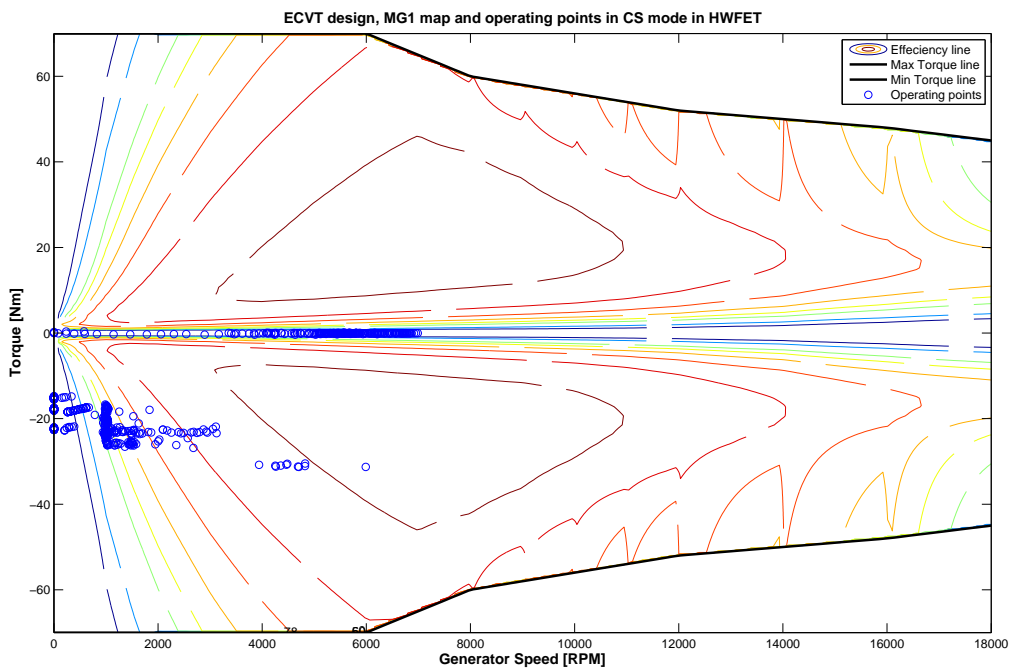


Figure F.12: ECVT design, MG1 map and operating points in CS mode in HWFET

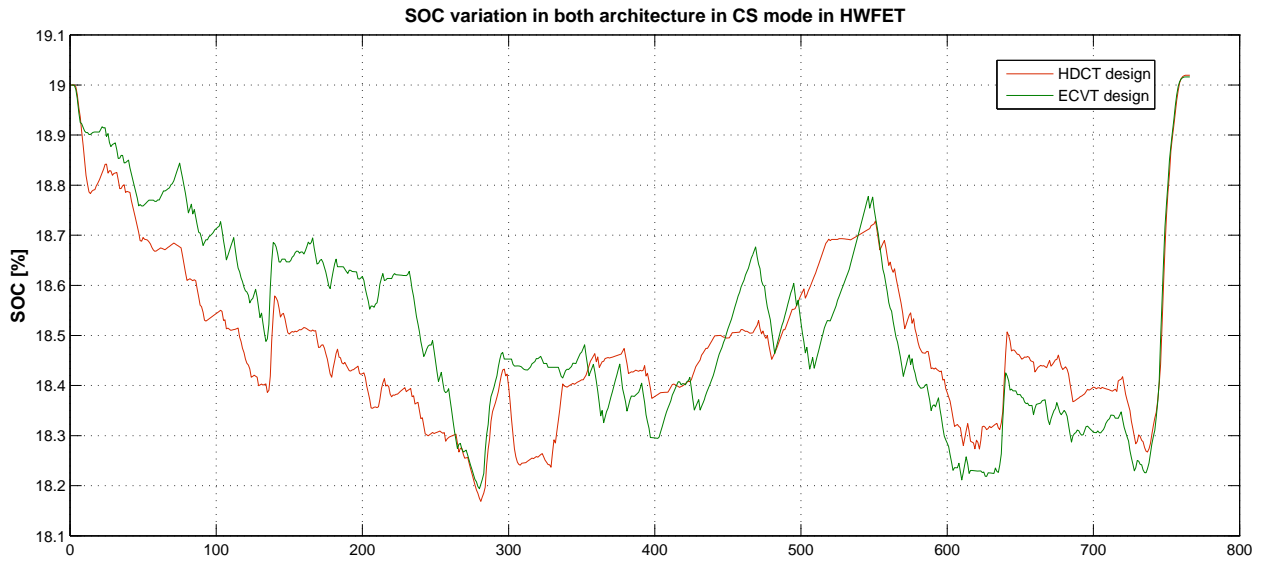


Figure F.13: SOC variation in both architectures in CS mode in HWFET

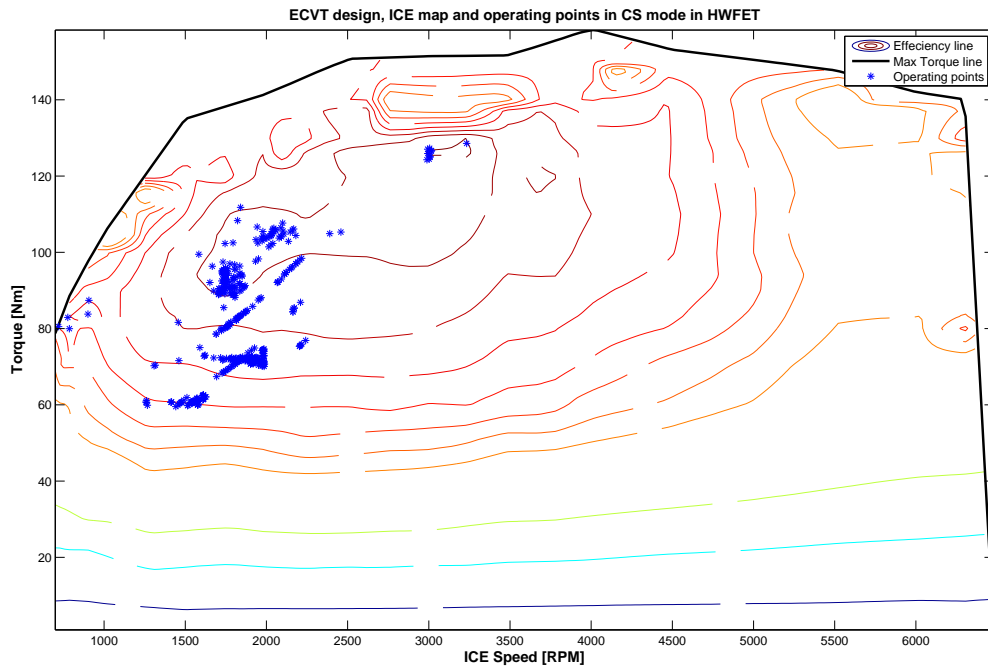


Figure F.14: ECVT design, ICE map and operating points in CS mode in HWFET

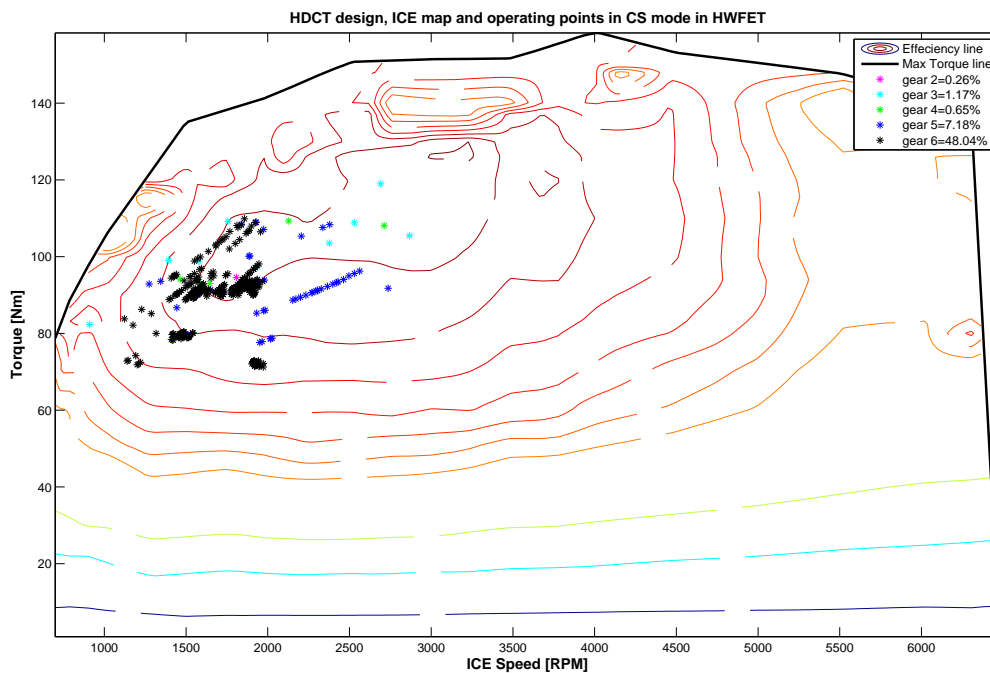


Figure F.15: HDCT design, ICE map and operating points in CS mode in HWFET

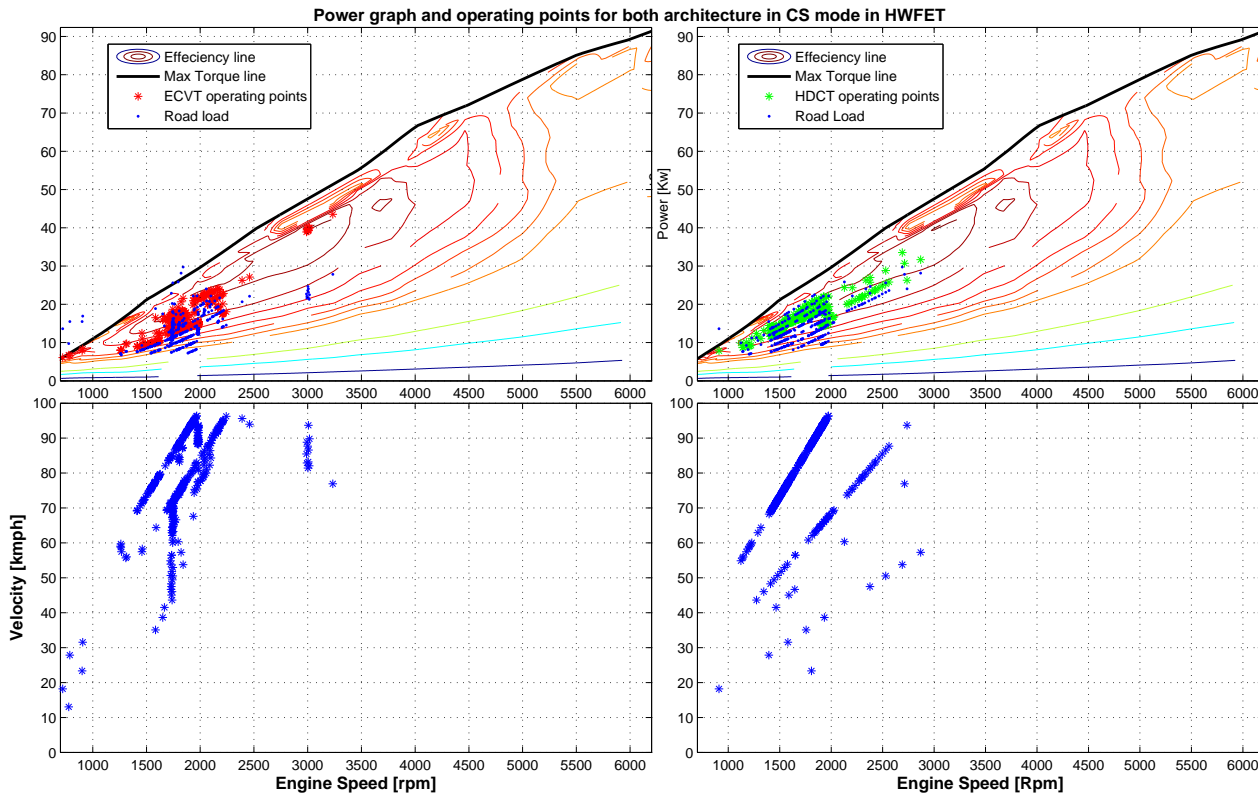


Figure F.16: Power map for both architecture with operating points and road load in HWFET

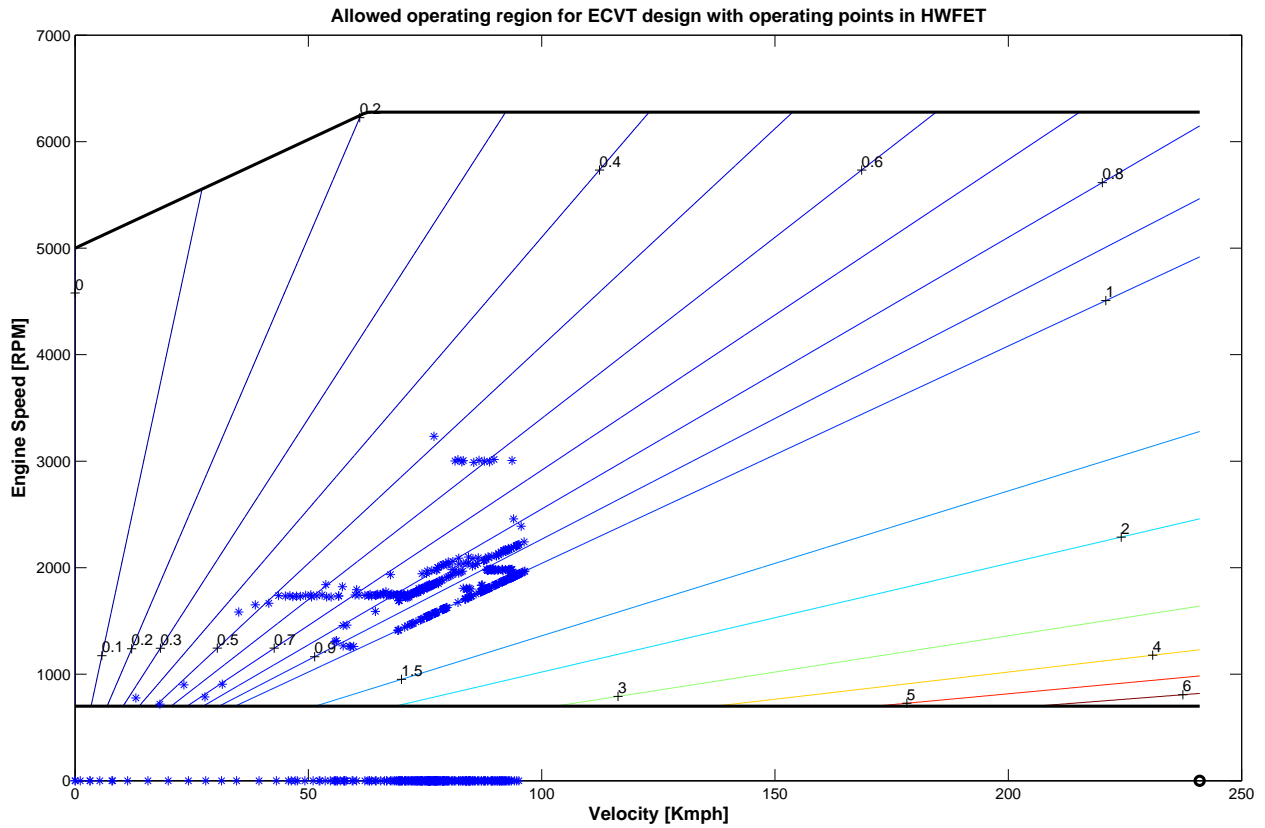


Figure F.17: Separation factor chosen by power-train control in CS mode in ECVT in HWFET design

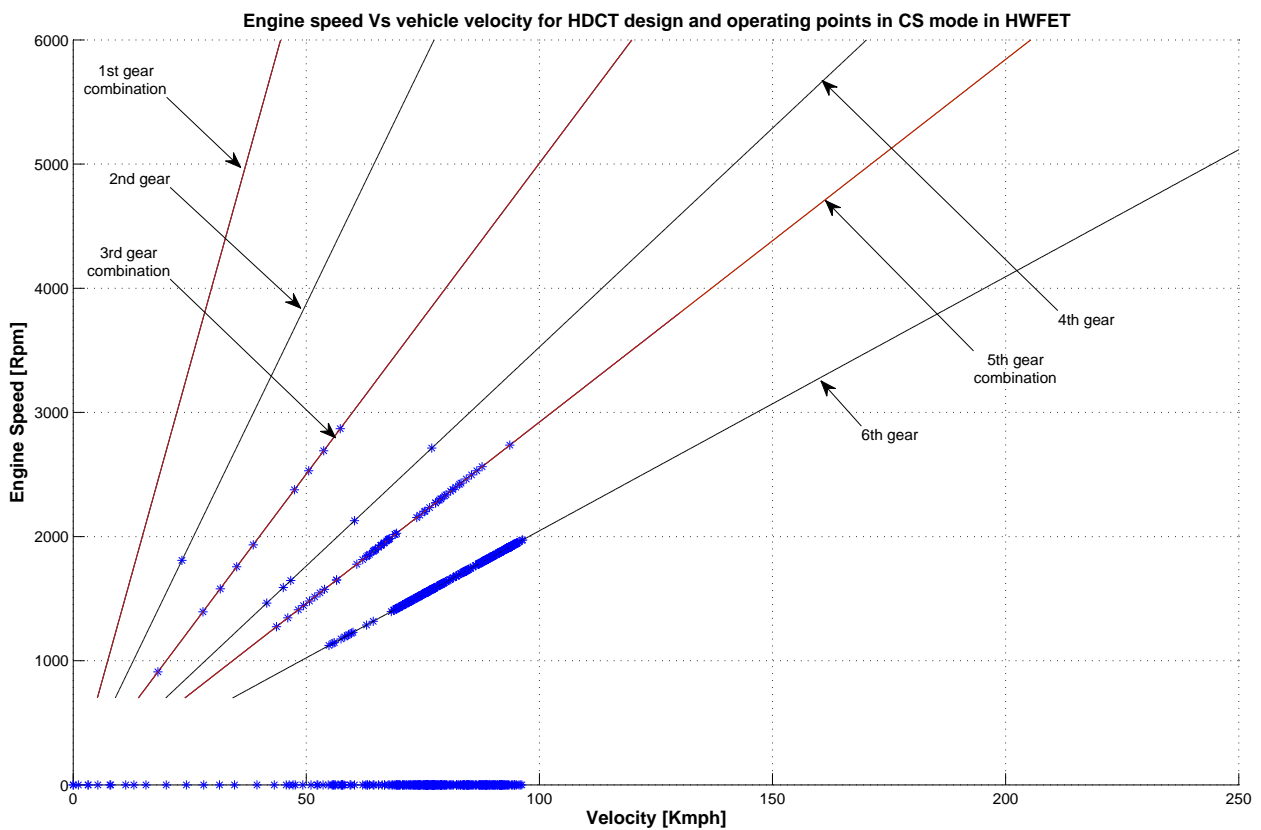


Figure F.18: Engine speed vs vehicle velocity and operating points in CS mode in HDCT in HWFET design

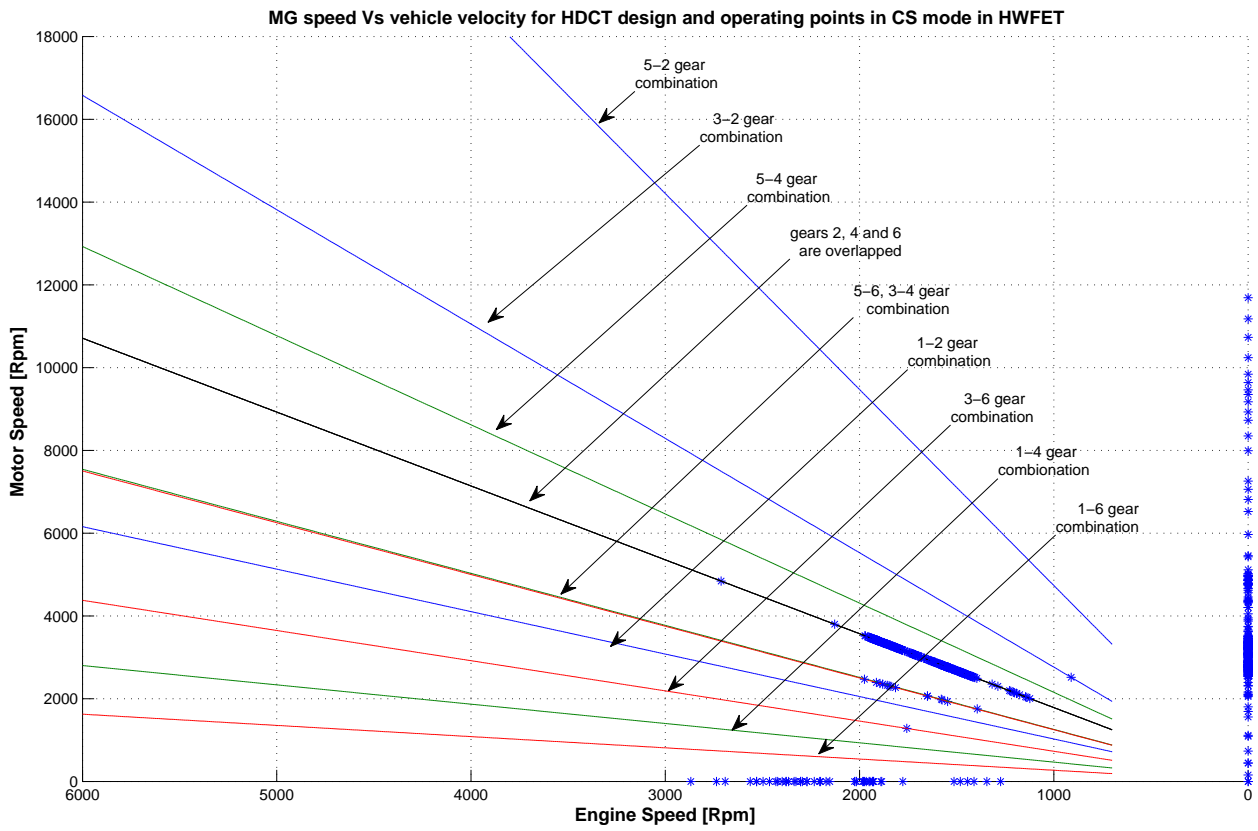


Figure F.19: MG speed vs vehicle velocity and operating points in CS mode in HWFET in HDCT design

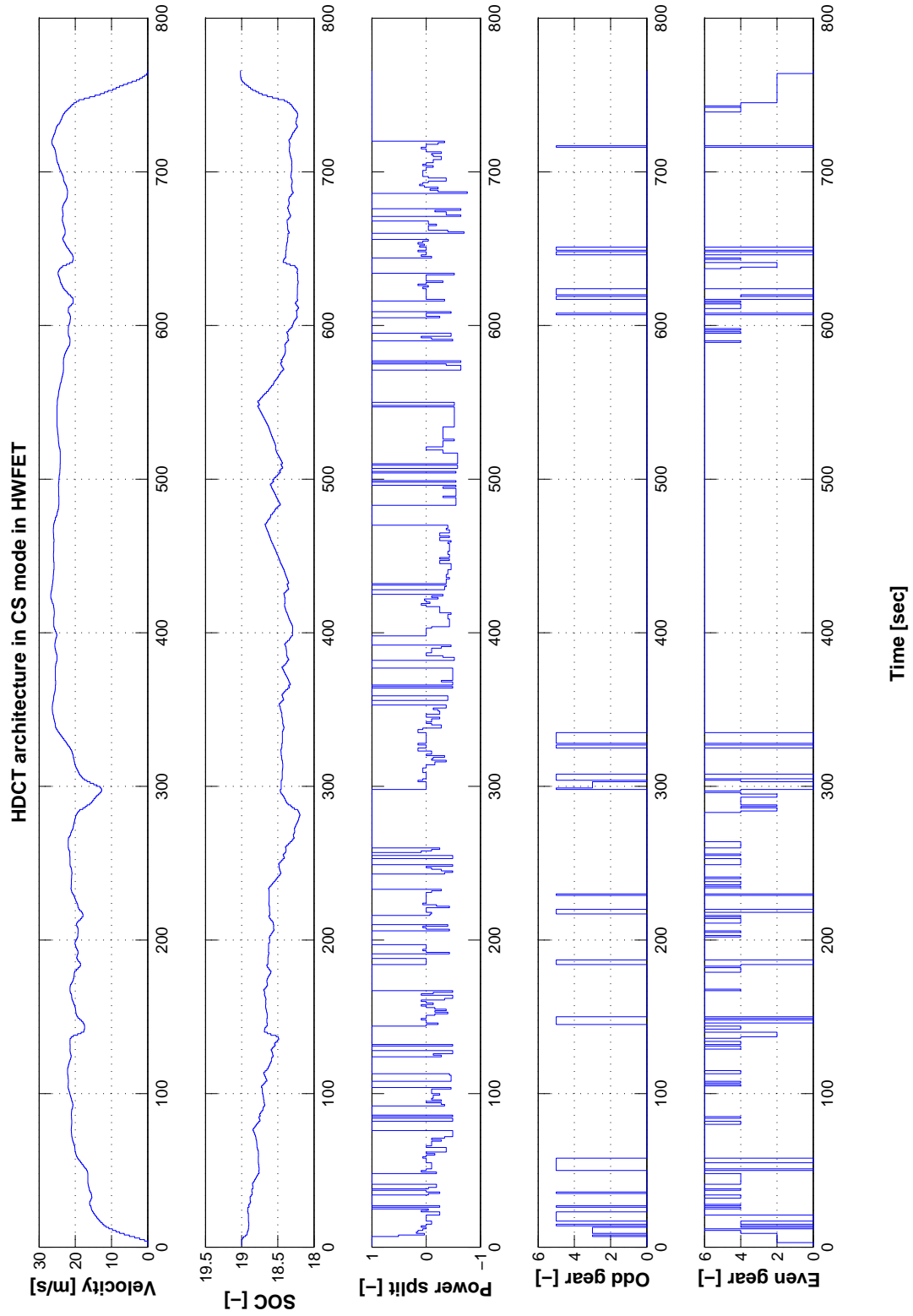


Figure F.20: *HDCT architecture, power-train control signals in HWFET in CS mode*

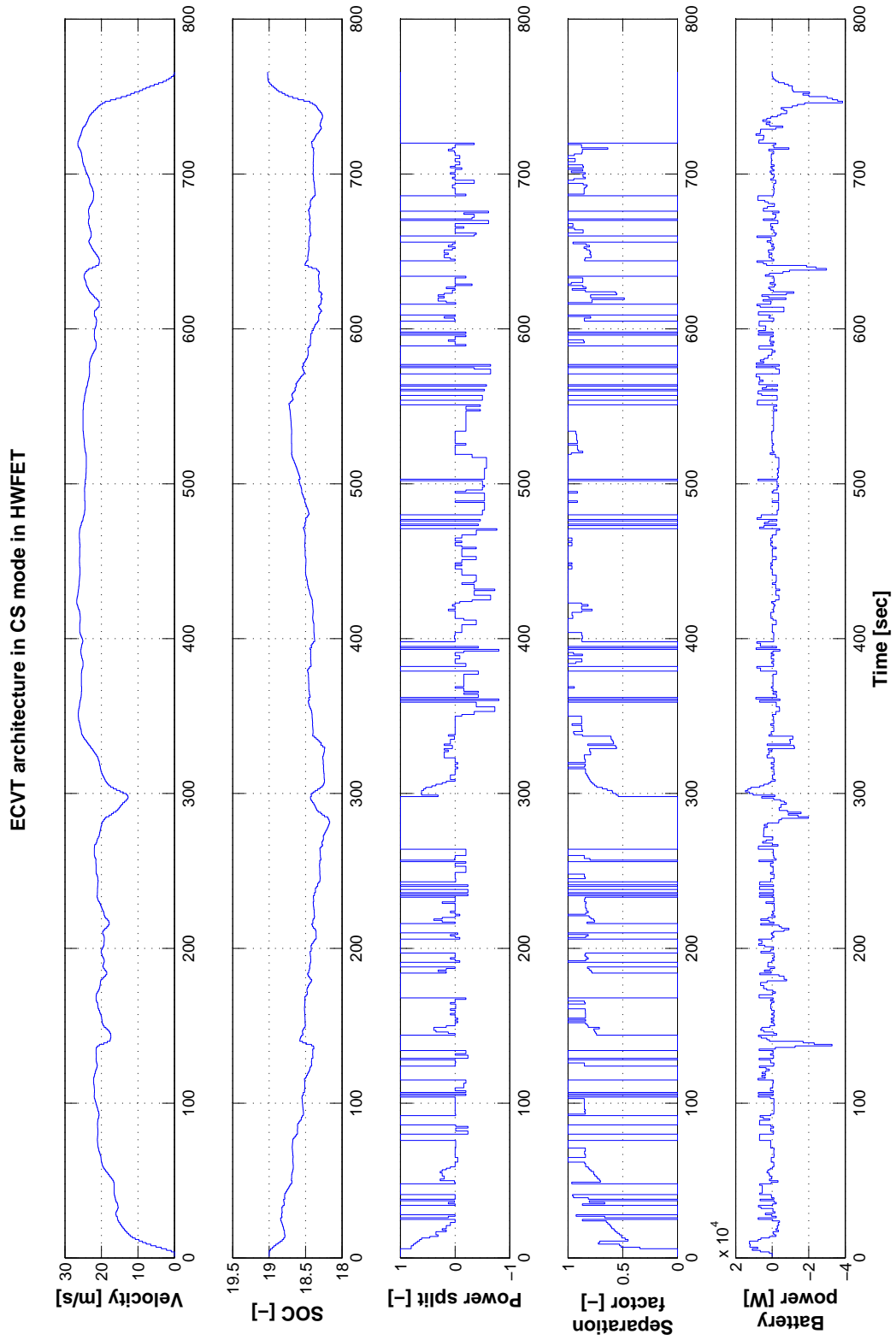


Figure F.21: *ECVT architecture, power-train control signals in HWFET in CS mode*